

Supporting Information

Modifying the liquid crystalline chessboard tiling - Soft reticular self-assembly of side-chain fluorinated polyphiles

Christian Anders,^a Virginia-Marie Fischer,^b Tianyi Tan,^c Mohamed Alaasar,^a Rebecca Waldecker,^b Yubin Ke,^d Yu Cao,^{c*} Feng Liu,^c Carsten Tschierske^{a*}

^aInstitute of Chemistry, Martin-Luther University Halle-Wittenberg, Kurt-Mothes Str. 2, D-06120 Halle/Saale, German. E-mail: Carsten.tschierske@chemie.uni-halle.de

^bInstitute of Mathematics, Martin-Luther University Halle-Wittenberg, Theodor-Lieser-Str. 5, 06120 Halle, Germany.

^cShannxi International Research Center for Soft Matter, State Key Laboratory for Mechanical Behavior of Materials, Xi'an Jiaotong University, Xi'an 710049, P. R. China. E-mail: yu.cao@xjtu.edu.cn

^dChina Spallation Neutron Source, Institute of High Energy Physics, Chinese Academy of Science, Dongguan 523000, P. R. China.

Content

1. Methods.....	S3
2. Additional data.....	S5
2.1 DSC traces and POM textures.....	S5
2.2 Scattering data and additional discussion.....	S15
2.2.1 WAXS patterns.....	S15
2.2.2 Additional SAXS patterns.....	S18
2.2.3 Numerical SAXS data.....	S19
2.2.4 Electron density maps.....	S25
2.2.5 SANS data.....	S25
2.2.6 Structural data.....	S26
2.2.7 Additional figures and discussion.....	S27
3. Synthesis and analytical data.....	S31
3.1 General.....	S31
3.2 Synthesis of intermediates.....	S32
3.2.1 Branched semiperfluorinated alkyl alcohols 5OH/m	S32
3.2.2 Branched semiperfluorinated alkyl bromides 5/m	S33
3.2.3 Synthesis of the 1-alkyloxy-4-benzyloxybenzenes (4Bz/n).....	S34
3.2.4 Synthesis of the hydroquinone monoethers 4/n	S34
3.2.5 Synthesis of the hydroquinone diethers 4/m/n	S35
3.2.6 Synthesis of the 2,6-diiodohydroquinone diether with two semiperfluorinated side-chains 7/m	S36
3.2.7 Synthesis of the 2,6-diiodohydroquinone diethers with different side-chains 7/m/n	S36
3.2.8 Syntheses of the acetonides Hm/nA , H8₂A , Fm/nA and F8₂A	S37
3.3 Syntheses of compounds Hm/n , H8₂ , Fm/n and F8₂	S39
3.4 Representative NMR spectra	S43
4. References.....	S49

1. Methods

Polarizing Optical Microscopy (POM)

Optical textures of all compounds were characterized by polarizing optical microscopy (Olympus BX51-P) with the combination of a heating stage (Linkam LTS420E) and controller (T95-HS). Optical investigations were carried out under equilibrium conditions between two glass slides that were used without further treatment. A full wavelength retardation plate was used to determine the sign of birefringence.

DSC measurements

Transition enthalpies were determined as obtained from differential scanning calorimetry (DSC) which were recorded on a TA DSC250 and DSC-8000 (Perkin Elmer) in sealed 30 μL aluminum pans with heating and cooling rates of 10 K/min under an N_2 stream; peak temperatures are given in Tables 1a,b.

X-ray scattering

X-ray investigations were carried out with an Incoatec (Geesthacht, Germany) $1\mu\text{S}$ microfocus source with a monochromator for CuK_{α} radiation ($\lambda = 0.154$ nm), calibration with the powder pattern of $\text{Pb}(\text{NO}_3)_2$. A droplet of the sample was placed on a glass plate on a Linkam hot stage HFS-X350-GI (rate: 1 Kmin^{-1} – 0.01 Kmin^{-1}). Exposure time was 5 min; the sample-detector distance was 9.00 cm for WAXS and 26.80 cm for SAXS. The diffraction patterns were recorded with a Vantec 500 area detector (Bruker AXS, Karlsruhe) and transformed into 1D plots using GADDS software.

Synchrotron-based Scattering

High-resolution small-angle powder diffraction experiments were recorded on Beamline BL16B1 at the Shanghai Synchrotron Radiation Facility (SSRF). Samples were held in evacuated 1 mm capillaries. A modified Linkam hot stage with thermal stability within 0.2 °C was used, with a hole for the capillary drilled through the silver heating block and mica windows attached to it on each side. A Pilatus 2M detector was used. q Calibration and linearization were verified using several orders of layer reflections from silver behenate and a series of n -alkanes. Experimental diffractograms are fitted using Gaussian-shaped peaks to determine the positions and intensities of the diffraction peaks. The diffraction peaks are indexed based on their peak positions, and the lattice parameters and the space groups are subsequently determined.

Small-angle neutron scattering was conducted on beamline at China Spallation Neutron Source (CSNS). The liquid crystal sample is placed in self-made quartz holder with 2.5 mm path length and empty cell with diameter of 4 mm. For each of the sample measurements, SANS measurements of corresponding holder as well as air are also carried out for background reduction. The measured scattering intensity is corrected for detector sensitivity, and placed on an absolute scale using a calibrated standard. The SANS data are processed under Lorentz correction and indexed by Nika and Irena macro of Igor platform.

Once the diffraction intensities are measured, and the corresponding plane group determined, 2D scattering length maps (electron density for SAXS and hydrogen density for SANS) can be reconstructed based on the general formula.

$$E(xy) = \sum_{hk} F(hk) e^{[i2\pi(hx+ky)]} \quad (1)$$

Here $F(hk)$ is the structure factor of a diffraction peak with index (hk) . It is normally a complex number, and the experimentally observed diffraction intensity is

$$I(xy) = K \cdot F(hk) = F * (hk) = K \cdot |F(hk)|^2 \quad (2)$$

Here K is a constant related to the sample volume, incident beam intensity etc. If the constant is equal to 1, then the electron density is

$$E(xy) = \sum_{hk} \sqrt{I(hk)} e^{[i2\pi(hx+ky)+\Phi_{hk}]} \quad (3)$$

As the observed diffraction intensity $I(hk)$ is only related to the amplitude of the structure factor $|F(hk)|$, the information about the phase of $F(hk)$, Φ_{hk} , cannot be determined directly from the experiment. However, the problem is much simplified when the structure of the ordered phase is centrosymmetric; hence, the structure factor $F(hk)$ is always real, and Φ_{hk} is either 0 or π .

This makes it possible for a trial-and-error approach, where candidate electron density maps are reconstructed for all possible phase combinations. The “correct” phase combination is then selected on the merit of the maps, helped by prior physical and chemical knowledge of the system. This is especially useful for studying nanostructures, where typically only a limited number of diffraction peaks are observed.

2. Additional Data

2.1. DSC traces and POM textures

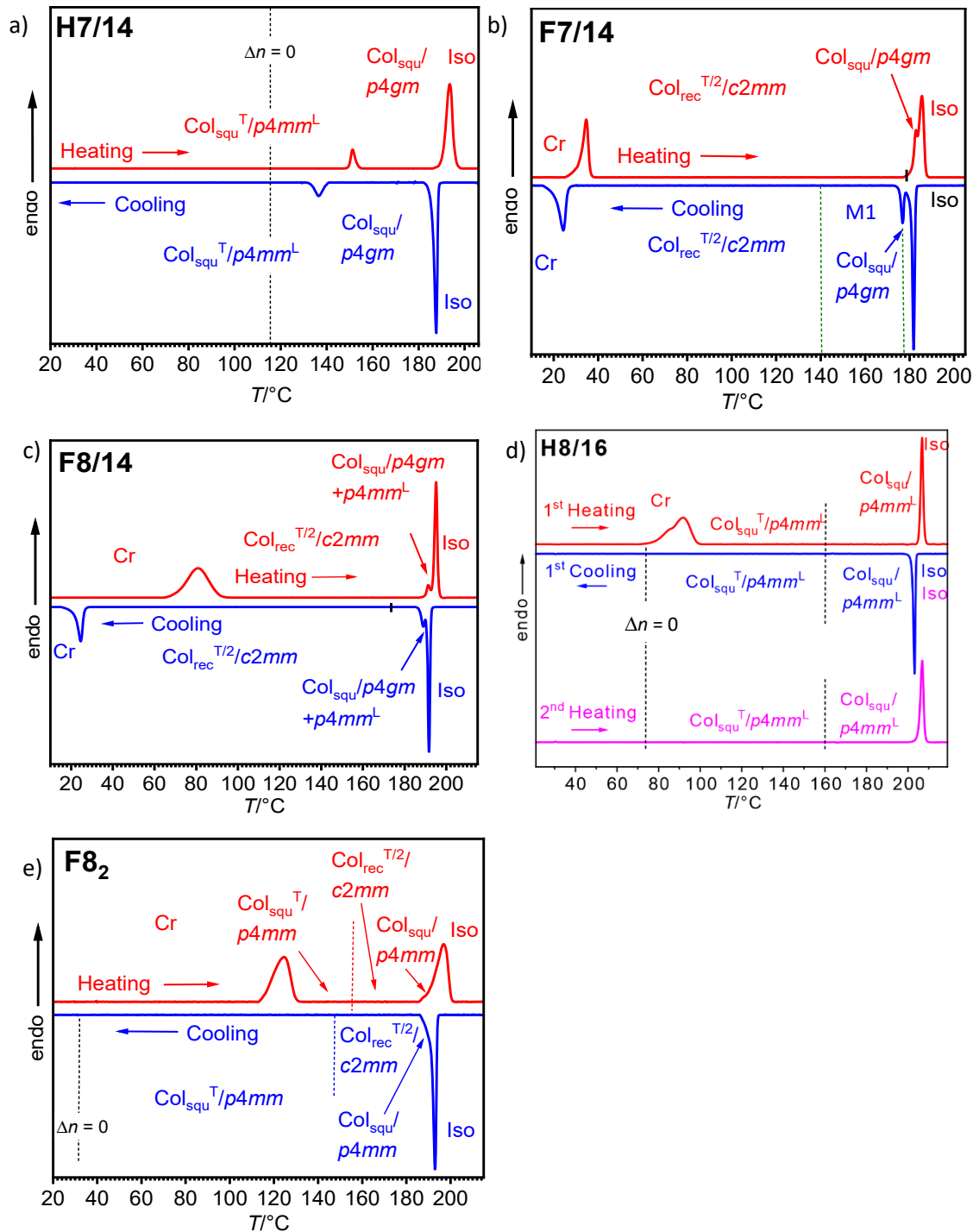


Figure S1: DSC heating & cooling traces of compounds **Hm/n**, **Fm/n** and **F8₂** recorded at 10 K min⁻¹.

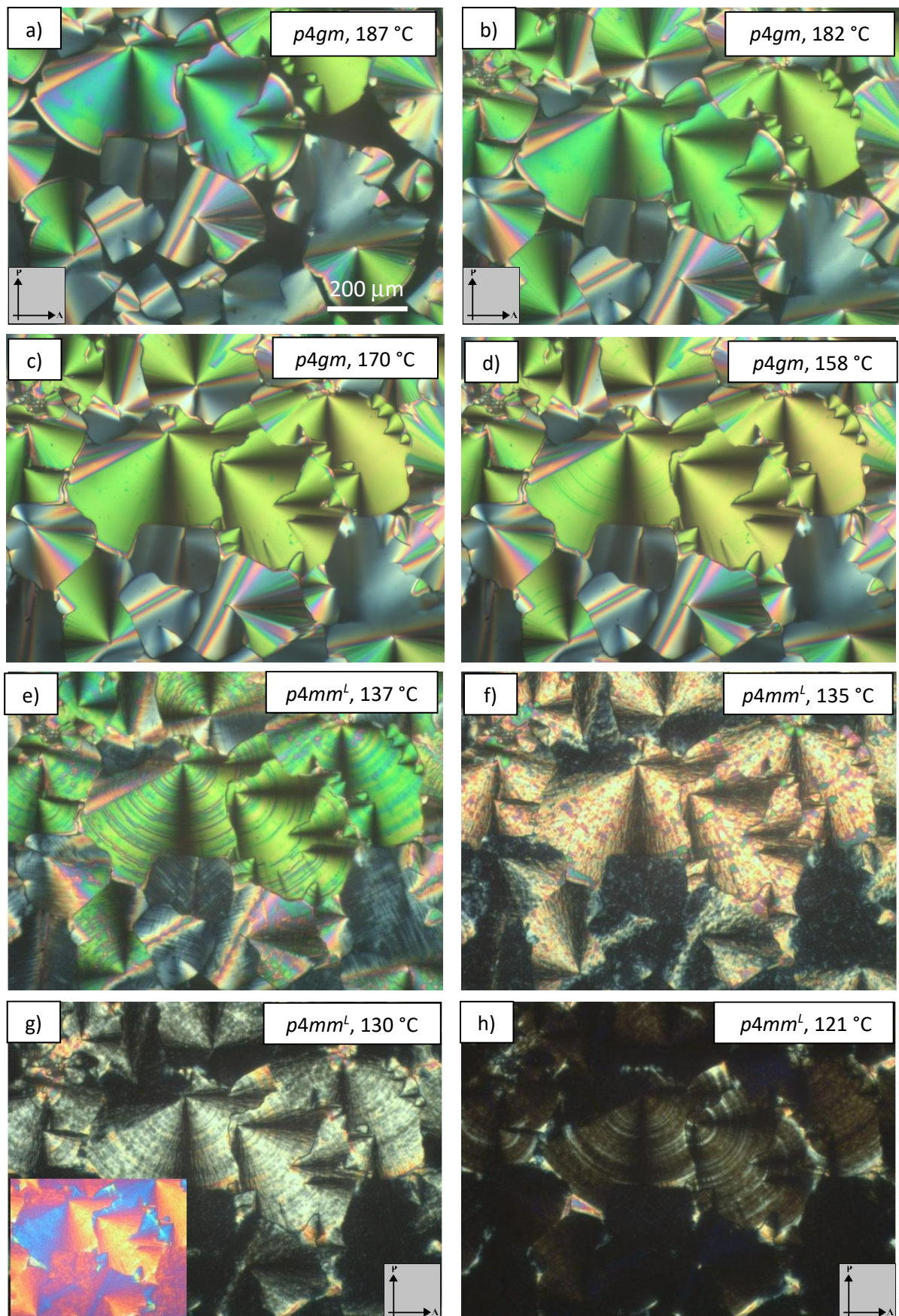


Figure S2: POM textures of compounds **H7/14**, observed between crossed polarizers on cooling at the indicated temperatures; the insets in e, h) show textures with additional λ -plate, the indicatrix slow axis is SW-NE.

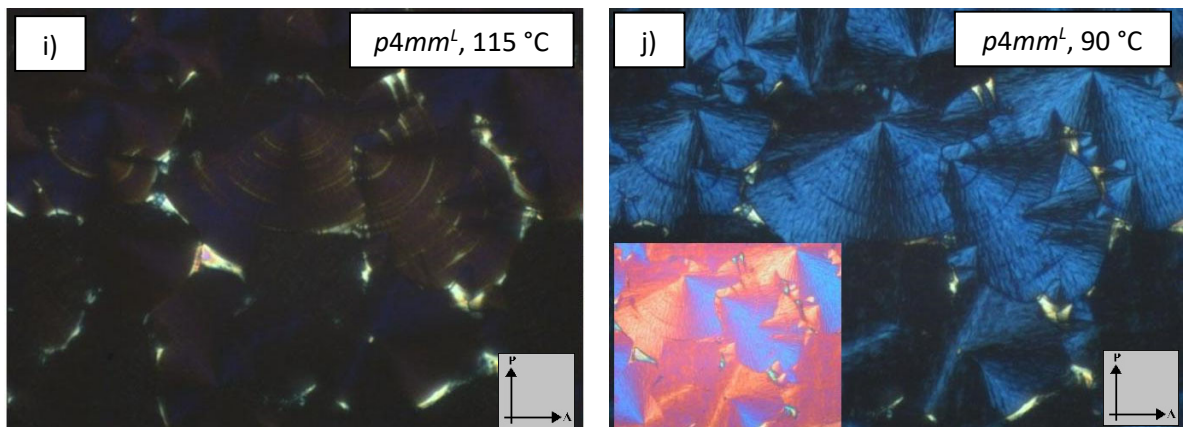


Figure S2 (cont.): POM textures of compounds **H7/14**, observed between crossed polarizers on cooling at the indicated temperatures; the insets in e, h) show textures with additional λ -plate, the indicatrix slow axis is SW-NE.

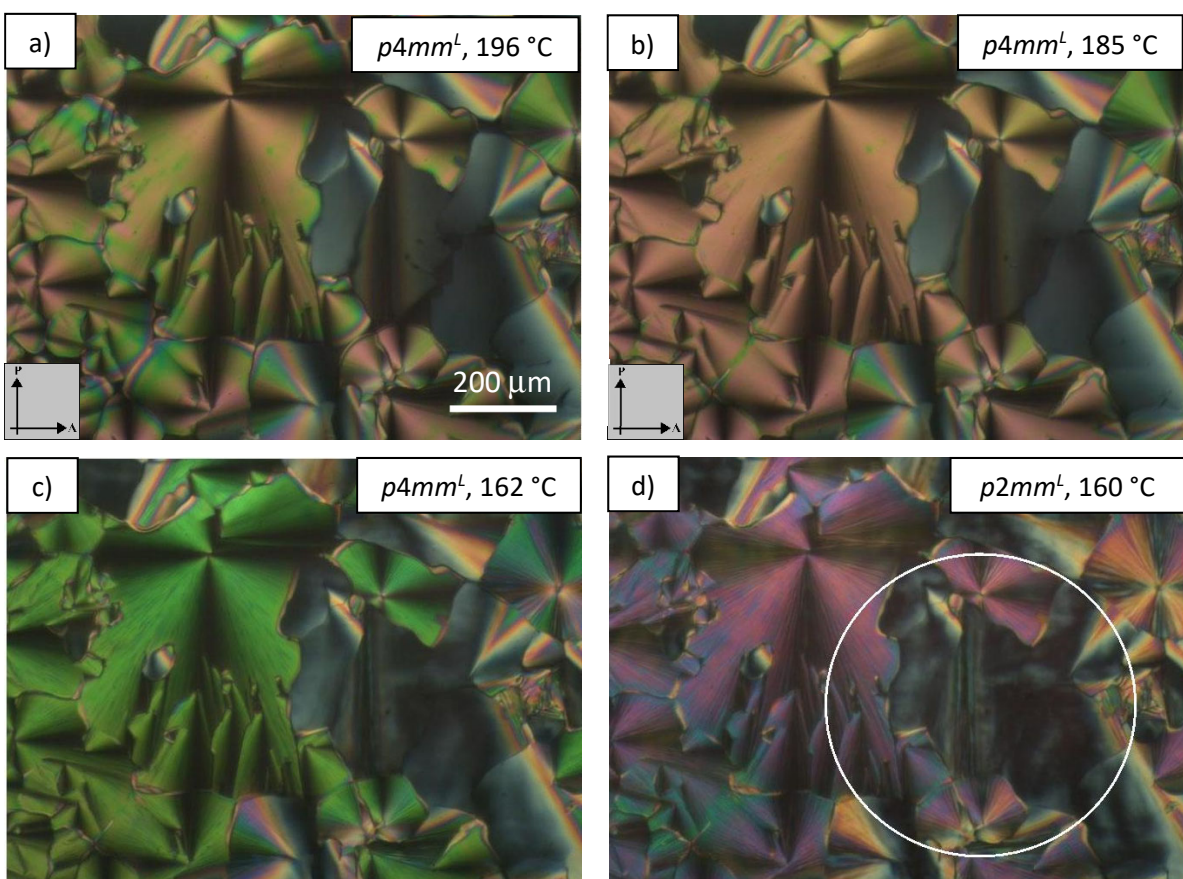


Figure S3: POM textures of compound **H8/14** observed between crossed polarizers on cooling at the indicated temperatures; the stripe pattern in the almost homeotropically aligned areas (inside the ring) indicates the phase biaxiality in the $p2mm^L$ range.

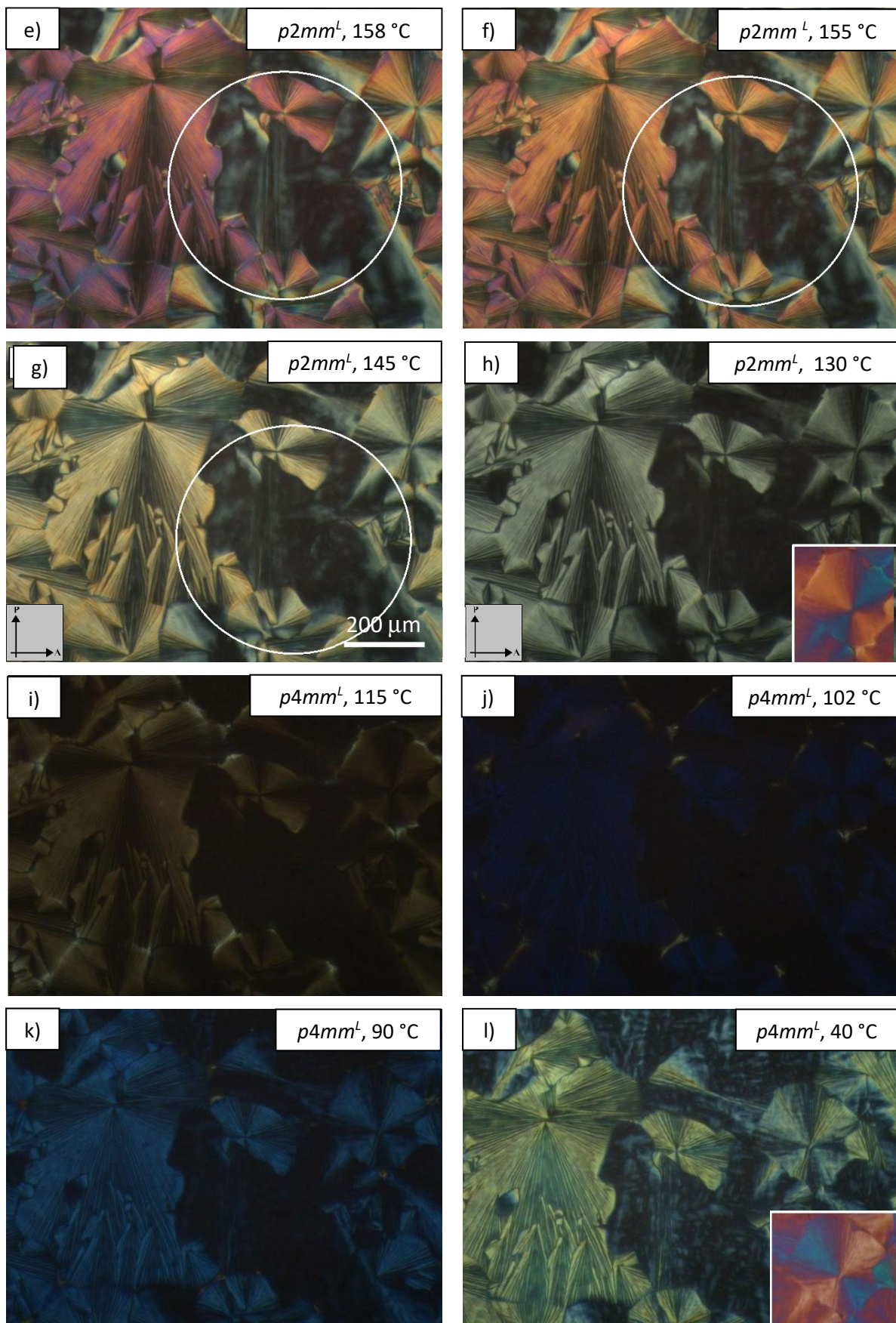


Figure S3 (cont.): POM textures of compound **H8/14**, observed between crossed polarizers on cooling at the indicated temperatures; the insets in h, j) show textures with additional λ -plate, the indicatrix slow axis is SW-NE.

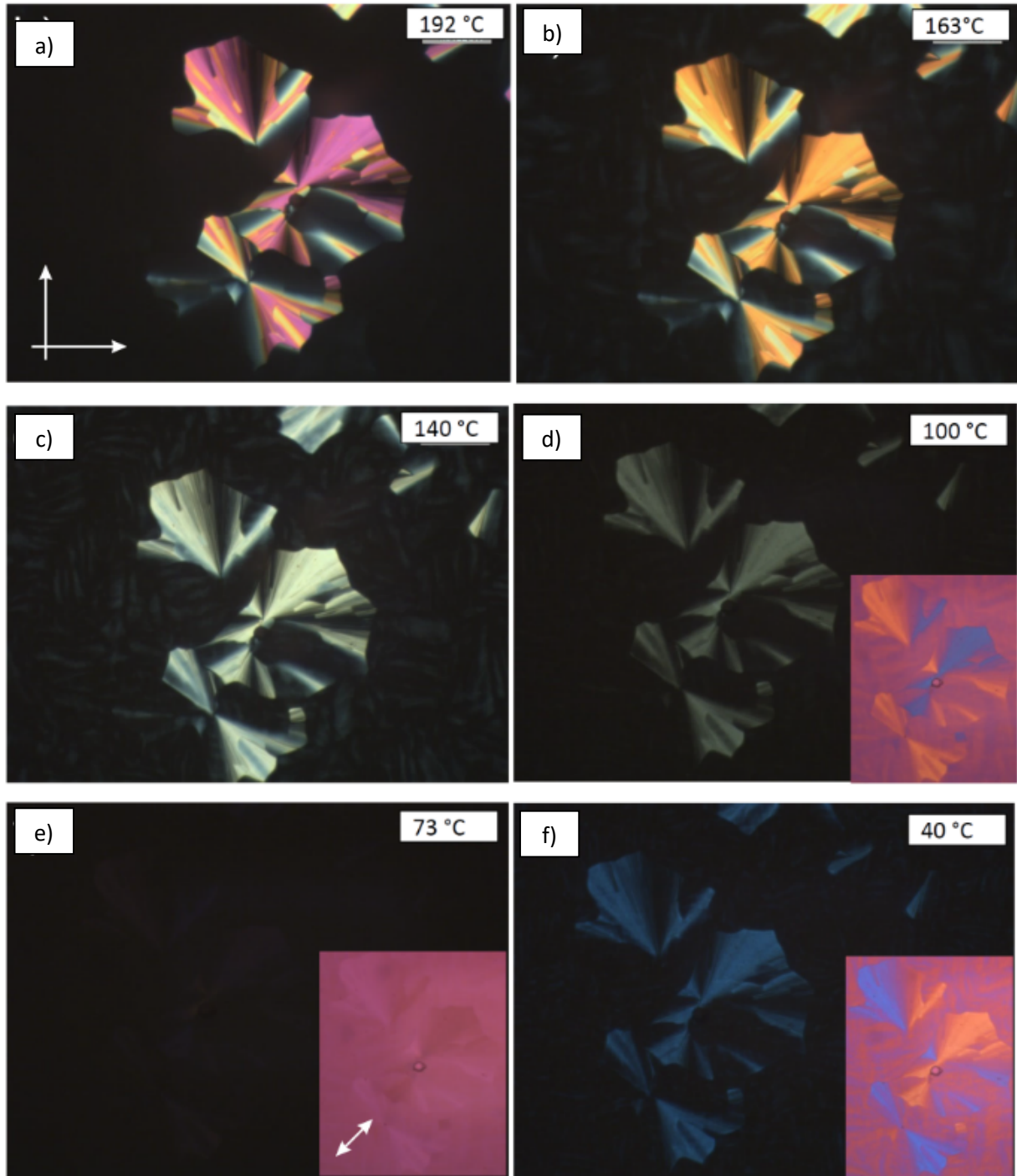


Figure S4. Textures of compound **H8/16** a) in the $\text{Col}_{\text{squ}}/\text{p}4\text{mm}^{\text{L}}$ phase and b-f) the $\text{Col}_{\text{squ}}^{\text{T}}/\text{p}4\text{mm}^{\text{L}}$ phase of as observed on cooling between crossed polarizers at the indicated temperatures; the dark regions represent homeotropic aligned areas. The insets show the textures with additional λ -plate, indicating a change of the blue-shifted fans from NE/SW to NW/SE with lowering temperature, in line with an inversion of birefringence from positive to negative; white arrows indicate the directions of polarizer and analyzer and the blue/yellow arrows indicate the indicatrix orientation of the λ -plate;

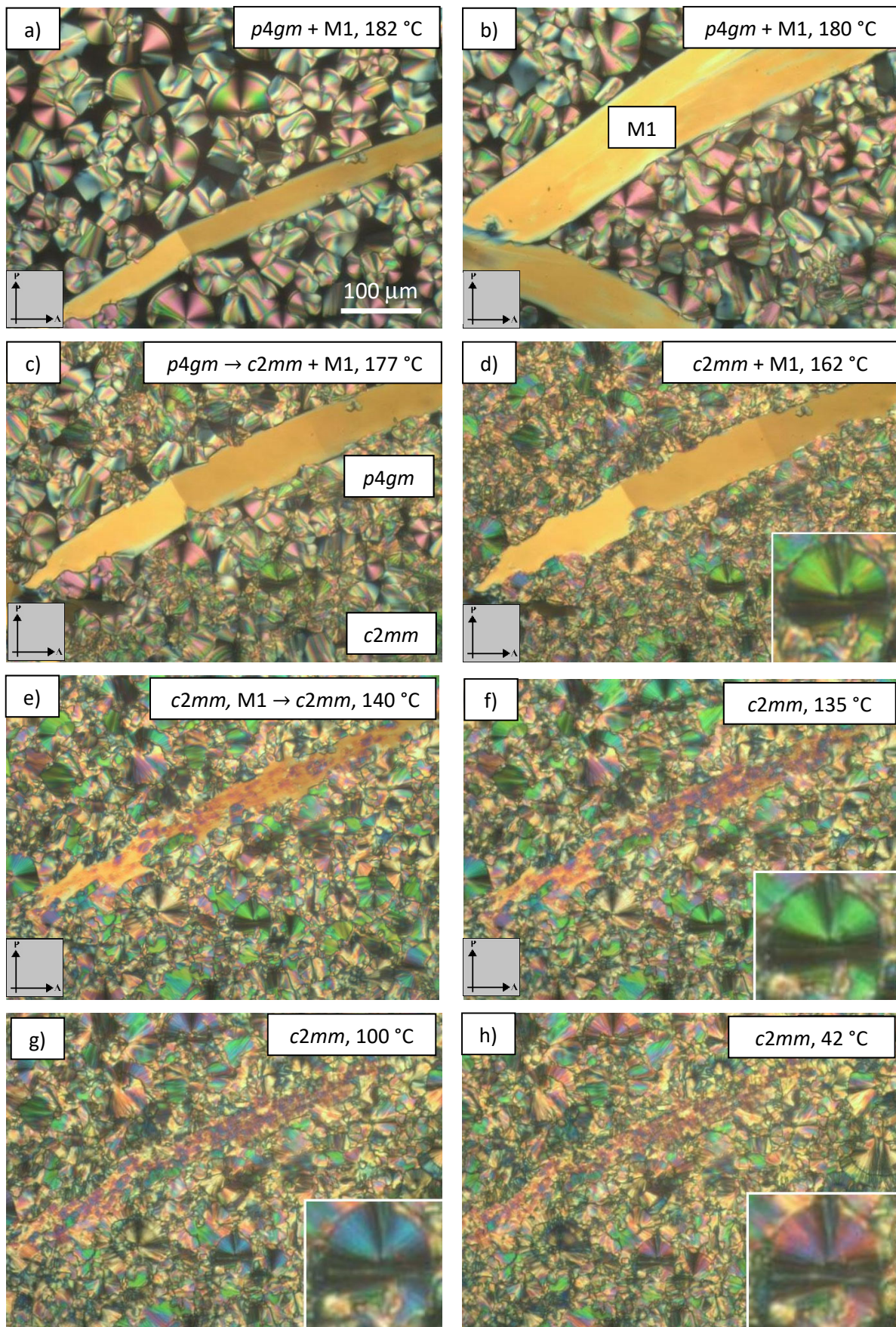


Figure S5: POM textures of compound **F7/14**, observed between crossed polarizers on cooling at the indicated temperatures.

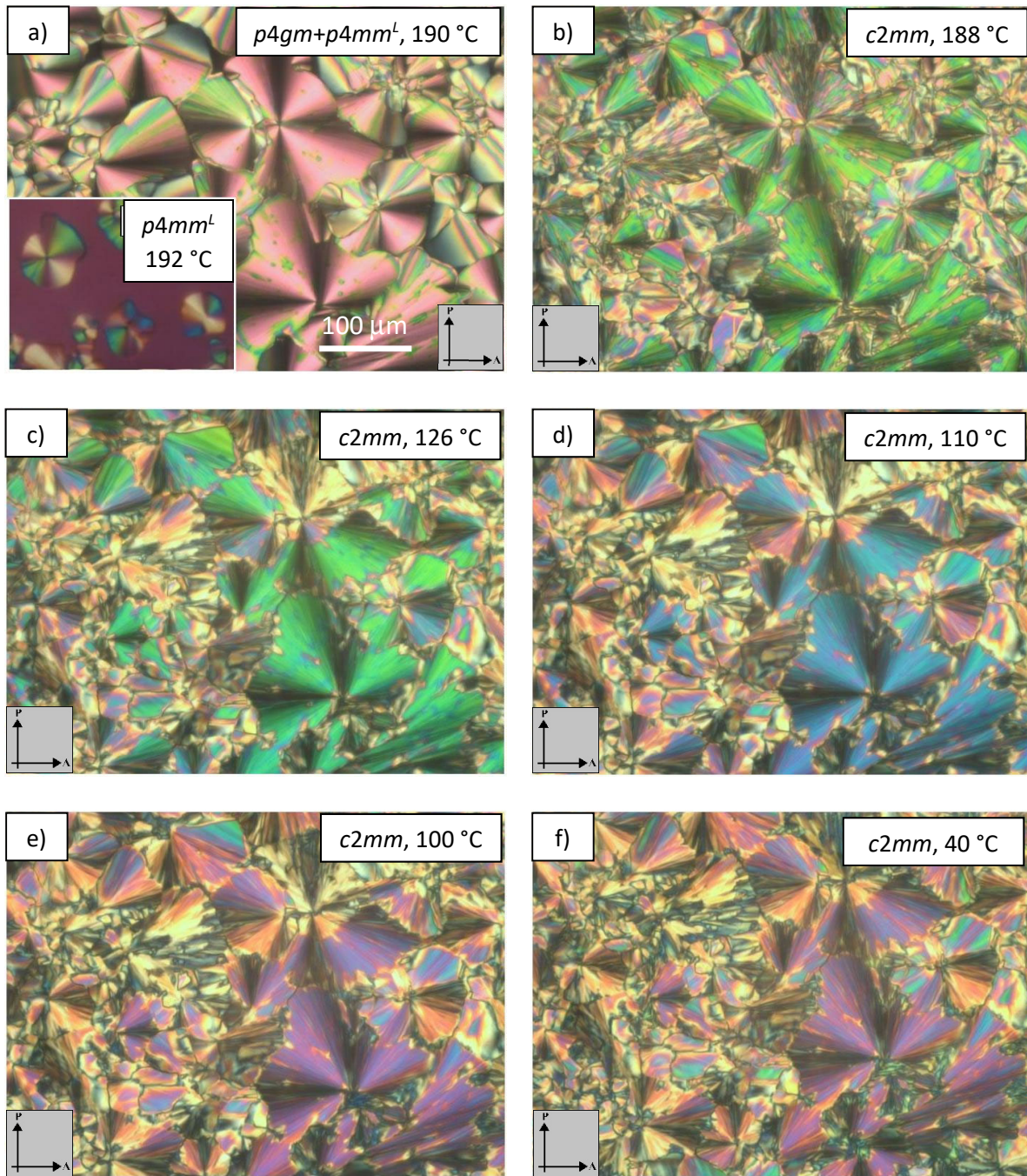


Figure S6: POM textures of compound **F8/14**, observed between crossed polarizers on cooling at the indicated temperatures; the inset in a) show textures with additional λ -plate, the indicatrix slow axis is SW-NE.

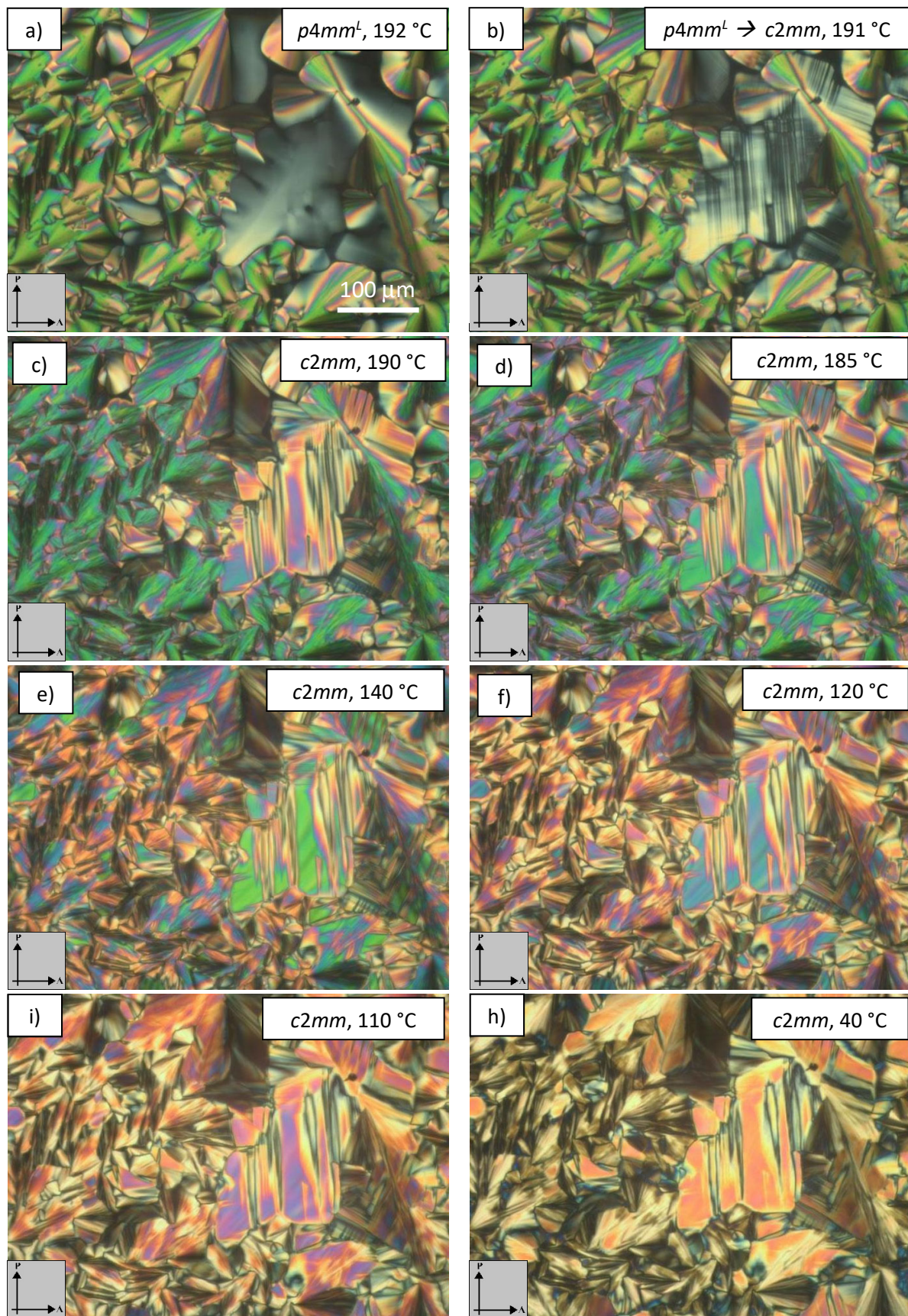


Figure S7: POM textures of compound **F8/16** observed between crossed polarizers on cooling at the indicated temperatures (different region than those shown in Fig. 7).

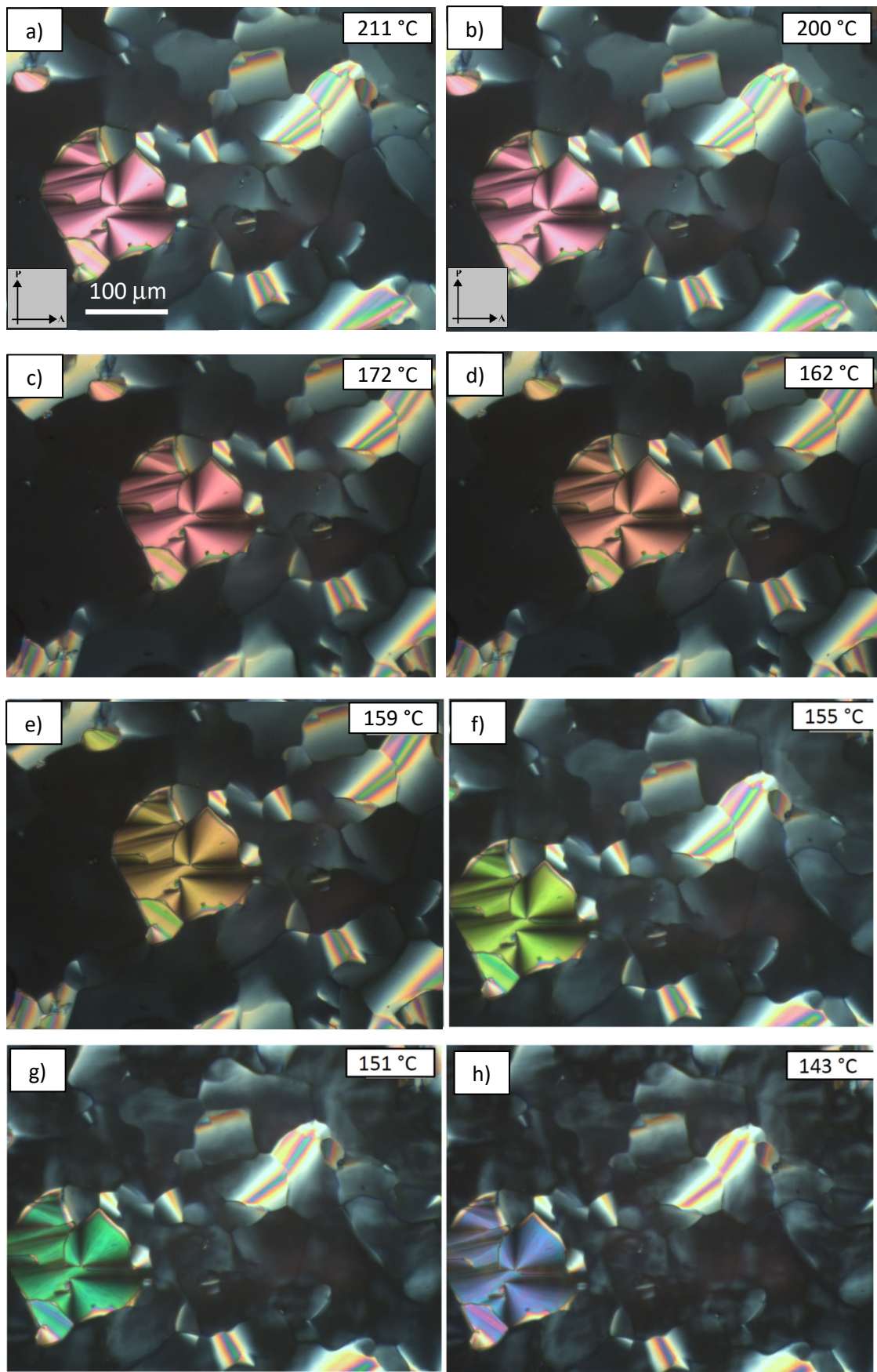


Figure S8. POM textures of compound **H8₂**, observed between crossed polarizers on cooling at the indicated temperatures.

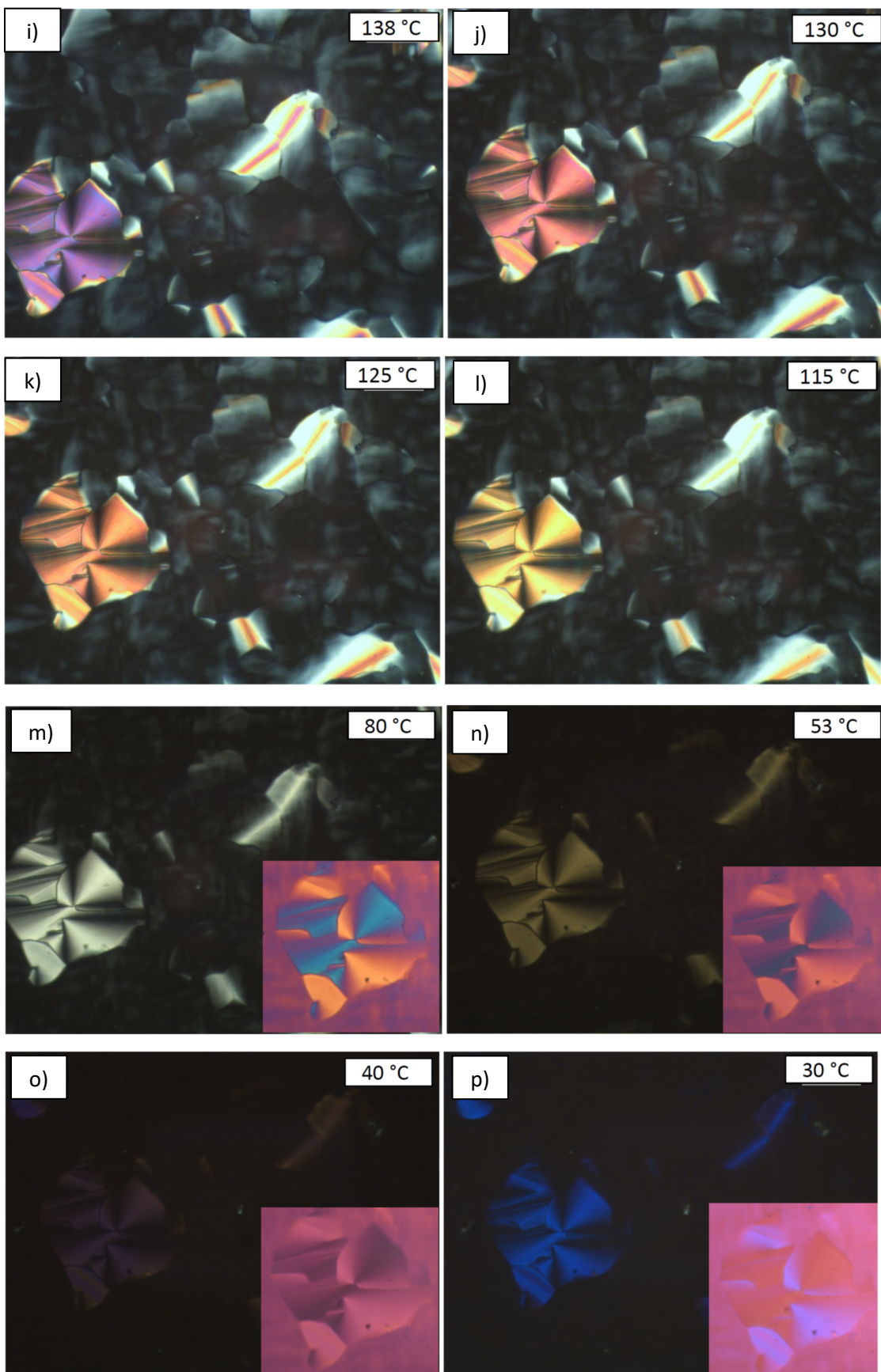


Figure S8 (cont.). POM textures of compound **H8₂**, observed between crossed polarizers on cooling at the indicated temperatures; the insets show textures with additional λ -plate, the indicatrix slow axis is SW-NE.

2.2. Scattering data and additional discussion

2.2.1. WAXS patterns

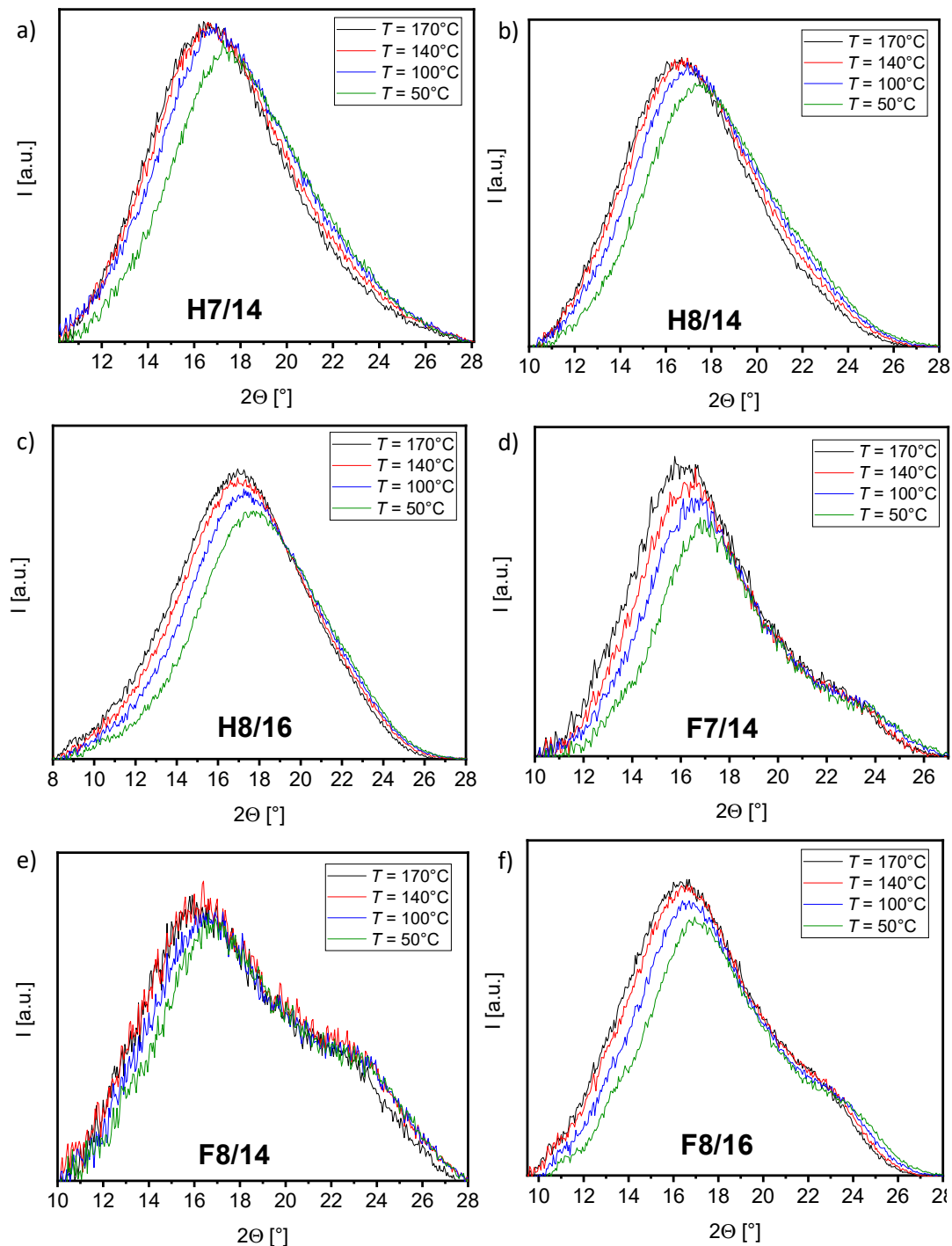


Figure S9. WAXS patterns of compounds **Hm/n** and **Fm/n** at the indicated temperatures.

Table S1. WAXS maxima of the LC phases of compounds **Hm/n** and **Fm/n**.

Comp.	T [°C]	2θ [°]	d [nm]
H7/14	170	16.772	0.53
	140	16.939	0.52
	100	16.994	0.52
	50	17.466	0.51
H8/14	170	16.644	0.53
	140	16.812	0.53
	100	17.058	0.52
	50	17.545	0.51
H8/16	170	17.125	0.52
	140	17.380	0.51
	100	17.545	0.51
	50	17.749	0.50
F7/14	170	16.196	0.55
	140	16.384	0.54
	100	16.617	0.53
	50	16.967	0.52
		22.833	0.39
F8/14	170	16.353	0.54
	140	16.462	0.54
	100	16.697	0.53
	50	16.956	0.52
		23.051	0.39
F8/16	170	16.508	0.54
	140	16.614	0.53
	100	16.832	0.53
	50	17.146	0.52
		23.141	0.38

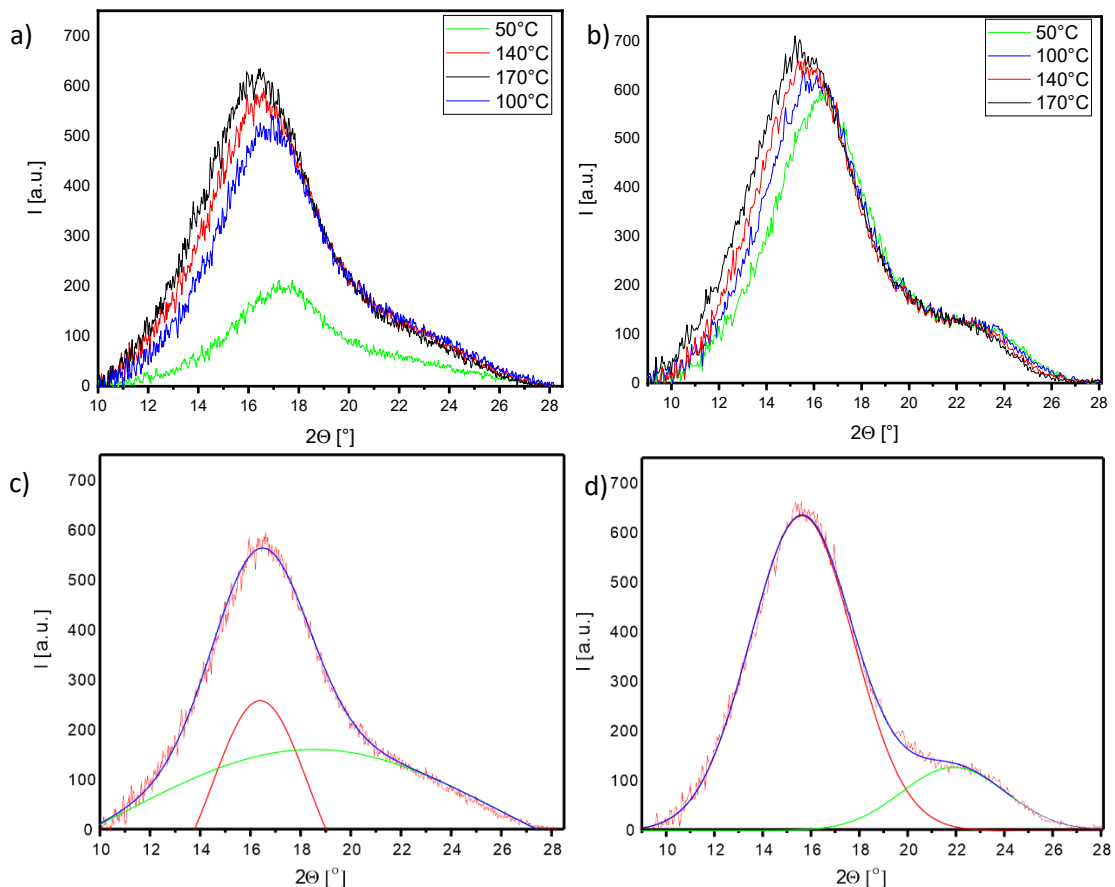


Figure S10. WAXS patterns of compounds a, c) **H8₂** and b, d) **F8₂** at the indicated temperatures with c, d) deconvolutions of the curves at 140°C into two scatterings.

Table S2. WAXS maxima of the LC phases of compounds **H8₂** and **F8₂**.

Comp.	T [°C]	2θ [°]	d [nm]
H8₂	170	16.399	0.541
	140	16.555	0.535
	100	16.866	0.526
	50	17.385	0.510
		18.511	0.479
F8₂	170	15.515	0.571
	140	15.711	0.564
	100	16.004	0.554
	50	16.370	0.541
		23.319	0.381

2.2.2. Additional SAXS patterns

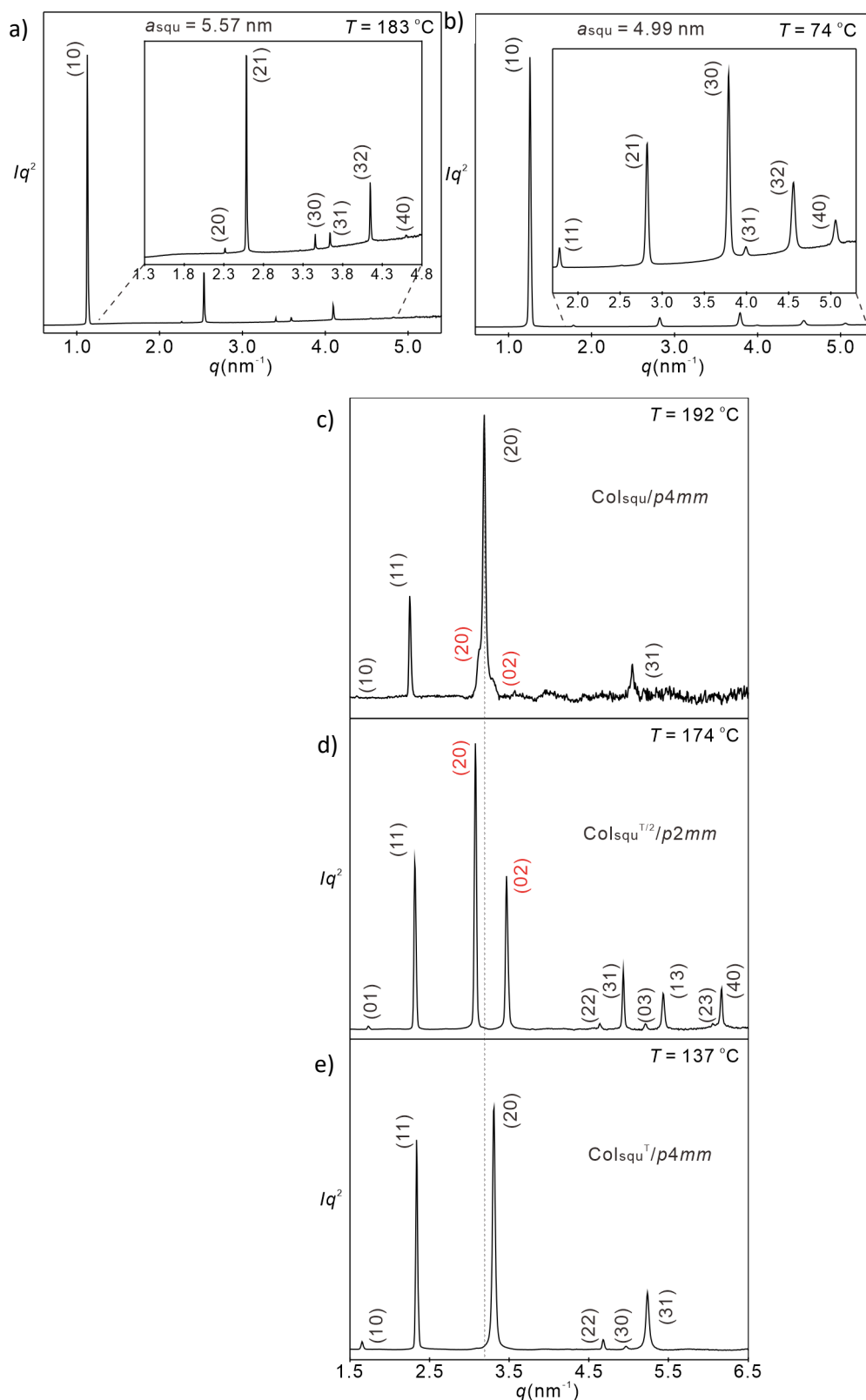


Figure S11. SAXS patterns a, b) of the square chessboard phases of **H8/14**, a) $\text{Col}_{\text{squ}}/p4mm^L$ phase at 183°C and b) $\text{Col}_{\text{squ}}^T/p4mm^L$ phase at 74°C , and c-e) the LC phases of **F8₂** as observed upon cooling; at 192°C a mixture of $p2mm$ and $p4mm$ can be observed.

2.2.3. Numerical SAXS data

Table S3. Experimental and calculated d -spacing of the observed SAXS reflection of the $\text{Col}_{\text{sq}}/p4gm$ phase of compound **H7/14** at $T = 169$ °C. All intensity values are Lorentz and multiplicity corrected.

(hk)	$d_{\text{obs.}}$ - spacings (nm)	$d_{\text{cal.}}$ - spacings (nm)	Intensity	Phase
(11)	5.71	5.71	100.0	0
(20)	4.04	4.04	14.3	0
(21)	3.61	3.61	9.8	π
(31)	2.55	2.55	10.3	0
(32)	2.23	2.24	0.7	/
(40)	2.01	2.02	0.6	/
(41)	1.95	1.96	1.8	/
(33)	1.90	1.90	1.2	/
(42)	1.80	1.81	0.2	/
(43)	1.61	1.62	2.6	/
(51)	1.58	1.58	0.9	/
(52)	1.49	1.50	1.1	/
(60)	1.34	1.35	1.6	/
(62)	1.27	1.28	0.5	/
$a = 8.07$ nm				

Table S4. Experimental and calculated d -spacing of the observed SAXS reflection of the $\text{Col}_{\text{sq}}^{\text{T}}/p4mm^{\text{L}}$ phase of compound **H7/14** at $T = 101$ °C. All intensity values are Lorentz and multiplicity corrected.

(hk)	$d_{\text{obs.}}$ - spacings (nm)	$d_{\text{cal.}}$ - spacings (nm)	Intensity	Phase
(10)	4.96	4.96	100.0	0
(11)	3.51	3.51	0.8	0
(21)	2.22	2.22	1.7	0
(30)	1.65	1.65	4.2	0
(32)	1.37	1.38	1.3	π
(40)	1.23	1.24	0.7	π
$a = 4.96$ nm				

Table S5. Experimental and calculated d -spacing of the observed SAXS reflection of the $\text{Col}_{\text{sq}}/p4mm^{\text{L}}$ phase of compound **H8/14** at $T = 183$ °C. All intensity values are Lorentz and multiplicity corrected.

(hk)	$d_{\text{obs.}}$ - spacings (nm)	$d_{\text{cal.}}$ - spacings (nm)	Intensity	Phase
(10)	5.57	5.56	100.0	0
(20)	2.77	2.78	0.4	/
(21)	2.48	2.49	9.6	0
(30)	1.85	1.85	0.8	π
(31)	1.75	1.76	0.8	π
(32)	1.53	1.54	3.0	π
(40)	1.38	1.39	0.3	π
$a = 5.57$ nm				

Table S6. Experimental and calculated d -spacing of the observed SAXS reflection of the $\text{Col}_{\text{rec}}/\text{p}2\text{mm}^{\text{L}}$ phase of compound **H8/14** at $T = 119$ °C. All intensity values are Lorentz and multiplicity corrected.

($h k$)	$d_{\text{obs.}}\text{- spacings}$ (nm)	$d_{\text{cal.}}\text{- spacings}$ (nm)	Intensity	Phase
(20)	5.22	5.20	100	π
(11)	4.71	4.69	0.3	π
(21)	3.67	3.70	0.7	π
(02)	2.61	2.63	0.3	π
(12)	2.56	2.55	0.04	/
(41)	2.32	2.33	5.0	π
(60)	1.73	1.73	7.0	π
(61)	1.64	1.64	0.4	0
(62)	1.44	1.45	4.0	0

$$a_{\text{rec}} = 10.39 \text{ nm } b_{\text{rec}} = 5.26 \text{ nm}$$

Table S7. Experimental and calculated d -spacing of the observed SAXS reflection of the $\text{Col}_{\text{squ}}/\text{p}4\text{mm}^{\text{L}}$ phase of compound **H8/14** at $T = 74$ °C. All intensity values are Lorentz and multiplicity corrected.

($h k$)	$d_{\text{obs.}}\text{- spacings}$ (nm)	$d_{\text{cal.}}\text{- spacings}$ (nm)	Intensity	Phase
(10)	4.99	4.99	100.0	0
(11)	3.53	3.53	0.6	0
(21)	2.23	2.23	2.2	0
(30)	1.66	1.66	7.1	0
(31)	1.57	1.58	0.2	/
(32)	1.38	1.38	1.7	π
(40)	1.24	1.25	1.2	π

$$a = 4.99 \text{ nm}$$

Table S8. Experimental and calculated d -spacing of the observed SAXS reflection of the $\text{Col}_{\text{squ}}/\text{p}4\text{mm}^{\text{L}}$ phase of compound **H8/16** at $T = 169$ °C. All intensity values are Lorentz and multiplicity corrected.

($h k$)	$d_{\text{obs.}}\text{- spacings}$ (nm)	$d_{\text{cal.}}\text{- spacings}$ (nm)	Intensity	Phase
(10)	5.55	5.55	100.0	0
(11)	3.92	3.92	0.8	0
(20)	2.77	2.77	0.8	π
(21)	2.48	2.48	4.1	0
(30)	1.84	1.85	1.7	π
(31)	1.75	1.75	0.6	π
(32)	1.53	1.54	1.2	π
(40)	1.38	1.39	0.7	π

$$a = 5.55 \text{ nm}$$

Table S9. Experimental and calculated d -spacing of the observed SAXS reflection of the $\text{Col}_{\text{squ}}^{\text{T}}/\text{p}4\text{mm}^{\text{L}}$ phase of compound **H8/16** at $T = 46$ °C. All intensity values are Lorentz and multiplicity corrected.

($h k$)	$d_{\text{obs.}}\text{- spacings}$ (nm)	$d_{\text{cal.}}\text{- spacings}$ (nm)	Intensity	Phase
(10)	5.02	5.02	100.0	0
(11)	3.55	3.55	0.1	0
(20)	2.50	2.51	0.1	π
(21)	2.24	2.24	1.7	0
(30)	1.67	1.67	5.1	π
(32)	1.38	1.39	0.4	π

$$a = 5.01 \text{ nm}$$

Table S10. Experimental and calculated d -spacing of the observed SAXS reflection of the $\text{Col}_{\text{sq}}/\text{p}4\text{mm}$ phase of compound **H8₂** at $T = 169$ °C. All intensity values are Lorentz and multiplicity corrected.

(<i>hk</i>)	$d_{\text{obs.}}$ - spacings (nm)	$d_{\text{cal.}}$ - spacings (nm)	Intensity	Phase
(10)	3.97	3.97	34.9	0
(11)	2.81	2.81	5.1	0
(20)	1.98	1.98	100.0	0
(21)	1.77	1.77	4.5	π
(22)	1.40	1.40	9.1	π
(30)	1.32	1.32	0.7	/
$a = 3.97$ nm				

Table S11. Experimental and calculated d -spacing of the observed SAXS reflection of the $\text{Col}_{\text{sq}}^{\text{T}}/\text{p}4\text{mm}$ phase of compound **H8₂** at $T = 83$ °C. All intensity values are Lorentz and multiplicity corrected.

(<i>hk</i>)	$d_{\text{obs.}}$ - spacings (nm)	$d_{\text{cal.}}$ - spacings (nm)	Intensity	Phase
(10)	3.78	3.77	56.7	0
(11)	2.67	2.66	39.7	0
(20)	1.88	1.88	100.0	0
(21)	1.6	1.68	0.2	π
(22)	1.33	1.33	31.5	π
$a = 3.77$ nm				

Table S12. Experimental and calculated d -spacing of the observed SAXS reflection of the $\text{Col}_{\text{sq}}/\text{p}4\text{gm}$ phase of compound **F7/14** at $T = 178$ °C. All intensity values are Lorentz and multiplicity corrected.

(<i>hk</i>)	$d_{\text{obs.}}$ - spacings (nm)	$d_{\text{cal.}}$ - spacings (nm)	Intensity	Phase
(11)	5.80	5.80	100.0	0
(20)	4.10	4.10	2.1	0
(21)	3.67	3.67	50.7	π
(22)	2.90	2.90	0.3	/
(31)	2.59	2.59	13.2	0
(32)	2.27	2.27	1.1	0
(40)	2.05	2.05	1.8	π
(41)	1.99	1.99	0.5	/
(33)	1.93	1.93	0.3	/
(42)	1.83	1.83	1.1	0
(43)	1.64	1.64	5.2	0
(52)	1.52	1.52	0.5	/
(53)	1.40	1.41	1.4	0
(60)	1.36	1.37	5.8	0
(62)	1.29	1.30	0.2	/
(54)	1.28	1.28	0.5	/
$a = 8.20$ nm				

Table S13. Experimental and calculated d -spacing of the observed SAXS reflection of the $\text{Col}_{\text{rec}}^{\text{T}2}/c2mm$ phase of compound **F7/14** at $T = 156$ °C. All intensity values are Lorentz and multiplicity corrected.

($h k$)	$d_{\text{obs.}}$ - spacings (nm)	$d_{\text{cal.}}$ - spacings (nm)	Intensity	Phase
(11)	4.84	4.83	100.0	0
(20)	4.05	4.05	4.4	π
(02)	3.01	3.01	16.2	π
(31)	2.47	2.46	1.5	0
(40)	2.02	2.03	0.2	/
(13)	1.95	1.95	0.3	/
(42)	1.68	1.68	0.1	/
(33)	1.61	1.61	2.2	π
(51)	1.56	1.56	1.1	0
(04)	1.50	1.51	0.5	/
(62)	1.23	1.23	0.8	/
(15)	1.19	1.19	2.2	0
$a_{\text{rec}} = 8.10 \text{ nm } b_{\text{rec}} = 6.02 \text{ nm}$				

Table S14. Experimental and calculated d -spacing of the observed SAXS reflection of the $\text{Col}_{\text{squ}}/\text{p}4\text{mm}^{\text{L}}$ + $\text{p}4\text{gm}$ phase of compound **F8/14** at $T = 189$ °C. All intensity values are Lorentz and multiplicity corrected.

($h k$)	$d_{\text{obs.}}$ - spacings (nm)	$d_{\text{cal.}}$ - spacings (nm)	Intensity	Phase
(11)	5.72	5.72	100.0	0
(10)	5.54	5.54	100	/
(20)	4.05	4.04	1.6	π
(11)	3.93	3.92	6.9	/
(21)	3.63	3.62	14.3	π
(22)	2.86	2.86	0.9	/
(31)	2.56	2.56	11.5	0
(21)	2.48	2.48	5.3	/
(32)	2.24	2.24	0.5	/
(41)	1.96	1.96	0.4	/
(33)	1.91	1.91	0.2	/
(42)	1.81	1.81	0.2	/
(43)	1.62	1.62	0.9	/
(51)	1.59	1.59	0.7	/
(52)	1.50	1.50	0.5	/
(53)	1.38	1.39	0.9	/
(60)	1.35	1.35	2.2	0
(61)	1.33	1.33	0.3	/
(62)	1.28	1.28	0.4	/
(63)	1.20	1.21	0.8	/
$a_{\text{p}4\text{gm}} = 8.09 \text{ nm}; a_{\text{p}4\text{mm}} = 5.54 \text{ nm}$				

Table S15. Experimental and calculated d -spacing of the observed SAXS reflection of the $\text{Col}_{\text{rec}}^{\text{T}2}/c2mm$ phase of compound **F8/14** at $T = 74$ °C. All intensity values are Lorentz and multiplicity corrected.

(hkl)	$d_{\text{obs.}}$ - spacings (nm)	$d_{\text{cal.}}$ - spacings (nm)	Intensity	Phase
(11)	4.88	4.88	100.0	0
(20)	3.93	3.93	6.8	π
(02)	3.11	3.11	10.6	π
(31)	2.41	2.41	6.5	0
(13)	2.00	2.00	0.2	/
(40)	1.96	1.97	0.1	/
(42)	1.66	1.66	0.3	/
(33)	1.62	1.63	5.8	π
(04)	1.55	1.56	0.2	/
(51)	1.52	1.52	2.3	0
(53)	1.25	1.25	0.05	/
(15)	1.22	1.23	2.0	0
(62)	1.20	1.21	3.6	0
$a_{\text{rec}} = 7.86$ nm $b_{\text{rec}} = 6.22$ nm				

Table S16. Experimental and calculated d -spacing of the observed SAXS reflection of the $\text{Col}_{\text{squ}}/p4mm^{\text{L}}$ phase of compound **F8/16** at $T = 192$ °C. All intensity values are Lorentz and multiplicity corrected.

(hk)	$d_{\text{obs.}}$ - spacings (nm)	$d_{\text{cal.}}$ - spacings (nm)	Intensity	Phase
(10)	5.62	5.62	100.0	0
(11)	3.98	3.97	11.6	π
(20)	2.81	2.81	0.1	/
(21)	2.51	2.51	5.3	0
(30)	1.87	1.87	1.0	π
(32)	1.56	1.56	1.5	π
(42)	1.25	1.26	1.2	π
$a_{\text{squ}} = 5.62$ nm				

Table S17. Experimental and calculated d -spacing of the observed SAXS reflection of the $\text{Col}_{\text{rec}}^{\text{T}2}/c2mm$ phase of compound **F8/16** at $T = 147$ °C. All intensity values are Lorentz and multiplicity corrected.

(hk)	$d_{\text{obs.}}$ - spacings (nm)	$d_{\text{cal.}}$ - spacings (nm)	Intensity	Phase
(11)	5.26	5.25	100.0	0
(20)	4.15	4.15	7.4	π
(02)	3.39	3.39	8.8	π
(22)	2.63	2.63	0.4	/
(31)	2.56	2.56	4.4	0
(13)	2.18	2.18	0.9	/
(33)	1.75	1.75	3.3	π
(51)	1.61	1.61	0.9	/
(15)	1.33	1.34	1.0	0
(62)	1.28	1.28	1.9	0
(71)	1.17	1.17	0.1	/
$a_{\text{rec}} = 8.30$ nm $b_{\text{rec}} = 6.78$ nm				

Table S18. Experimental and calculated d -spacing of the observed SAXS reflection of the $\text{Col}_{\text{rec}}^{\text{T}2}/p2mm$ phase of compound **F8₂** at $T = 174$ °C. All intensity values are Lorentz and multiplicity corrected.

(<i>hk</i>)	$d_{\text{obs.-}}$ spacings (nm)	$d_{\text{cal.-}}$ spacings (nm)	Intensity	Phase
(01)	3.63	3.62	0.7	0
(11)	2.71	2.71	28.6	0
(20)	2.04	2.05	100.0	0
(02)	1.81	1.81	61.0	0
(22)	1.36	1.36	0.8	π
(31)	1.27	1.28	9.0	π
(03)	1.21	1.21	1.8	0
(13)	1.16	1.16	7.7	π
(23)	1.04	1.04	0.6	π
(40)	1.02	1.02	11.5	0
$a_{\text{rec}} = 4.09 \text{ nm } b_{\text{rec}} = 3.62 \text{ nm}$				

Table S19. Experimental and calculated d -spacing of the observed SAXS reflection of the $\text{Col}_{\text{rec}}^{\text{T}}/p4mm$ phase of compound **F8₂** at $T = 137$ °C. All intensity values are Lorentz and multiplicity corrected.

(<i>hk</i>)	$d_{\text{obs.-}}$ spacings (nm)	$d_{\text{cal.-}}$ spacings (nm)	Intensity	Phase
(10)	3.80	3.80	2.0	0
(11)	2.69	2.69	54.5	0
(20)	1.90	1.90	100.0	0
(22)	1.34	1.34	2.8	0
(30)	1.26	1.27	1.0	π
(31)	1.20	1.20	13.7	π
$a = 3.80 \text{ nm}$				

2.2.4. Electron density maps

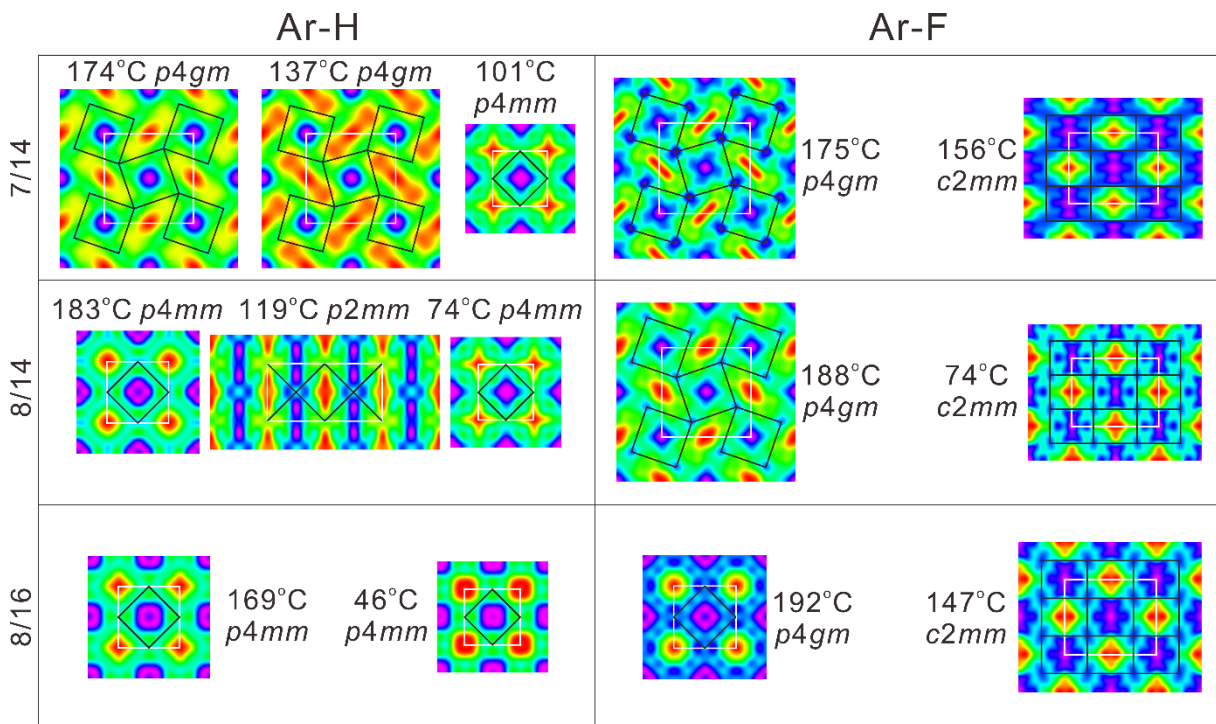


Figure S12. Representative ED maps of all investigated compounds **Hm/n** and **Fm/n** in their honeycomb LC phases, all representing two- or multicolor tilings with the noted plane groups.

2.2.5 SANS data

Table S20. Experimental and calculated *d*-spacing of the observed SANS reflection of the Col_{sq}/*p4gm* phase of compound **H7/14** at *T* = 174 °C. All intensity values are Lorentz and multiplicity corrected.

(<i>hk</i>)	<i>d</i> _{obs.-} spacings (nm)	<i>d</i> _{cal.-} spacings (nm)	Intensity	Phase
(11)	5.77	5.77	100.0	0
(20)	4.07	4.08	14.9	0
(21)	3.66	3.65	8.5	0
(31)	2.58	2.58	20.6	0
(32)	2.27	2.26	10.4	0
<i>a</i> = 8.16 nm				

Table S21. Scattering length density of **H7/14** for SAXS and SANS.

Components	SAXS	SANS
R _H chains	320	-32
OPE core	494	369
Glycerol end	516	119
R _F chains	686	509

2.2.6 Structural data

Table S22: Structural data of the LC phases of compounds **Hm/n**, **Fm/n**, **H8₂**, and **F8₂**. ^a

Comp.	T/°C (Phase)	a.b/nm	V _{mol;cr} /nm ³	V _{cell} /nm ³	n _{cell;cr}	n _{cell;liq}	n _{cell;LC}	n _{wall}
H7/14	169 (p4gm)	<i>a</i> = 8.08	2.39	29.36	12.29	9.66	10.98	1.4
	101 (p4mm ^{TL})	<i>a</i> = 4.96		11.07	4.63	3.64	4.14	1.0
H8/14	183 (p4gm)	<i>a</i> = 5.57	2.46	13.98	5.68	4.47	5.07	1.3
	119 (p2mm ^{TL})	<i>a</i> = 10.41		24.38	9.91	7.79	8.84	1.1
	74 (p4mm ^{TL})	<i>b</i> = 5.20		11.22	4.56	3.58	4.07	1.0
H8/16	169 (p4mm ^L)	<i>a</i> = 5.55	2.56	13.86	5.41	4.25	4.83	1.2
	46 (p4mm ^{TL})	<i>a</i> = 5.02		11.34	4.43	3.48	3.95	1.0
F7/14	178 (p4gm)	<i>a</i> = 8.20	2.44	30.18	12.37	9.72	11.05	1.4
	156 (c2mm ^{T/2})	<i>a</i> = 8.13		22.02	9.02	7.09	8.07	1.0
	<i>b</i> = 6.02							
F8/14	189 (p4mm ^L)	<i>a</i> = 5.54	2.51	13.81	5.50	4.32	4.91	1.2
	189 (p4gm)	<i>a</i> = 8.09		29.64	11.81	9.28	10.55	1.3
	156 (c2mm ^{T/2})	<i>a</i> = 8.17		23.63	9.41	7.40	8.41	1.1
	<i>b</i> = 6.43							
	74 (c2mm ^{T/2})	<i>a</i> = 7.86		22.00	8.76	6.89	7.83	1.0
F8/16	<i>b</i> = 6.22							
	192 (p4mm ^L)	<i>a</i> = 5.61	2.61	14.15	5.42	4.26	4.84	1.2
	146 (c2mm ^{T/2})	<i>a</i> = 8.32		25.33	9.70	7.63	8.67	1.1
	<i>b</i> = 6.77							
H8₂	169 (p4mm)	<i>a</i> = 3.98	2.56	7.13	2.79	2.19	2.49	1.2
	83 (p4mm ^T)	<i>a</i> = 3.76		6.36	2.48	1.96	2.22	1.1
F8₂	174 (p2mm ^{T/2})	<i>a</i> = 4.09	2.61	6.66	2.55	2.01	2.28	1.1
	<i>b</i> = 3.62							
	137 (p4mm ^T)	<i>a</i> = 3.78		6.43	2.46	1.94	2.20	1.1

^a V_{cell} = a_{squ}² * h (Col_{squ}); a_{rec} * b_{rec} * h (Col_{rec}) where h represents the height of the unit cell and is assumed to be 0.45 nm. V_{mol} = volume of the molecule as determined by the crystal volume increments.^{S1} n_{cell,cr} = number of molecules per unit cell in the crystalline state, calculated according to n_{cell,cr} = V_{cell}/V_{mol} (average packing coefficient in the crystal is *k* = 0.7). n_{cell,liq} = the number of molecules in the unit cell of an isotropic liquid with an average packing coefficient *k* = 0.55, calculated according to n_{cell,liq} = 0.55/0.7. n_{cell,LC} = number of molecules in the unit cell in the LC state as estimated from the average of n_{cell,cr} and n_{cell,Liq}^{S2}, n_{wall} = the number of molecules in the cross-section of the honeycomb walls, n_{wall} = $\frac{n_{cell,LC}}{2}$ for p4mm and p2mm cells, n_{wall} = $\frac{n_{cell,LC}}{4}$ for p4mm^L cells, n_{wall} = $\frac{n_{cell,LC}}{8}$ for p4gm, c2mm^L and p2mm^L cells.

2.2.7 Additional figures and discussion

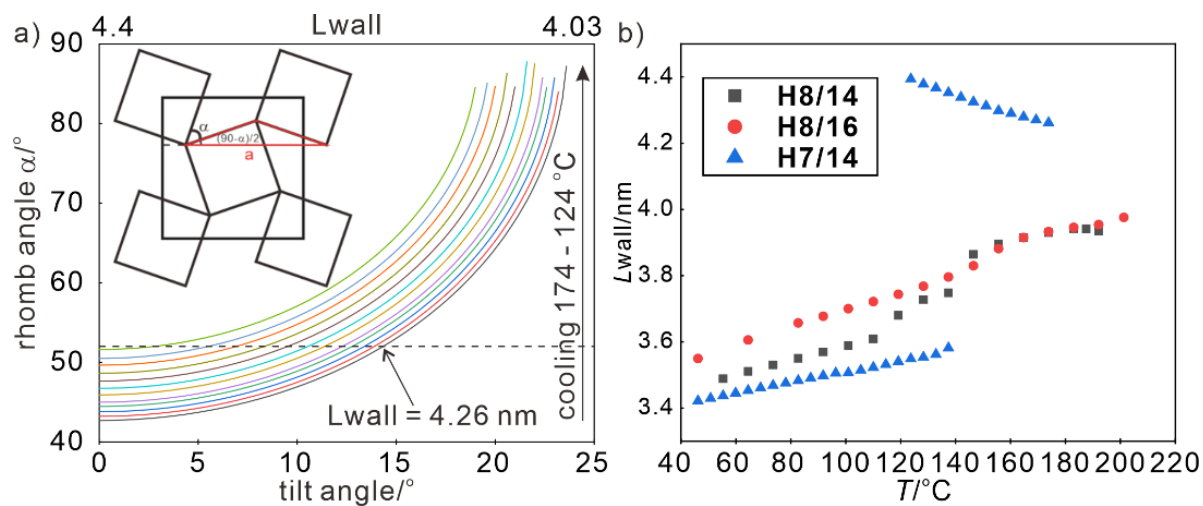


Figure S13. The $\text{Col}_{\text{rec}}^{\text{T}}/\text{p}4\text{gm}$ phase. a) Relation between tilt angle side length and rhombic angle depending on temperature for **H7/14**; inset: schematic showing the relations between L_{wall} and rhombic angle α and b) temperature dependence of aromatic wall length of compounds **Hm/n** upon cooling.



Figure S14. Space filling CPK models showing the complete space filling in a regular triangular cell with a hypothetical side length 4.3 nm and filled by one branched R_H chains with $n = 14$ from each molecule. Any reduction of a side length would cause a significant overcrowding of the triangular cell.

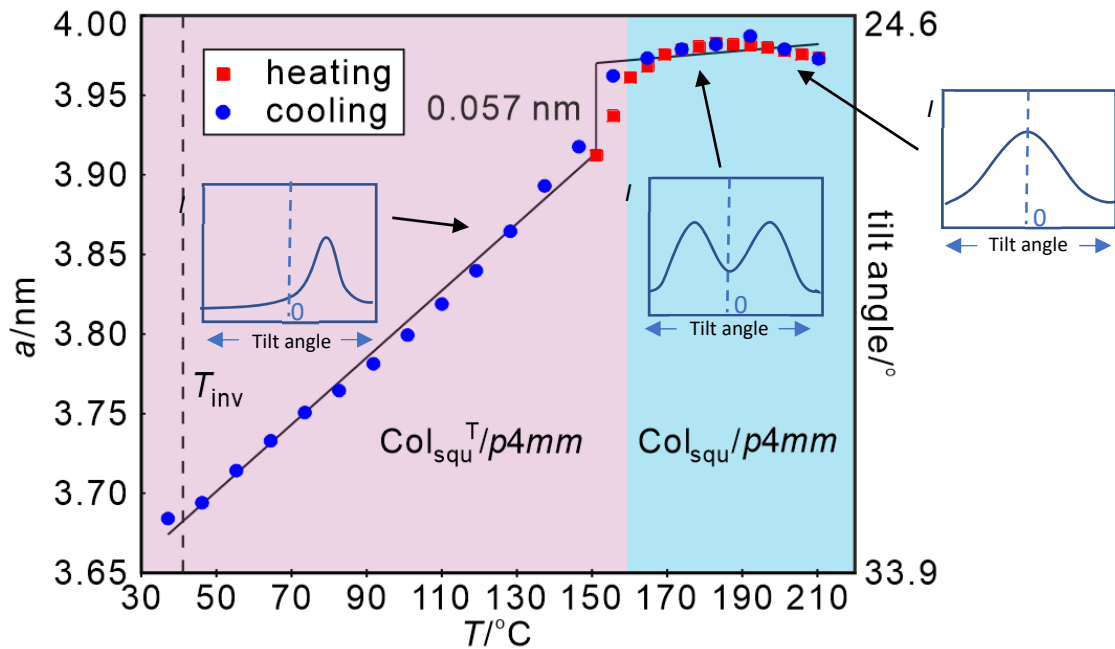


Figure S15. Schematic showing the development of the orientational order parameter distribution function depending on temperature, shown for **H8₂** as example.

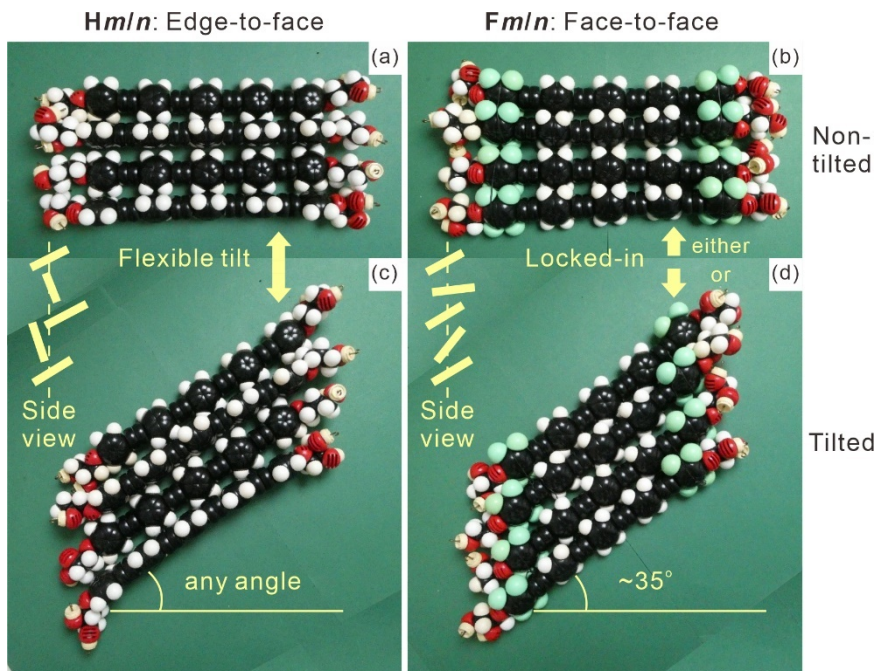


Figure S16: Effect of core-fluorination on the mode of core-packing in the honeycomb walls: (a, c) Non-fluorinated OPEs can easily rotate around their long axis and assume different modes of packing including the shown edge-to-face packing which allows any longitudinal shift, i.e. any tilt angle of the OPEs, while (b, d) the face-to-face packing of the fluorinated FOPEs allows either (b) a non-shifted packing of the fluorinated benzenes on top of each other without tilt, or alternatively, (d) a significant longitudinal shift allowing the fluorinated benzenes to be located on top of adjacent acetylene units, thus leading to a tilt around 30-50 ° (see also Fig. S17), but not any value other from it; in general any transversal shift competes with the desire of the polar glycerols to stay segregated from the polyaromatic cores. On the left sides of (c,d) the side-views on the walls along the rod-long axes are shown (view on the edges of individual benzene rings) in yellow color: (c) the almost free rotation or (d) the transversal

shift of the benzenes providing a tilt of the benzene rings with respect to the column direction, this retains a mean distance of about 0.45 nm for the unit cell height (h) along the c direction.

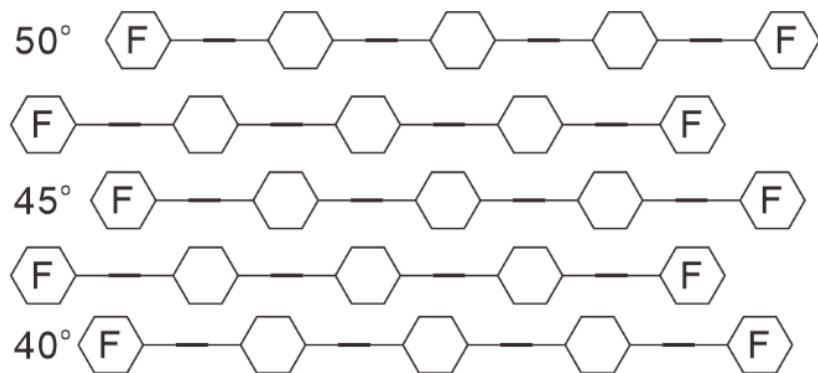


Figure S17. Tilt angles achieved with the different shift modes of the FOPE cores in a face-to-face stacking mode with Ar-F rings besides the triple bonds.



Figure S18. Space filling CPK models showing the organization in the square cells of a) compounds **H8₂** and b) **F8₂** and showing the development of sparsely packed space in the corners of the square cells; note that the restricted R_F chain length and their rigidity provide a significant limitation for the possible arrangements of the R_F segments; in the ED maps (Figs. 3f,h and 10c,e) the red low ED areas are located in the corners, while, as shown in a, b), the low ED oligomethylene spacers are fixed to the middle of the OPE cores and therefore cannot be located there; therefore, a significant contribution to reduced ED in the red dots is likely to result from the loose packing of the rigid R_F segments in the corners; c) shows a R_F filled square cell of **H8/16** with one molecule giving its R_H chain into the shell around the R_F core; the cell size is in all cases 4.0 nm. Note that the larger diameter of the R_F segments leads to a contribution of these units also to the space filling in the two neighboring 0.45 nm slices of the honeycomb, therefore, there is denser space filling than actually suggested by the shown models. Moreover, it must be considered that n_{wall} is somewhat larger ($n_{\text{wall}} = 1.1-1.2$, see Table S22) than in the actually shown structure with exactly one molecule in the wall cross section ($n_{\text{wall}} = 1.0$).

Discussion of the development of the side lengths in the rectangular cells of the *p2mm* phases of compounds **Fm/n**.

Reduction of the chain volume, by reduction of the alkyl chain length in **F8/14**, and in addition the R_F chain length in **F7/14**, reduces only the shorter parameter b_{rec} where the short (tilted) side length reaches

2.82 nm, corresponding to a large tilt angle of 50° for **F7/14** (Fig. 9a). There is only a small effect on the larger parameter a_{rec} of the non-tilted side, which is attributed to a changing order parameter. The shape of this curve indicates a slight increase of the side-length due to an increasing order parameter with lowering temperature between 180 and 160 °C, followed by a decrease due to a decreasing order parameter with growing tilt in the shorter walls. Increasing tilt along b_{rec} leads to a growing distance between the glycerols along the c -direction and this causes a reduction of the order parameter along a_{rec} , dominating below ~160 °C. In the high temperature range between 180 and 160 °C the increasing order parameter expands a_{rec} and requires a stronger increase of tilt along b_{rec} to reduce the cell area (Fig. 9a). Interestingly, upon cooling, the occupied area shrinks almost linearly with the same rate for all $c2mm$ phases of the series **Fm/n** (see dashed lines in Fig. 9b). For large enough side chain volume, and minor gap between prismatic cell volume and side chain volume, i.e. for compound **F8/16** (red symbols), the $p4mm^L$ phase can be found at high temperature with a minor jump of normalized lattice area (unit cell area divided by the number of honeycomb walls per unit cell) from 7.9 to 7.4 nm². For insufficient side-chain volume and different volumes of R_H and R_F chains (compound **F7/14**, blue symbols) the $p4gm$ phase is preferred. In contrast to the $c2mm$ lattice, the $p4gm$ lattice grows on cooling because the chain volume shrinkage is in this phase compensated by increasing n_{wall} . With the onset of out-of-plane tilt n_{wall} decreases suddenly from ~1.4 to ~1.2 at the $p4gm$ - $c2mm$ transition, giving rise to the large jump of the normalized lattice area from 8.5 to 6.2 nm². At high temperature, side chain volume expansion pushes the frustrated $p4gm$ phase to $p4mm^L$ phase, which decreases the normalized lattice area and exhibits an opposite trend compared with $c2mm$ phase.

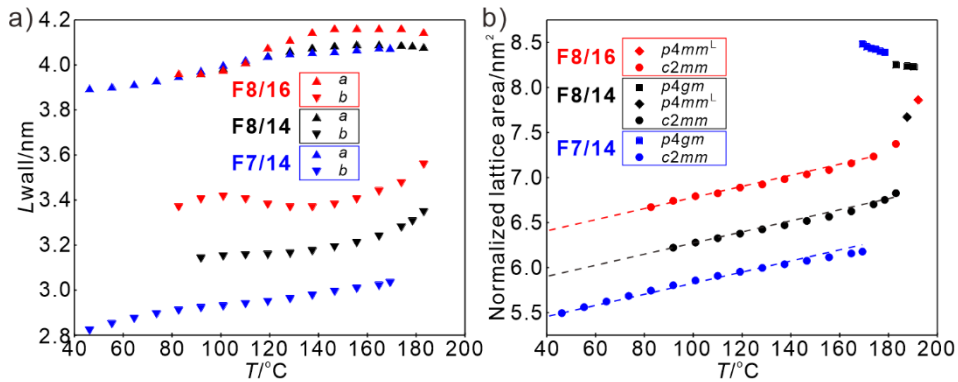
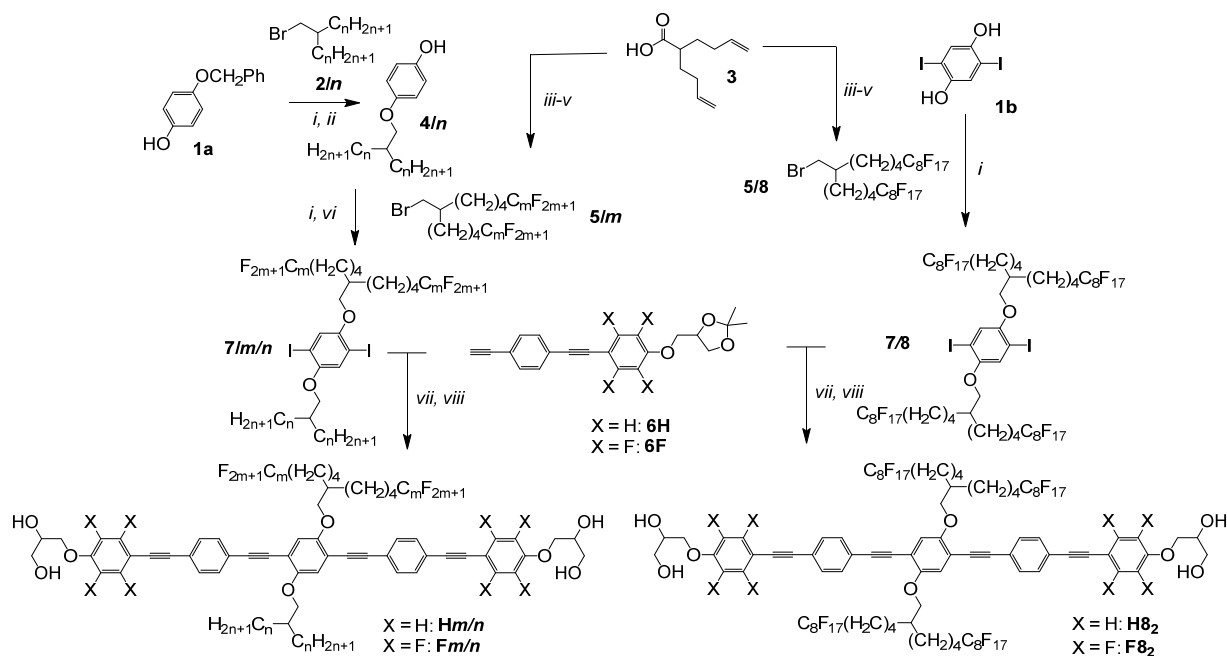


Figure S19: a) Temperature dependence of aromatic wall length in the temperature ranges of the $c2mm$ phases of **F8/16** (red), **F8/14** (black) and **F7/14** (blue) upon cooling and b) temperature dependence of the normalized lattice area of $p4mm$ (diamond), $p4gm$ (square) and $c2mm$ (circle) which is calculated by A_{cell}/N_{cell} , where A_{cell} is unit cell area and N_{cell} is the number of aromatic wall per unit cell, 2 for $p4mm$ and $c2mm$ phase; 4 for $p4gm$ phase. The M phase of **F7/14** is cancelled probably due to the relatively fast and continuous cooling in capillary.

3. Synthesis and analytical data

3.1. General

The preparation of the compounds is outlined in Scheme S1. The synthesis of compounds **H_m/8₂** and **F_m/8₂** with two identical fluorinated side-chains was conducted in an analogous way as reported for compounds **H_n** by alkylation of 2,6-diiodohydroquinone with the branched semiperfluorinated alkyl bromide **5/8^{S3}**, followed by Sonogashira coupling^{S4} with two equivalents of **6H** or **6F**, and deprotection of the glycerol groups (see Scheme 1, right side).^{S5} The syntheses of the tolane based building blocks **6H** and **6F** have been reported previously,^{S5} and the synthesis of **5/8** was conducted as reported in ref.^{S6}. The synthesis strategy to compounds **H_{m/n}** and **F_{m/n}** with different side-chains is shown at the left side of Scheme 1: Here monoalkylation of 4-benzyloxyphenol (**1a**) with the branched alkyl bromide **2/n**^{S5} followed by hydrogenolysis of the benzyl group leads to the hydroquinone monoethers **4/n**.^{S7} Alkylation with **5/m** and iodination^{S8} yielded the 2,6-diiodohydroquinone diethers **7/m/n**, which were coupled in a Sonogashira cross-coupling reaction^{S4} with **6H** or **6F**, followed by acidolytic deprotection of the acetonide protecting groups^{S9} leading to compounds **H_{m/n}** and **F_{m/n}**.



Scheme S1. Synthesis of compounds **H_{m/n}**, **F_{m/n}**, **H8₂** and **F8₂**. Reagents and conditions: *i*: K₂CO₃, Bu₄N⁺I⁻, DMF, 80 °C, 3d; *ii*: H₂, Pd⁰ (10% on charcoal) dioxane, 50 °C, 1d; *iii*: I-C_mF_{2m+1}, Pd[PPh₃]₄, *n*-hexane, 25 °C, 2 weeks; *iv*: LiAlH₄, Et₂O, 40 °C, 1d; *v*: Bu₄N⁺Br⁻, DDQ, PPh₃, CH₂Cl₂, 25 °C, 1d; *vi*: PhI(OCOCF₃)₂, I₂, CH₂Cl₂, 50 °C, 1d; *vii*: Pd[PPh₃]₄, CuI, Et₃N, 80 °C, 1d; *viii*: Py⁺TosO⁻, MeOH / THF, 50 °C, 1d.

The compound numbers are given in Scheme S1. 4-Benzyloxyphenol (**1a**), LiAlH₄, tetrabutylammonium bromide (TBABr), triphenylphosphine, (bis(trifluoroacetoxy)iodo)-benzene, (PhI(OCOCF₃)₂), 2,3-dichloro-5,6-dicyano-1,4-benzoquinone (DDQ), CuI and pyridinium-*p*-toluenesulfonate (PPTS) were obtained from Sigma-Aldrich. 2,5-Diiodohydroquinone (**1b**) and iodine were obtained from ABCR. Pd(PPh₃)₄ was purchased from

TCI Chemicals, 1,1,1,2,2,3,3,4,4,5,5,6,6,7,7-pentadecafluoro-7-iodoheptane and 1,1,1,2,2,3,3,4,4,5,5,-6,6,7,7,8,8-heptadecafluoro-8-iodooctane from APOLLO SCIENTIFIC. These compounds were used as received. Triethylamine was distilled from CaH₂ and stored over the molecular sieve. The synthesis of the isopropylidene functionalized bistolane derivatives **6H** and **6F**, and the branched alkylbromides **2n** was reported previously.^{S5} 2-(But-3-en-1-yl)hex-5-enoic acid **3** was prepared as reported in ref.^{S10}

All compounds were synthesized from racemic *rac*-1,2-*O*-isopropylidene glycerol and therefore **Hm/n**, **Fm/n**, **H8₂**, and **F8₂** represent racemic mixtures of diastereomers.

Column chromatography was performed with silica gel 60 (0.063-0.2, Merck), and flash-chromatography with silica gel 60 (0.040-0.063, Merck). The purity of all compounds was checked by thin-layer chromatography (TLC, silica gel 60 F254, Merck).

¹H-, ¹³C-NMR spectra (Varian Unity 500 and Varian Unity 400 spectrometers) were recorded in CDCl₃ or THF-d₈ solutions, with tetramethylsilane as the internal standard for ¹H- and ¹³C-NMR and CFCl₃ as standard for ¹⁹F-NMR. All measurements were operated at 27 °C. Mass spectra were recorded with a Bruker HR-ESI-TOF. The measurements were performed in THF (1 mg/mL) with 0.1 mg/mL LiCl.

3.2 Synthesis of intermediates

3.2.1 Branched semiperfluorinated alcohols **5OH/m**^{S3}

A solution of 2-(but-3-en-1-yl)hex-5-enoic acid **3** (1 eq) in dry hexane (5 mL / mmol **3**) is purged with argon for 5 minutes. After the addition of the perfluoroalkyl iodide (2 eq), Pd(PPh₃)₄ (5 mol%) was added and the suspension was stirred for 2 weeks at room temperature. After this the mixture was filtered through silica gel and the residue was washed with Et₂O (150 mL). The solvent was removed under reduced pressure and the residue was taken up in dry Et₂O (50 mL). This solution was added dropwise to a solution of LiAlH₄ (3 eq) in dry Et₂O (50 mL) followed by heating the suspension to reflux for an additional 6 h. After the reaction is completed the suspension is cooled to room temperature and unreacted LiAlH₄ was hydrolyzed by careful addition of water. Then 30% aqueous H₂SO₄ (20 mL) was added to dissolve all precipitated solids. The organic layer was separated and the aqueous layer was extracted with Et₂O (3x 50 mL). The combined organic layers were washed with 10% Na₂S₂O₃ until the aqueous layer remained colorless. After washing with water (2x 100 mL) and brine (100 mL), the solution was dried over Mg₂SO₄, and the solvent was removed under reduced pressure. The crude product was purified by column chromatography.

7,7,8,8,9,9,10,10,11,11,12,12,13,13,13-Pentadecafluoro-2-(5,5,6,6,7,7,8,8,9,9,10,10,11,11,-11-pentadecafluoroundecyl)tridecan-1-ol 5OH/7: Synthesized form **3** (3.9 g, 17.9 mmol), 1,1,1,2,2,3,3,4,4,5,5,6,6,7,7-pentadecafluoro-7-iodoheptane (19.6 g, 39.4 mmol), with Pd(Ph₃)₄ as catalyst (1.1 g, 1.0 mmol) and LiAlH₄ (2.4 g, 59.1 mmol) as reducing agent, purification by column chromatography (eluent: CHCl₃); solid, C₂₄H₂₀F₃₀O, M = 894.38 g/mol, yield: 612.3 g (70 %), mp.: 50 °C, ¹H- NMR (CDCl₃, 500 MHz): δ / ppm = 3.57 (d, ³J_{H,H} = 5.4 Hz, 2H, -OCH₂-), 2.14 – 2.01 (m, 4H, -CH₂CF₂-), 1.68 – 1.57 (m, 4H, -CH₂CH₂CF₂-), 1.55 – 1.47 (m, 1H -CH-), 1.47 – 1.28 (m, 8H, -CH₂-). ¹⁹F-NMR (CDCl₃, 470 MHz): δ / ppm = -80.86 (m, 6F,

-CF₃), -114.44 (m, 4F, -CF₂-), -121.81 (m, 4F, -CF₂-), -122.13 (m, 4F, -CF₂-), -122.79 (m, 4F, -CF₂-), -123.59 (m, 4F, -CF₂-), -126.18 (m, 4F, -CF₂-).

7,7,8,8,9,9,10,10,11,11,12,12,13,13,14,14,14-Heptadecafluoro-2-(5,5,6,6,7,7,8,8,9,9,10,10,-11,11,-12,12,12-heptadecafluorododecyl)tetradecan-1-ol 5OH/8: Synthesized from **3** (3.0 g, 15.3 mmol), 1,1,1,2,2,3,3,4,4,5,5,6,6,7,7,8,8-heptadecafluoro-8-iodooctane (16.7 g, 30.6 mmol), with Pd(Ph₃)₄ as catalyst (0.9 g, 0.8 mmol) and LiAlH₄ (1.7 g, 45.9 mmol), purification by column chromatography (eluent: CHCl₃); solid, C₂₆H₂₀F₃₄O, M = 994.39 g/mol, yield: 6.7 g (44 %), mp.: 69 °C, **¹H-NMR** (CDCl₃, 400 MHz): δ / ppm = 3.59 (d, ³J_{H,H} = 5.4 Hz, 2H, -OCH₂-), 2.16 – 1.97 (m, 4H, -CH₂CF₂-), 1.67 – 1.57 (m, 4H, -CH₂CH₂CF₂-), 1.56 – 1.50 (m, 1H -CH-), 1.49 – 1.24 (m, 8H, -CH₂-). **¹⁹F-NMR** (CDCl₃, 376 MHz): δ / ppm = -80.91 (m, 6F, -CF₃), -114.45 (m, 4F, -CF₂-), -121.63 – -122.19 (m, 12F, -CF₂-), -122.80 (m, 4F, -CF₂-), -123.60 (m, 4F, -CF₂-), -126.13 (m, 4F, -CF₂-).

3.2.2 Branched semiperfluorinated alkyl bromides **5/m**^{S6}

DDQ (1.2 eq), and PPh₃ (1.2 eq) were solved in dry CH₂Cl₂ (2 mL / mmol **5OH/m**). TBABr (1.2 eq) solved in dry CH₂Cl₂ (1 mL / mmol **5OH/m**) was added to the suspension. Afterward, the semiperfluorinated alcohol **5OH/m** was dissolved in dry CH₂Cl₂ (1 mL / mmol) and added to the suspension. The reaction is stirred for 1 day at room temperature. When the reaction is completed the solvent is distilled off in a vacuum. The residue is taken up in hot hexane, filtered through silica gel (3x 75 mL) and the crude product is purified by column chromatography.

12-Bromomethyl-1,1,1,2,2,3,3,4,4,5,5,6,6,7,7,17,17,18,18,19,19,20,20,21,21,22,22,23,23,-23-triacontafluorotricosane 5/7: Synthesized from **5OH/7** (6.1 g, 6.9 mmol), DDQ (1.9 g, 8.2 mmol), PPh₃ (2.2 g, 8.2 mmol), TBABr (2.7 g, 8.2 mmol), purified by column chromatography (eluent: *n*-hexane), solid, C₂₄H₁₉BrF₃₀, M = 957.27 g/mol, yield: 5.1 g (77%), mp.: 40 °C, **¹H-NMR** (CDCl₃, 400 MHz): δ / ppm = 3.44 (d, ³J_{H,H} = 4.6 Hz, 2H, -BrCH₂-), 2.16 – 1.99 (m, 4H, -CH₂CF₂-), 1.71 – 1.56 (m, 5H, -CH₂CH₂CF₂-, -CH-), 1.51 – 1.30 (m, 8H, -CH₂-). **¹⁹F-NMR** (CDCl₃, 376 MHz): δ / ppm = -80.94 (m, 6F, -CF₃), -114.18 – -114.84 (m, 4F, -CF₂-), -121.85 (m, 4F, -CF₂-), -122.19 (m, 4F, -CF₂-), -122.87 (m, 4F, -CF₂-), -123.63 (m, 4F, -CF₂-), -126.29 (m, 4F, -CF₂-).

13-Bromomethyl-1,1,1,2,2,3,3,4,4,5,5,6,6,7,7,8,8,18,18,19,19,20,20,21,21,22,22,23,23,-24,24,25,25,25-tetratriacontafluoropentacosane 5/8: Synthesized from **5OH/8** (3.8 g, 3.8 mmol), DDQ (1.0 g, 4.2 mmol), PPh₃ (1.1 g, 4.2 mmol), TBABr (1.4 g, 4.2 mmol), purified by column chromatography (eluent: *n*-hexane), solid, C₂₄H₁₉BrF₃₄, M = 1057.29 g/mol, yield: 5.1 g (77%) mp.: 52 °C, **¹H-NMR** (CDCl₃, 400 MHz): δ / ppm = 3.44 (d, ³J_{H,H} = 4.6 Hz, 2H, -BrCH₂-), 2.18 – 1.98 (m, 4H, -CH₂CF₂-), 1.72 – 1.56 (m, 5H, -CH₂CH₂CF₂-, -CH-), 1.51 – 1.31 (m, 8H, -CH₂-). **¹⁹F-NMR** (CDCl₃, 376 MHz): δ / ppm = -80.81 (m, 6F, -CF₃), -114.02 – -114.79 (m, 4F, -CF₂-), -121.14 – -122.28 (m, 12F, -CF₂-), -122.76 (m, 4F, -CF₂-), -123.53 (m, 4F, -CF₂-), -126.16 (m, 4F, -CF₂-).

3.2.3 Synthesis of the 1-alkyloxy-4-benzyloxybenzenes (**4Bz/n**)

A mixture of 4-benzyloxyphenol **1a** (1 equ.), the branched alkylbromide **2/n** (1 equ.), K_2CO_3 (2.5 equ.), and Bu_4NI (tip of a spatula) in anhydrous DMF (10 mL/ mmol **1a**) was stirred at 80 °C for 3 days. After cooling to room temperature, the reaction was quenched with water (10 mL / 10 mL DMF), and the aqueous layer was extracted with Et_2O (3x50 mL). The combined organic layers were washed with saturated aq. $LiCl$, water, and brine. After drying over anhydrous Na_2SO_4 , filtration, and solvent evaporation, the crude product was purified by column chromatography.

1-Benzyl-4-(2-tetradec-1-ylhexadec-1-yloxy)benzene (4Bz/14**):** Synthesized from **2/14** (5.0 g, 10.0 mmol), **1a** (2.0 g, 10.0 mmol), K_2CO_3 (3.5 g, 25.0 mmol), TBAI (0.3 g, 0.8 mmol), purified by column chromatography (eluent: $CHCl_3$ / *n*-hexane (1:1)), solid, $C_{43}H_{72}O_2$, M = 621.05 g/mol; yield: 3.6 g (58 %), mp.: 46 °C, **1H-NMR** ($CDCl_3$, 400 MHz): δ / ppm = 7.49 – 7.28 (m, 5H, Aryl-*H*), 6.95 – 6.86 (m, 2H, Aryl-*H*), 6.86 – 6.78 (m, 2H, Aryl-*H*), 5.02 (s, 2H, - OCH_2 -), 3.77 (d, $^3J_{H,H}$ = 5.8 Hz, 2H, - OCH_2 -), 1.81 – 1.68 (m, 1H, - CH -), 1.56 – 1.19 (m, 52H, - CH_2 -), 0.89 (t, $^3J_{H,H}$ = 7.1 Hz, 6H, - CH_3).

1-Benzyl-4-(2-hexadec-1-yloctadec-1-yloxy)benzene (4Bz/16**):** Synthesized from **2/16** (5.6 g, 10.0 mmol), **1a** (2.0 g, 10.0 mmol), K_2CO_3 (3.5 g, 25.0 mmol), TBAI (0.3 g, 0.8 mmol), purified by column chromatography (eluent: $CHCl_3$ / *n*-hexane (1:1)), solid, $C_{47}H_{80}O_2$, M = 677.16 g/mol; yield: 3.5 g (52 %), mp.: 40 °C, **1H-NMR** ($CDCl_3$, 400 MHz): δ / ppm = 7.47 – 7.27 (m, 5H, Aryl-*H*), 6.92 – 6.86 (2H, m, Aryl-*H*), 6.86 – 6.79 (2H, m Aryl-*H*), 5.01 (2H, s, - OCH_2 -), 3.77 (2H, d, $^3J_{H,H}$ = 5.7 Hz, - OCH_2 -), 1.80 – 1.66 (1H, m, - CH -), 1.38 – 1.19 (60H, m, - CH_2 -), 0.88 (6H, t, $^3J_{H,H}$ = 6.8 Hz, - CH_3).

3.2.4 Synthesis of the hydroquinone monoethers **4/n**

A mixture of **4Bz/n** (1 equ.), $Pd(OH)_2$ on activated carbon (20 w%) is placed in a 2-neck flask in anhydrous 1,4-dioxane (5 mL/ mmol phenol) and stirred at room temperature for 1 day under a hydrogen atmosphere. After the reaction is completed, the suspension is filtered and the solvent is distilled off under reduced pressure. The crude product was purified by column chromatography.

4-(2-Tetradec-1-ylhexadec-1-yloxy)phenol **4/14:** Synthesized from **4Bz/14** (3.6 g, 5.9 mmol), purified by column chromatography (eluent: $CHCl_3$), solid, $C_{36}H_{66}O_2$, M = 530.92 g/mol; yield: 2.1 g (67 %), mp.: 40 °C, **1H-NMR** ($CDCl_3$, 400 MHz): δ / ppm = 6.82 – 6.70 (m, 4H, Aryl-*H*), 3.76 (d, $^3J_{H,H}$ = 5.7 Hz, 2H, - OCH_2 -), 1.78 – 1.69 (m, 1H, - CH -), 1.48 – 1.20 (m, 52H, - CH_2 -), 0.88 (t, $^3J_{H,H}$ = 6.7 Hz, 6H, - CH_3).

4-(2-Hexadec-1-yloctadec-1-yloxy)phenol **4/16:** Synthesized from **4Bz/16** (3.5 g, 5.2 mmol) purified by column chromatography (eluent: $CHCl_3$), solid, $C_{40}H_{74}O_2$, M = 587.03 g/mol; yield: 2.0 g (65 %), mp.: 55 °C, **1H-NMR** ($CDCl_3$, 400 MHz): δ / ppm = 6.81 – 6.71 (m, 4H, Aryl-*H*), 3.75 (d, $^3J_{H,H}$ = 5.7 Hz), 2H, - OCH_2 -), 1.81 – 1.68 (m, 1H, - CH -), 1.50 – 1.11 (m, 60H, - CH_2 -), 0.89 (t, $^3J_{H,H}$ = 7.2 Hz, 6H, - CH_3).

3.2.5 Synthesis of the hydroquinone diethers **4/m/n**

A mixture of **4/n** (1 equ.), the branched semifluorinated alkylbromide **5/m** (1.1 equ.), K₂CO₃ (5 equ.), and Bu₄NI (tip of a spatula) in anhydrous DMF (10 mL/ mmol **4/n**) was stirred at 80 °C for 3 days. After cooling to room temperature, the reaction was quenched with water (10 mL / 10 mL DMF), and the aqueous layer was extracted with Et₂O (3x50 mL). The combined organic layers were washed with saturated aq. LiCl, water, and brine. After drying over anhydrous Na₂SO₄, filtration, and solvent evaporation (850 mbar, 60 °C), the crude product was purified by column chromatography.

1-[7,7,8,8,9,9,10,10,11,11,12,12,13,13,13-Pentadecafluoro-2-(5,5,6,6,7,7,8,8,9,9,10,10,-11,11,11-pentadecafluoroundec-1-yl)tridec-1-yloxy]-4-(2-tetradec-1-ylhexadec-1-yloxy)benzene 4/7/14: Synthesized from **4/14** (2.1 g, 4.0 mmol), **2/7** (4.2 g, 4.4 mmol), K₂CO₃ (2.7 g, 19.8 mmol), TBAI (0.3 g, 0.8 mmol), purified by column chromatography (eluent: CHCl₃ / *n*-hexane (1:9)), solid, C₆₀H₈₄F₃₀O₂, M = 1407.28 g/mol; yield: 2.6 g (54 %), mp.: 44 °C, **¹H-NMR** (CDCl₃, 400 MHz): δ / ppm = 6.86 – 6.78 (m, 4H, Aryl-H), 3.78 (dd, ²J_{H,H} = 7.8, ³J_{H,H} = 5.6 Hz, 4H, -OCH₂-), 2.16 – 1.99 (m, 4H, -CH₂CF₂-), 1.84 – 1.68 (m, 2H, -CH-), 1.69 – 1.57 (m, 4H, -CH₂CH₂CF₂-), 1.52 – 1.22 (m, 60H, -CH₂-), 0.88 (t, ³J_{H,H} = 7.1 Hz, 6H, -CH₃). **¹⁹F-NMR** (CDCl₃, 376 MHz): δ / ppm = -80.87 (m, 6F, -CF₃), -114.35 (m, 4F, -CF₂-), -121.78 (m, 4F, -CF₂-), -122.11 (m, 4F, -CF₂-), -122.77 (m, 4F, -CF₂-), -123.55 (m, 4F, -CF₂-), -126.13 (m, 4F, -CF₂-).

1-[7,7,8,8,9,9,10,10,11,11,12,12,13,13,14,14-Heptadecafluoro-2-(5,5,6,6,7,7,8,8,9,9,-10,10,11,11,12,12,12-heptadecafluorododec-1-yl)tetradec-1-yloxy]-4-(2-tetradec-1-ylhexadec-1-yloxy)benzene 4/8/14: Synthesized from **4/14** (1.1 g, 2.1 mmol), **2/8** (2.4 g, 2.3 mmol), K₂CO₃ (1.4 g, 10.4 mmol), TBAI (0.3 g, 0.8 mmol), purified by column chromatography (eluent: CHCl₃ / *n*-hexane (1:9)), solid, C₆₂H₈₄F₃₄O₂, M = 1507.30 g/mol; yield: 0.6 g (40 %), mp.: 50 °C, **¹H-NMR** (CDCl₃, 400 MHz): δ / ppm = 6.85 – 6.77 (m, 4H, Aryl-H), 3.78 (dd, ²J_{H,H} = 7.9, ³J_{H,H} = 5.6 Hz, 4H, -OCH₂-), 2.16 – 1.95 (m, 4H, -CH₂CF₂-), 1.84 – 1.70 (m, 2H, -CH-), 1.70 – 1.58 (m, 4H, -CH₂CH₂CF₂-), 1.56 – 1.17 (m, 60H, -CH₂-), 0.88 (t, ³J_{H,H} = 6.7 Hz, 6H, -CH₃). **¹⁹F-NMR** (CDCl₃, 376 MHz): δ / ppm = -80.81 (m, 6F, -CF₃), -114.32 (m, 4F, -CF₂-), -121.55 – -122.10 (m, 12F, -CF₂-), -122.73 (m, 4F, -CF₂-), -123.53 (m, 4F, -CF₂-), -126.12 (m, 4F, -CF₂-).

1-[7,7,8,8,9,9,10,10,11,11,12,12,13,13,14,14-Heptadecafluoro-2-(5,5,6,6,7,7,8,8,9,9,-10,10,11,11,12,12,12-heptadecafluorododec-1-yl)tetradec-1-yloxy]-4-(2-hexadec-1-yloctadec-1-yloxy)benzene 4/8/16: Synthesized from **4/16** (0.6 g, 1.0 mmol), **2/8** (1.1 g, 1.1 mmol), K₂CO₃ (0.6 g, 4.2 mmol), TBAI (0.3 g, 0.8 mmol), purified by column chromatography (eluent: CHCl₃ / *n*-hexane (1:9)), solid, C₆₆H₉₂F₃₄O₂, M = 1563.41 g/mol; yield: 1.0 g (77 %), mp.: 42 °C, **¹H-NMR** (CDCl₃, 400 MHz): δ / ppm = 6.91 – 6.72 (m, 4H, Aryl-H), 3.78 (dd, ²J_{H,H} = 7.7, ³J_{H,H} = 5.6 Hz, 4H, -OCH₂-), 2.17 – 1.96 (m, 4H, -CH₂CF₂-), 1.85 – 1.70 (m, 1H, -CH-), 1.68 – 1.59 (m, 4H, -CH₂CH₂CF₂-), 1.54 – 1.48 (m, 1H, -CH-), 1.48 – 1.20 (m, 68H, -CH₂-), 0.88 (t, ³J_{H,H} = 7.0 Hz, 6H, -CH₃). **¹⁹F-NMR** (CDCl₃, 376 MHz): δ / ppm = -80.77 – -80.91 (m, 6F, -CF₃), -114.35 (m, 4F, -CF₂-), -121.50 – -122.18 (m, 12F, -CF₂-), -122.77 (m, 4F, -CF₂-), -123.55 (m, 4F, -CF₂-), -126.15 (m, 4F, -CF₂-).

3.2.6 Synthesis of the 2,6-diiodohydroquinone diether with two semiperfluorinated side-chains 7/m

1,4-Bis[7,7,8,8,9,9,10,10,11,11,12,12,13,13,14,14,14-heptadecafluoro-2-(5,5,6,6,7,7,8,8,-9,9,10,10,11,11,12,12,12-heptadecafluorododecyl)tetradec-1-yloxy]-2,5-diido-benzene 7/8: A mixture of **1b** (1 equ., 0.2 g, 0.5 mmol), **5/8** (2.2 equ., 1.3 g, 1.2 mmol), K₂CO₃ (10 equ.), and Bu₄NI (tip of a spatula) in anhydrous DMF (10 mL / 1 mmol **1b**) was stirred at 80 °C for 3 days. After cooling to room temperature, the reaction was quenched with water (10 mL / 10 mL DMF), and the aqueous layer was extracted with Et₂O (3x50 mL). The combined organic layers were washed with saturated aq. LiCl, water, and brine. After drying over anhydrous Na₂SO₄, filtration, and evaporation of the solvent, the crude product was purified by column chromatography (eluent: *n*-hexane); colorless liquid C₅₈H₄₀F₆₈I₂O₂, M = 2314.66 g/mol, yield: 600 g (50%), mp.: 86 °C, ¹H-NMR (CDCl₃, 400 MHz): δ / ppm = 7.15 (s, 2H, Aryl-H), 3.83 (d, ³J_{H,H} = 5.1 Hz, 4H, -OCH₂-), 2.16 – 1.99 (m, 8H, -CH₂CF₂-), 1.83 (s, 2H, -CH-), 1.70 – 1.41 (m, 24H, -CH₂-). ¹⁹F-NMR (CDCl₃, 376 MHz): δ / ppm = -80.83 (m, 12F, -CF₃), -114.32 (m, 8F, -CF₂-), -121.34 – -122.27 (m, 24F, -CF₂-), -122.74 (m, 8F, -CF₂-), -123.52 (m, 8F, -CF₂-), -126.24 (m, 8F, -CF₂-).

3.2.7 Synthesis of the 2,6-diiodohydroquinone diethers with different side-chains 7/m/n^{S8}

A mixture of **4/m/n** (1 equ.), PhI(OCOCF₃)₂ (1.1 equ) and I₂ (1.1 equ) in CH₂Cl₂ (10 mL / mmol **4/m/n**) was refluxed for 1d. After cooling to 25 °C the reaction was quenched with saturated Na₂S₂O₄ solution. The aqueous layer was extracted with Et₂O (3x50 mL) The combined organic layers were washed with water, and brine (50 mL each), and dried over Na₂SO₄. The solvent was evaporated (850 mbar, 60 °C) and the crude product was purified by column chromatography (eluent: *n*-hexane).

1,4-Diido-2-(2-tetradecylhexadecyl-1-yloxy)-5-(1,1,2,2,3,3,4,4,5,5,6,6,7,7,17,17,18,-19,19,20,20,21,21,22,22,23,23,23-triacontafluorotricosylmethoxy)benzene 7/7/14: Synthesized from **4/7/14** (2.6 g, 1.8 mmol), PhI(OCOCF₃)₂ (0.9 g, 2.0 mmol), I₂ (0.5 g, 2.0 mmol) in CH₂Cl₂ (20 mL); purification by column chromatography (eluent: *n*-hexane); colorless liquid C₆₂H₈₂F₃₀I₂O₂, M = 1659.08 g/mol, yield: 1.1 g (35 %), mp.: 54 °C, ¹H-NMR (CDCl₃, 400 MHz): δ / ppm = 7.15 (d, ³J_{H,H} = 1.0 Hz, 2H, Aryl-H), 3.81 (dd, ²J_{H,H} = 7.4, ³J_{H,H} = 5.3 Hz, 4H, -OCH₂-), 2.18 – 2.01 (m, 4H, -CH₂CF₂-), 1.87 – 1.73 (m, 2H, -CH-), 1.72 – 1.20 (m, 64H, -CH₂-), 0.88 (t, ³J_{H,H} = 6.9 Hz, 6H, -CH₃). ¹⁹F-NMR (CDCl₃, 376 MHz): δ / ppm = -80.82 (m, 6F, -CF₃), -114.31 (m, 4F, -CF₂-), -121.75 (m, 4F, -CF₂-), -122.09 (m, 4F, -CF₂-), -122.74 (m, 4F, -CF₂-), -123.51 (m, 4F, -CF₂-), -126.13 (m, 4F, -CF₂-).

1,4-Diido-2-(2-tetradecylhexadecyl-1-yloxy)-5-(1,1,2,2,3,3,4,4,5,5,6,6,7,7,8,8,18,-19,19,20,20,21,21,22,22,23,23,24,24,25,25,25-tetratriacontafluoropentacosylmethoxy)benzene 7/8/14: Synthesized from **4/8/14** (1.0 g, 0.6 mmol), PhI(OCOCF₃)₂ (0.3 g, 0.7 mmol), I₂ (0.2 g, 0.7 mmol) in CH₂Cl₂ (20 mL); purification by column chromatography (eluent: *n*-hexane); colorless liquid C₆₂H₈₂F₃₄I₂O₂, M = 1759.09 g/mol, yield: 540 mg (49 %), mp.: 60 °C, ¹H-NMR (CDCl₃, 500 MHz): δ / ppm = 7.17 (d, ³J_{H,H} = 1.5 Hz, 2H, Aryl-H), 3.83 (dd, ²J_{H,H} = 8.2, ³J_{H,H} = 5.2 Hz, 4H, -OCH₂-), 2.17 – 2.04 (m, 4H, -CH₂CF₂-), 1.89 – 1.77 (m, 2H, -CH-), 1.71 – 1.27 (m, 64H, -CH₂-), 0.90 (t, ³J_{H,H} = 6.8 Hz, 6H, -CH₃). ¹⁹F-NMR (CDCl₃,

470 MHz): δ / ppm = -80.89 (m, 6F, -CF₃), -114.37 (m, 4F, -CF₂-), -121.56 – -122.15 (m, 12F, -CF₂-), -122.79 (m, 4F, -CF₂-), -123.54 (m, 4F, -CF₂-), -126.19 (m, 4F, -CF₂-).

1-(2-Hexadec-1-yloctadec-1-yloxy)-2,5-diido-4-(1,1,1,2,2,3,3,4,4,5,5,6,6,7,7,8,8,18,18,-19,19,20,20,21,21,22,22,23,23,24,24,25,25,25-tetratriacontafluoropentacos-13-ylmethoxy)benzene 7/8/16:

Synthesized from **4/8/16** (1.1 g, 0.7 mmol), PhI(OCOCF₃)₂ (0.3 g, 0.7 mmol), I₂ (0.2 g, 0.7 mmol) in CH₂Cl₂ (20 mL); purification by column chromatography (eluent: *n*-hexane); colorless liquid C₆₀H₉₀F₃₄I₂O₂, M = 1815.20 g/mol, yield: 450 mg (37 %), mp.: 62 °C, **¹H-NMR** (CDCl₃, 400 MHz): δ / ppm = 7.15 (d, ³J_{H,H} = 1.0 Hz, 2H, Aryl-*H*), 3.89 – 3.74 (m, 4H, -OCH₂-), 2.16 – 2.01 (m, 4H, -CH₂CF₂-), 1.94 – 1.72 (m, 2H, -CH-), 1.69 – 1.19 (m, 72H, -CH₂-), 0.88 (t, ³J_{H,H} = 6.8 Hz, 6H, -CH₃). **¹⁹F-NMR** (CDCl₃, 376 MHz): δ / ppm = -80.79 (m, 6F, -CF₃), -114.31 (m, 4F, -CF₂-), -121.58 – -122.07 (m, 12F, -CF₂-), -122.71 (m, 4F, -CF₂-), -123.47 (m, 4F, -CF₂-), -126.11 – (m, 4F, -CF₂-).

3.2.8 Syntheses of the acetonides H_{m/n}A, H₈₂A, F_{m/n}A and F₈₂A

A mixture of the diiodoarene **7/m/n** or **7/m** (1 equ.) and the appropriate phenylacetylene **6H** or **6F** (2.1 equ.) was dissolved in purified NEt₃ (10 mL/~1 mmol **7**). After degassing with argon for 30 min [Pd(PPh₃)₄] (3 mol%) and CuI (3 mol%) were added and the mixture was stirred at 80°C for 24 h.^{S4,S5} After removing the solvent by evaporation the obtained residue was purified by column chromatography.

H7/14A: Synthesized from **7/7/14** (250 mg, 0.15 mmol), **6H** (110 mg, 0.33 mmol), [Pd(PPh₃)₄] (5.2 mg, 4.5·10⁻³ mmol), CuI (0.9 mg, 4.5·10⁻³ mmol) in NEt₃ (20 mL); purification by column chromatography (eluent: CHCl₃). Yellow solid, C₁₀₄H₁₂₀F₃₄O₈, M = 2068.05 g/mol, yield: 265 mg (85 %), mp.: 144 °C, **¹H-NMR** (CDCl₃, 400 MHz): δ / ppm = 7.50 – 7.43 (m, 12H, Aryl-*H*), 6.99 (s, 1H Aryl-*H*), 7.00 (s, 1H, Aryl-*H*), 6.93 – 6.86 (m, 4H, Aryl-*H*), 4.49 (m, 2H, -OCH-), 4.18 (dd, ²J_{H,H} = 8.5, ³J_{H,H} = 6.4 Hz, 2H, -OCH_AH_B-), 4.09 – 4.05 (m, 2H, -OCH_AH_B-), 4.01 – 3.87 (m, 6H, -ArCH_AH_B-), 3.86 (dd, ²J_{H,H} = 11.6, ³J_{H,H} = 4.1 Hz 2H, ArCH_AH_B-), 2.12 – 1.96 (m, 4H, -CH₂CF₂-), 1.95 – 1.80 (m, 2H, -CH-), 1.69 – 1.17 (m, 76H, -CH₂-, -CH₃), 0.87 (t, ³J_{H,H} = 6.7 Hz, 6H, -CH₃). **¹⁹F-NMR** (CDCl₃, 376 MHz): δ / ppm = -80.79 (m, 6F, -CF₃), -114.30 (m, 4F, -CF₂-), -121.76 (m, 4F, -CF₂-), -122.08 (m, 4F, -CF₂-), -122.74 (m, 4F, -CF₂-), -123.46 (m, 4F, -CF₂-), -125.11 (m, 4F, -CF₂-).

H8/14A: Synthesized from **7/8/14** (340 mg, 0.19 mmol), **6H** (141 mg, 0.43 mmol), [Pd(PPh₃)₄] (6.6 mg, 5.7·10⁻³ mmol), CuI (1.1 mg, 5.7·10⁻³ mmol) in NEt₃ (20 mL); purification by column chromatography (eluent: CHCl₃). Yellow solid, C₁₀₆H₁₂₀F₃₄O₈, M = 2168.06 g/mol, yield: 350 mg (84 %), mp.: 139 °C, **¹H-NMR** (CDCl₃, 400 MHz): δ / ppm = 7.50 – 7.44 (m, 12H, Aryl-*H*), 7.00 (s, 1H Aryl-*H*), 7.01 (s, 1H, Aryl-*H*), 6.94 – 6.88 (m, 4H, Aryl-*H*), 4.50 (m, 2H, -OCH-), 4.19 (dd, ²J_{H,H} = 8.5, ³J_{H,H} = 6.4 Hz, 2H, -OCH_AH_B-), 4.10 (dd, ²J_{H,H} = 5.7, ³J_{H,H} = 1.7 Hz, 2H, -OCH_AH_B-), 3.97 – 3.90 (m, 6H, ArOCH_AH_B-), 3.87 (dd, ²J_{H,H} = 11.4, ³J_{H,H} = 3.8 Hz, 2H, ArOCH_AH_B-), 2.14 – 1.96 (m, 4H, -CH₂CF₂-), 1.93 – 1.84 (m, 2H, -CH-), 1.71 – 1.21 (m, 76H, -CH₂-, -CH₃), 0.88 (t, ³J_{H,H} = 6.8 Hz, 6H, -CH₃). **¹⁹F-NMR** (CDCl₃, 376 MHz): δ / ppm = -80.77 (m, 6F, -CF₃), -114.35 (m, 4F, -CF₂-), -121.49 – -122.13 (m, 12F, -CF₂-), -122.70 (m, 4F, -CF₂-), -123.46 (m, 4F, -CF₂-), -125.96 – -126.24 (m, 4F, -CF₂-).

H8/16A: Synthesized from **7/8/16** (200 mg, 0.11 mmol), **6H** (81 mg, 0.24 mmol), [Pd(PPh₃)₄] (3.8 mg, 3.3·10⁻³ mmol), CuI (0.7 mg, 3.3·10⁻³ mmol) in NEt₃ (20 mL); purification by column chromatography (eluent: CHCl₃). Yellow solid, C₁₁₀H₁₂₈F₃₄O₈, M = 2224.17 g/mol, yield: 200 mg (81 %), mp.: 68 °C, **1H-NMR** (CDCl₃, 400 MHz): δ / ppm = 7.52 – 7.42 (m, 12H, Aryl-H), 6.99 (s, 1H Aryl-H), 7.00 (s, 1H, Aryl-H), 6.94 – 6.85 (m, 4H, Aryl-H), 4.49 (m, 2H, -OCH-), 4.18 (dd, ²J_{H,H} = 8.6, ³J_{H,H} = 6.4 Hz, 2H, -OCH_AH_B-), 4.09 (dd, ²J_{H,H} = 5.3, ³J_{H,H} = 1.6 Hz, 2H, -OCH_AH_B-), 3.95 – 3.89 (m, 6H, ArOCH_AH_B-), 3.86 (dd, ²J_{H,H} = 11.4, ³J_{H,H} = 3.8 Hz, 2H, ArOCH_AH_B-), 2.13 – 1.95 (m, 4H, -CH₂CF₂-), 1.94 – 1.78 (m, 2H, -CH-), 1.72 – 1.15 (m, 84H, -CH₂-, -CH₃), 0.87 (t, ³J_{H,H} = 6.8 Hz, 6H, -CH₃). **19F-NMR** (CDCl₃, 376 MHz): δ / ppm = -80.78 (m, 6F, -CF₃), -114.34 (m, 4F, -CF₂-), -121.51 – -122.15 (m, 12F, -CF₂-), -122.70 (m, 4F, -CF₂-), -123.45 (m, 4F, -CF₂-), -125.07 (m, 4F, -CF₂-).

H8₂A: Synthesized from **7/8** (600 mg, 0.26 mmol), **6H** (190 mg, 0.57 mmol), [Pd(PPh₃)₄] (32.9 mg, 28.5·10⁻³ mmol), CuI (5.4 mg, 28.5·10⁻³ mmol) in NEt₃ (20 mL); purification by column chromatography (eluent: CHCl₃). Yellow solid, C₁₀₂H₇₈F₆₈O₈, M = 2723.63 g/mol, yield: 500 mg (71 %), mp.: 138 °C, **1H-NMR** (CDCl₃, 400 MHz): δ / ppm = 7.50 – 7.42 (m, 12H, Aryl-H), 7.00 (s, 2H, Aryl-H), 6.91 – 6.86 (m, 4H, Aryl-H), 4.49 (m, 2H, -OCH-), 4.18 (dd, ²J_{H,H} = 8.5, ³J_{H,H} = 6.4 Hz, 2H, -OCH_AH_B-), 4.08 (dd, ²J_{H,H} = 9.6, ³J_{H,H} = 5.4 Hz, 2H, -OCH_AH_B-), 4.02 – 3.86 (m, 8H, ArOCH_AH_B-, ArOCH_AH_B-), 2.13 – 1.95 (m, 8H, -CH₂CF₂-), 1.94 – 1.85 (m, 2H, -CH-), 1.67 – 1.48 (m, 24H, -CH₂-), 1.47 (s, 6H, -CH₃), 1.41 (s, 6H, -CH₃). **19F-NMR** (CDCl₃, 376 MHz): δ / ppm = -80.80 (m, 12F, -CF₃), -114.34 (m, 8F, -CF₂-), -121.59 – -122.10 (m, 24F, -CF₂-), -122.73 (m, 8F, -CF₂-), -123.48 (m, 4F, -CF₂-), -125.99 – -126.24 (m, 8F, -CF₂-).

F7/14A: Synthesized from **7/7/14** (250 mg, 0.15 mmol), **6F** (134 mg, 0.33 mmol), [Pd(PPh₃)₄] (5.2 mg, 4.5·10⁻³ mmol), CuI (0.9 mg, 4.5·10⁻³ mmol) in NEt₃ (20 mL); purification by column chromatography (eluent: CHCl₃). Yellow solid, C₁₀₄H₁₁₂F₃₈O₈, M = 2211.97 g/mol, yield: 290 mg (87 %), mp.: 104 °C, **1H-NMR** (CDCl₃, 400 MHz): δ / ppm = 7.56 – 7.47 (m, 8H, Aryl-H), 7.00 (s, 1H Aryl-H), 7.01 (s, 1H, Aryl-H), 4.46 (m, 2H, -OCH-), 4.31 (dd, ²J_{H,H} = 7.2, ³J_{H,H} = 5.3 Hz, 2H, -OCH_AH_B-), 4.16 (dd, ²J_{H,H} = 8.6, ³J_{H,H} = 6.4 Hz, 2H, -OCH_AH_B-), 3.99 – 3.89 (m, 6H, ArOCH_AH_B-), 3.84 (dd, ²J_{H,H} = 7.7, ³J_{H,H} = 4.6 Hz, 2H, ArOCH_AH_B-), 2.11 – 1.96 (m, 4H, -CH₂CF₂-), 1.89 – 1.83 (m, 2H, -CH-), 1.66 – 1.18 (m, 76H, -CH₂-, -CH₃), 0.87 (t, ³J_{H,H} = 7.3 Hz, 6H, -CH₃). **19F-NMR** (CDCl₃, 376 MHz): δ / ppm = -80.82 (m, 6F, -CF₃), -114.38 (m, 4F, -CF₂-), -121.77 (m, 4F, -CF₂-), -122.13 (m, 4F, -CF₂-), -122.76 (m, 4F, -CF₂-), -123.50 (m, 4F, -CF₂-), -126.15 (m, 4F, -CF₂-), -137.14 – -137.90 (m, 4F, Aryl-F), -156.67 – -157.42 (m, 4F, Aryl-F).

F8/14A: Synthesized from **7/8/14** (340 mg, 0.19 mmol), **6F** (172 mg, 0.43 mmol), [Pd(PPh₃)₄] (6.6 mg, 5.7·10⁻³ mmol), CuI (1.1 mg, 5.7·10⁻³ mmol) in NEt₃ (20 mL); purification by column chromatography (eluent: CHCl₃). Yellow solid, C₁₀₆H₁₁₂F₄₂O₈, M = 2311.99 g/mol, yield: 340 mg (76 %), mp.: 111 °C, **1H-NMR** (CDCl₃, 400 MHz): δ / ppm = 7.58 – 7.48 (m, 8H, Aryl-H), 7.01 (s, 1H Aryl-H), 7.02 (s, 1H, Aryl-H), 4.46 (m, 2H, -OCH-), 4.32 (dd, ²J_{H,H} = 6.5, ³J_{H,H} = 5.6 Hz, 2H, -OCH_AH_B-), 4.17 (dd, ²J_{H,H} = 8.2, ³J_{H,H} = 6.1 Hz, 2H, -OCH_AH_B-), 4.00 – 3.89 (m, 6H, ArOCH_AH_B-), 3.86 (dd, ²J_{H,H} = 7.0, ³J_{H,H} = 4.7 Hz, 2H, ArOCH_AH_B-), 2.12 – 1.96 (m, 4H, -CH₂CF₂-), 1.95 – 1.82 (m, 2H, -CH-), 1.73 – 1.19 (m, 76H, -CH₂-, -CH₃), 0.91 – 0.84 (m, 6H, -CH₃). **19F-NMR** (CDCl₃, 376 MHz): δ / ppm = -80.82 (m, 6F, -CF₃), -114.36 (m, 4F, -CF₂-), -121.79 (m, 4F, -CF₂-), -122.73 (m, 4F, -CF₂-), -123.47 (m, 4F, -CF₂-), -126.10 (m, 4F, -CF₂-), -137.10 – -137.86 (m, 4F, Aryl-F), -156.74 – -157.53 (m, 4F, Aryl-F).

F8/16A: Synthesized from **7/8/16** (190 mg, 0.11 mmol), **6F** (108 mg, 0.27 mmol), [Pd(PPh₃)₄] (3.8 mg, 3.3·10⁻³ mmol), CuI (0.7 mg, 3.3·10⁻³ mmol) in NEt₃ (20 mL); purification by column chromatography (eluent: CHCl₃). Yellow solid, C₁₁₀H₁₂₀F₄₂O₈, M = 2368.09 g/mol, yield: 220 mg (88 %), mp.: 97 °C, **¹H-NMR** (CDCl₃, 400 MHz): δ / ppm = 7.60 – 7.46 (m, 8H, Aryl-H), 7.00 (s, 1H Aryl-H), 7.01 (s, 1H, Aryl-H), 4.46 (m, 2H, -OCH-), 4.37 – 4.28 (m, 2H, -OCH_AH_B-), 4.23 (dd, ²J_{H,H} = 10.0, ³J_{H,H} = 5.6 Hz, 2H, -OCH_AH_B-), 4.16 (dd, ²J_{H,H} = 8.6, ³J_{H,H} = 6.4 Hz, 2H, ArOCH_AH_B-), 4.00 – 3.89 (m, 6H, ArOH_AH_B-), 2.12 – 1.95 (m, 4H, -CH₂CF₂-), 1.93 – 1.79 (m, 2H, -CH-), 1.68 – 1.18 (m, 84H, -CH₂-, -CH₃), 0.87 (t, ³J_{H,H} = 6.7 Hz, 6H, -CH₃). **¹⁹F-NMR** (CDCl₃, 376 MHz): δ / ppm = -80.81 (m, 6F, -CF₃), -114.35 (m, 4F, -CF₂-), -121.56 – -122.10 (m, 12F, -CF₂-), -122.74 (m, 4F, -CF₂-), -123.46 (m, 4F, -CF₂-), -126.13 (m, 4F, -CF₂-), -137.32 – -137.81 (m, 4F, Aryl-F), -156.65 – -157.26 (m, 4F, Aryl-F).

F8₂A: Synthesized from **7/8** (170 mg, 0.07 mmol), **6F** (65 mg, 0.16 mmol), [Pd(PPh₃)₄] (4.0 mg, 3.5·10⁻³ mmol), CuI (0.7 mg, 3.5·10⁻³ mmol) in NEt₃ (20 mL); purification by column chromatography (eluent: CHCl₃). Yellow solid, C₁₀₂H₇₀F₇₆O₈, M = 2867.55 g/mol, yield: 110 mg (52 %), mp.: 135 °C, **¹H-NMR** (CDCl₃, 400 MHz): δ / ppm = 7.57 – 7.46 (m, 8H, Aryl-H), 7.01 (s, 2H, Aryl-H), 4.45 (m, 2H, -OCH-), 4.33 (dd, ²J_{H,H} = 10.1, ³J_{H,H} = 5.1 Hz, 2H, -OCH_AH_B-), 4.23 (dd, ²J_{H,H} = 10.1, ³J_{H,H} = 5.6 Hz, 2H, -OCH_AH_B-), 4.16 (dd, ²J_{H,H} = 8.6, ³J_{H,H} = 6.4 Hz, 2H, ArOCH_AH_B-), 3.99 – 3.92 (m, 6H, ArOCH_AH_B-), 2.11 – 1.94 (m, 8H, -CH₂CF₂-), 1.94 – 1.85 (m, 2H, -CH-), 1.67 – 1.45 (m, 24H, -CH₂-), 1.43 (s, 6H, -CH₃), 1.38 (s, 6H, -CH₃). **¹⁹F-NMR** (CDCl₃, 376 MHz): δ / ppm = -80.88 (m, 12F, -CF₃), -114.41 (m, 8F, -CF₂-), -121.64 – -122.22 (m, 24F, -CF₂-), -122.80 (m, 8F, -CF₂-), -123.54 (m, 8F, -CF₂-), -126.21 (m, 8F, -CF₂-), -137.75 (m, 4F, Aryl-F), -157.11 (m, 4F, Aryl-F).

3.3 Syntheses of compounds H_{m/n}, H8₂, F_{m/n} and F8₂^{S9}

H7/14: Synthesized from **H7/14A** (265 mg, 0.13 mmol), PPTS (64 mg, 0.27 mmol) in MeOH/THF (1:1, 30/30 mL), purification by column chromatography (eluent CHCl₃/THF 3:1). Yellow solid C₉₈H₁₁₂F₃₀O₈, M = 1987.92 g/mol, yield: 162 mg (0.08 mol, 64%), for phase transitions, see Table 1; **¹H NMR** (400 MHz, THF-d₈) δ / ppm = 7.48 (2s, 8H, Aryl-H), 7.46 – 7.39 (m, 4H, Aryl-H), 7.10 (2d, 2H, Aryl-H), 6.99 – 6.92 (m, 4H, Aryl-H), 4.25 (d, ³J_{H,H} = 5.1 Hz, 2H, -CH₂-OH), 4.06 (dd, ²J_{H,H} = 9.5, ³J_{H,H} = 4.8 Hz, 2H, -CH_AH_B-OAr), 4.00 (d, ³J_{H,H} = 5.3 Hz, 2H, CH-CH₂-OAr), 3.98 – 3.92 (m, 4H, CH-CH₂-OAr, -CH_AH_B-OAr), 3.89 (m, 2H, CH-OH), 3.83 (t, ³J_{H,H} = 5.8 Hz, 2H, -CH₂-OH), 3.5-3.7 (m, overlapping with THF, -CH₂OH), 2.25 – 2.08 (m, 4H, -CH₂-CF₂-), 1.98 – 1.83 (m, 2H, -CH-), 1.69 – 1.22 (m, 64H, -CH₂-), 0.88 (t, ³J_{H,H} = 6.7 Hz, 6H, -CH₃). **¹³C NMR** (101 MHz, THF-d₈) δ / ppm = 160.88, 155.24, 154.88 (C_{Aryl}-O), 133.94, 133.90, 132.32, 132.23 (C_{Aryl}-H), 125.01, 124.90, 124.19, 124.07 (C_{Aryl}-quart), 117.40, 117.38 (C_{Aryl}-H), 116.08, 116.07 (C_{Aryl}-quart), 115.71, 115.68 (C_{Aryl}-H), 115.06, 114.97 (C_{Aryl}-quart), 95.43, 95.36, 92.64, 92.61, 89.01, 88.96, 88.54, 88.41 (-C≡C-), 73.02, 72.66 (-OCH₂-CH), 71.58 (CH-OH), 71.03 (-CH₂-O-C_{Aryl}), 64.50 (-CH₂-OH), 39.49, 39.16 (-CH-), 33.05, 32.66, 32.26 (-CH₂-), 31.64 (t, ³J_{H,F} = 22.0 Hz, -CH₂-CF₂-), 31.26, 30.86 [2xC], 30.84 [3xC], 30.81, 30.79, 30.49, 28.07, 27.41, 23.73, 21.65 (-CH₂-), 14.60 (-CH₃). **¹⁹F-NMR** (376 MHz, THF-d₈) δ / ppm = -81.78 (m, 6F, -CF₃), -114.82 (m, 4F, -CF₂-), -122.30 (m, 4F, -CF₂-), -122.62 (m, 4F, -CF₂-), -123.32 (m, 4F, -CF₂-), -124.01 (m, 4F, -CF₂-), -126.78 (m, 4F, -CF₂-). **HRMS** (m/z): [M]⁺Cl⁻ calcd. for C₉₈H₁₁₂F₃₀O₈Cl: 2022.7595, found: 2022.7573.

H8/14: Synthesized from **H8/14A** (350 mg, 0.16 mmol), PPTS (81 mg, 0.32 mmol) in MeOH/THF (1:1, 30/30 mL), purification by column chromatography (eluent CHCl₃/THF 3:1). Yellow solid C₁₀₀H₁₁₂F₃₄O₈, $M = 2087.93$ g/mol, yield: 215 mg (0.10 mmol, 64 %), for phase transitions, see Table 1; **¹H NMR** (400 MHz, THF-*d*₈) δ / ppm = 7.48 (2s, 8H, Aryl-*H*), 7.45 – 7.38 (m, 4H, Aryl-*H*), 7.10 (s, 2H, Aryl-*H*), 6.98 – 6.92 (m, 4H, Aryl-*H*), 4.23 (d, $^3J_{H,H} = 5.1$ Hz, 2H, -CH₂-OH), 4.07 (dd, $^2J_{H,H} = 9.5$, $^3J_{H,H} = 4.8$ Hz, 2H, -CH_AH_B-OAr), 4.00 (d, $^3J_{H,H} = 5.3$ Hz, 2H, CH-CH₂-OAr), 3.99 – 3.93 (m, 4H, CH-CH₂-OAr, -CH_AH_B-OAr), 3.89 (m, 2H, CH-OH), 3.81 (t, $^3J_{H,H} = 5.8$ Hz, 2H, -CH₂-OH), 3.5–3.7 (m, overlapping with THF, -CH₂OH), 2.27 – 2.09 (m, 4H, -CH₂-CF₂-), 1.99 – 1.83 (m, 2H, -CH-), 1.68 – 1.19 (m, 64H, -CH₂-), 0.88 (t, $^3J_{H,H} = 6.7$ Hz, 6H, -CH₃). **¹³C NMR** (101 MHz, THF-*d*₈) δ / ppm = 160.87, 155.23, 154.88 (*C_{Aryl}-O*), 133.93, 133.89, 132.32, 132.30, 132.23 (*C_{Aryl}-H*), 125.00, 124.89, 124.18, 124.06 (*C_{Aryl}-quart*), 117.40 (*C_{Aryl}-H*), 116.06, 116.05 (*C_{Aryl}-quart*), 115.71, 115.68 (*C_{Aryl}-H*), 115.06, 114.97 (*C_{Aryl}-quart*), 95.44, 95.36, 92.64, 92.61, 89.00, 88.95, 88.53, 88.41 (-C≡C-), 73.03, 72.67 (-OCH₂-CH), 71.58 (CH-OH), 71.02 (-CH₂O-C_{Aryl}), 64.49 (-CH₂-OH), 39.47, 39.12 (-CH-), 33.04, 32.65, 32.22 (-CH₂-), 31.63 (t, $^3J_{H,F} = 21.6$ Hz, -CH₂-CF₂-), 31.25, 30.84 [2xC], 30.83 [3xC], 30.79, 30.78, 30.48, 28.05, 27.39, 23.72, 21.63 (-CH₂-), 14.59 (-CH₃). **¹⁹F NMR** (376 MHz, THF-*d*₈) δ / ppm = -79.92 (m, 6F, -CF₃), -113.02 (m, 4F, -CF₂-), -119.93 – -120.80 (m, 12F, -CF₂-), -121.41 (m, 4F, -CF₂-), -122.14 (m, 4F, -CF₂-), -124.45 – -125.32 (m, 4F, -CF₂-). **HRMS** (m/z): [M]⁺Cl⁻ calcd. for C₁₀₀H₁₁₂F₃₄O₈Cl: 2122.7531, found: 2122.7544.

H8/16: Synthesized from **H8/16A** (200 mg, 0.09 mmol), PPTS (45 mg, 0.18 mmol) in MeOH/THF (1:1, 30/30 mL), purification by column chromatography (eluent CHCl₃/THF 3:1). Yellow solid C₁₀₄H₁₂₀F₃₄O₈, $M = 2144.04$ g/mol, yield: 113 mg (0.05 mmol, 48 %), for phase transitions, see Table 1; **¹H NMR** (500 MHz, THF-*d*₈) δ / ppm = 7.48 (2s, 8H, Aryl-*H*), 7.46 – 7.39 (m, 4H, Aryl-*H*), 7.10 (s, 2H, Aryl-*H*), 6.99 – 6.91 (m, 4H, Aryl-*H*), 4.17 (d, $^3J_{H,H} = 5.1$ Hz, 2H, CH-OH), 4.05 (2 x dd, $^2J_{H,H} = 9.5$, $^3J_{H,H} = 4.9$, 2H, -CH_AH_B-OAr), 4.00 (d, $^3J_{H,H} = 5.3$ Hz, 2H, CH-CH₂-OAr), 3.98 – 3.93 (m, 4H, CH-CH₂-OAr, -CH_AH_B-OAr), 3.91 – 3.84 (m, CH-OH), 3.72–3.77 (2 x t, $^3J_{H,H} = 5.8$ Hz, 2H, -CH₂-OH), 3.5–3.7 (m, overlapping with THF, -CH₂OH), 2.25 – 2.09 (m, 4H, -CH₂-CF₂-), 1.98 – 1.82 (m, 2H, -CH-), 1.68 – 1.19 (m, 72H, -CH₂-), 0.88 (t, $^3J_{H,H} = 6.9$ Hz, 6H, -CH₃). **¹³C NMR** (126 MHz, Pyridine-*d*₅) δ / ppm = 160.76, 155.17, 154.80 (*C_{Aryl}-O*), 134.07, 134.01, 132.49, 132.41 (*C_{Aryl}-H*), 124.86, 124.76, 123.51 (*C_{Aryl}-quart*), 117.79, 115.87, 115.82 (*C_{Aryl}-H*), 115.67, 115.03, 114.96 (*C_{Aryl}-quart*), 96.01, 95.92, 93.18, 93.10, 89.53, 89.45, 88.98, 88.84 (-C≡C-), 73.10, 72.79 (-OCH₂-CH), 71.80 (CH-OH), 71.56, 71.54 (-CH₂O-C_{Aryl}), 64.72 (-CH₂-OH), 39.09, 38.60, (-CH-), 32.60, 32.42, 31.85 (-CH₂-), 31.20 (t, $^3J_{C,F} = 22.1$ Hz, -CH₂-CF₂-), 30.94, 30.51 [3xC], 30.50 [2xC], 30.48, 30.47, 30.45, 30.40, 30.09, 27.78, 27.01, 23.40, 21.32 (-CH₂-), 14.72 (-CH₃). **¹⁹F NMR** (470 MHz, THF-*d*₈) δ / ppm = -79.92 (m, 6F, -CF₃), -112.94 (m, 4F, -CF₂-), -120.29 – 120.72 (m, 12F, -CF₂-), -121.41 (m, 4F, -CF₂-), -122.14 (m, 4F, -CF₂-), -124.92 (m, 4F, -CF₂-). **HRMS** (m/z): [M]⁺Cl⁻ calcd. for C₁₀₄H₁₂₀F₃₄O₈Cl: 2178.8157, found: 2178.8208.

H8₂: Synthesized from **H8₂A** (500 mg, 0.18 mmol), PPTS (92 mg, 0.37 mmol) in MeOH/THF (1:1, 30/30 mL), purification by column chromatography (eluent CHCl₃/THF 3:1). Yellow solid C₉₆H₇₀F₆₈O₈, $M = 2643.50$ g/mol, yield: 314 mg (0.12 mmol, 64 %), for phase transitions, see Fig. 3a; **¹H NMR** (400 MHz, THF-*d*₈) δ / ppm = 7.48 (s, 8H, Aryl-*H*), 7.42 (d, $^3J_{H,H} = 8.7$ Hz, 4H, Aryl-*H*), 7.12 (s, 2H, Aryl-*H*), 6.94 (d, $^3J_{H,H} = 8.6$ Hz, 4H, Aryl-*H*), 4.20 (d, $^3J_{H,H} = 5.1$ Hz, 2H, CH-OH), 4.06 (dd, $^2J_{H,H} = 9.5$, $^3J_{H,H} = 4.8$ Hz, 2H, -CH_AH_B-OAr), 4.01 (d, $^3J_{H,H} = 5.3$ Hz, 4H, CH-CH₂-OAr), 3.95 (dd, $^2J_{H,H} = 9.5$, 6.0 Hz, 2H, -CH_AH_B-OAr), 3.88 (m, 2H, CH-OH), 3.78 (t, $^3J_{H,H} = 5.8$ Hz, 2H, -CH₂-OH), 3.5–3.7 (m, overlapping with THF, -CH₂-OH), 2.27 –

2.06 (m, 8H, -CH₂-CF₂-), 1.99 – 1.86 (m, 2H, -CH-), 1.71 – 1.50 (m, overlapped with THF, 24H, -CH₂-). **¹³C NMR** (101 MHz, THF-*d*₈) δ / ppm = 160.89, 155.01 (*C_{Aryl}*-O), 133.90, 132.34, 132.21 (*C_{Aryl}*-H), 125.09, 123.97 (*C_{Aryl}*-quart), 120.0 (m, br., CF₂), 117.43 (*C_{Aryl}*-H), 116.9 (m, CF₂), 116.03 (*C_{Aryl}*-quart), 115.68 (*C_{Aryl}*-H), 115.01 (*C_{Aryl}*-quart), 111.5 – 114 (m, br., -CF₂-), 109 – 111 (m, br., -CF₃), 95.45, 92.67, 88.83, 88.37 (-C≡C-), 72.63 (-OCH₂-CH), 71.58 (CH-OH), 71.03 (-CH₂-O-C_{Aryl}), 64.49 (-CH₂-OH), 39.11 (-CH-), 32.23 (-CH₂-), 31.53 (t, ³*J*_{H,F} = 22.2 Hz, -CH₂-CF₂-), 27.39, 21.63 (-CH₂-). **¹⁹F NMR** (376 MHz, THF-*d*₈) δ / ppm = -81.80 (m, 12F, -CF₃), -114.82 (m, 8F, -CF₂-), -122.11 – -122.56 (m, 24F, -CF₂-), -123.29 (m, 8F, -CF₂-), -124.03 (m, 8F, -CF₂-), -126.80 (m, 8F, -CF₂-). **HRMS** (m/z): [M]+Cl⁻ calcd. for C₉₆H₇₀F₆₈O₈Cl: 2678.3702, found: 2678.3745.

F7/14: Synthesized from **F7/14A** (290 mg, 0.13 mmol), PPTS (66 mg, 0.26 mmol) in MeOH/THF (1:1, 30 mL : 30 mL), purification by column chromatography (eluent CHCl₃/THF 3:1). Yellow solid C₉₈H₁₀₄F₃₈O₈, *M* = 2131.84 g/mol, yield: 199 mg (0.09 mmol, 71 %), for phase transitions, see Table 2; **¹H NMR** (400 MHz, THF-*d*₈) δ / ppm = 7.61 – 7.52 (m, 8H, Aryl-H), 7.12 (2s, 2H, Aryl-H), 4.43 – 4.38 (m, 2H, -CH_AH_B-OAr_F), 4.32 (2 d, ³*J*_{H,H} = 5.1 Hz, 2H, CH-OH), 4.38 – 4.24 (m, 2H, -CH_AH_B-OAr_F), 4.01 (d, ³*J*_{H,H} = 5.4 Hz, 2H, -CH-CH₂-OAr), 3.97 (d, ³*J*_{H,H} = 5.4 Hz, 2H, CH-OCH₂-OAr), 3.93 – 3.84 (m, 4H, -CH₂-OH, CH-OH), 3.5-3.7 (m, overlapping with THF, -CH₂OH), 2.25 – 2.06 (m, 4H, -CH₂-CF₂-), 1.98 – 1.83 (m, 2H, -CH-), 1.70 – 1.22 (m, 64H, -CH₂-), 0.88 (t, ³*J*_{H,H} = 6.3 Hz, 6H, -CH₃). **¹³C NMR** (101 MHz, THF-*d*₈) δ / ppm = 155.32, 154.96 (*C_{Aryl}*-O), 149.33, 147.44, 143.25, 141.30 (m, broad, *C_{Aryl}*-F), 140.50 (m, *C_{Aryl}F*-O), 132.80, 132.49, 132.40 (*C_{Aryl}*-H), 125.86, 125.72, 122.87, 122.75 (*C_{Aryl}*-quart), 121.96, 119.96, (2x m, broad, -CF₂-), 117.39 (*C_{Aryl}*-H), 117.19 (m, broad, -CF₂-), 115.00, 114.94 (*C_{Aryl}*-quart), 113.5 – 114.5, 111.5 – 112.5 (2x m, broad, -CF₂-), 109 – 110 (m, broad, -CF₃), 100.70 (t, ³*J*_{C,F} = 3.6 Hz, -C≡C-C_{Aryl}F), 100.57 (t, ³*J*_{C,F} = 3.0 Hz, -C≡C-C_{Aryl}F), 98.23 (t, ²*J*_{C,F} = 17.9 Hz, *C_{Aryl}F*-quart), 95.16, 95.10, 89.83, 89.76 (-C≡C-), 77.88 (t, ⁴*J*_{C,F} = 3.4 Hz, -CH₂-O-C_{Aryl}F), 76.62 (2t, overlapped, ³*J*_{C,F} = 3.8 Hz, -C≡C-C_{Aryl}F), 73.03, 72.75 (-OCH₂-CH), 72.25 (CH-OH), 63.99 (-CH₂-OH), 39.47, 39.17 (-CH-), 33.04, 32.66, 32.28 (-CH₂-), 31.52 (t, ²*J*_{C,F} = 22.0 Hz, -CH₂-CF₂-), 31.26, 30.85 [2xC], 30.83 [3xC], 30.80, 30.78, 30.48, 28.06, 27.43, 23.71, 21.65 (-CH₂-), 14.57 (-CH₃). **¹⁹F NMR** (376 MHz, THF-*d*₈) δ / ppm = -81.82 (m, 6F, -CF₃), -114.83 (m, 4F, -CF₂-), -122.32 (m, 4F, -CF₂-), -122.61 (m, 4F, -CF₂-), -123.32 (m, 4F, -CF₂-), -123.98 (m, 4F, -CF₂-), -126.81 (m, 4F, -CF₂-), -140.04 (m, 4F, CAryl-F), -158.35 (m, 4F, CAryl-F). **HRMS** (m/z): [M]+Cl⁻ calcd. for C₉₈H₁₀₄F₃₈O₈Cl: 2166.6841, found: 2166.6804.

F8/14: Synthesized from **F8/14A** (340 mg, 0.15 mmol), PPTS (74 mg, 0.29 mmol) in MeOH/THF (1:1, 30/30 mL), purification by column chromatography (eluent CHCl₃/THF 3:1). Yellow solid C₁₀₀H₁₀₄F₄₂O₈, *M* = 2231.86 g/mol, yield: 236 mg (0.11 mmol, 72 %), for phase transitions, see Table 2; **¹H NMR** (400 MHz, THF-*d*₈) δ / ppm = 7.62 – 7.51 (m, 8H, Aryl-H), 7.12 (2s, 2H, Aryl-H), 4.43 – 4.37 (m, 2H, -CH_AH_B-OAr_F), 4.32 (d, 2H, -CH-OH), 4.31-4.25 (m, 2H, -CH_AH_B-OAr_F), 4.01 (d, ³*J*_{H,H} = 5.4 Hz, 2H, CH-CH₂-OAr), 3.97 (d, ³*J*_{H,H} = 5.5 Hz, 2H, CH-CH₂-OAr), 3.92 – 3.85 (m, 4H, -CH₂-OH, CH-OH), 3.5-3.7 (m, overlapping with THF, -CH₂OH), 2.25 – 2.07 (m, 4H, -CH₂-CF₂-), 1.98 – 1.83 (m, 2H, -CH-), 1.69 – 1.23 (m, 64H, -CH₂-), 0.88 (t, ³*J*_{H,H} = 6.3 Hz, 6H, -CH₃). **¹³C NMR** (101 MHz, THF-*d*₈) δ / ppm = 155.31, 154.96 (*C_{Aryl}*-O), 132.80, 132.49, 132.41 (*C_{Aryl}*-H), 125.85, 125.71, 122.86, 122.74 (*C_{Aryl}*), 117.40 (*C_{Aryl}*-H), 114.99, 114.93 (*C_{Aryl}*), 100.68, 100.53 (m, -C≡C-C_{Aryl}F), 98.20 (m, *C_{Aryl}F*-

quart) 95.16, 95.10, 89.82, 89.76 ($-C\equiv C-$), 77.84 (m, $-CH_2-O-C_{ArylF}-$), 76.62 (m, $-C\equiv C-C_{ArylF}$), 73.03, 72.77 ($-OCH_2-CH$), 72.25 (CH-OH), 63.97 ($-CH_2-OH$), 39.47, 39.14 ($-CH-$), 33.03, 32.65, 32.25 ($-CH_2-$), 31.51 (t, $^3J_{C,F} = 22.1$ Hz, $-CH_2-CF_2-$), 31.25, 30.85 [2xC], 30.83 [3xC], 30.80, 30.77, 30.47, 28.05, 27.42, 23.71, 21.64 ($-CH_2-$), 14.57 ($-CH_3$). **^{19}F NMR** (376 MHz, THF-*d*8) δ / ppm = -79.94 (m, 6F, $-CF_3$), -112.95 (m, 4F, $-CF_2-$), -120.20 – -120.78 (m, 12F, $-CF_2-$), -121.45 (m, 4F, $-CF_2-$), -122.12 (m, 4F, $-CF_2-$), -124.94 (m, 4F, $-CF_2-$), -138.39 (m, 4F, *Caryl-F*), -156.50 (m, 4F, *Caryl-F*). **HRMS** (m/z): [M] $+\text{Cl}^-$ calcd. for $C_{100}H_{104}F_{42}O_8\text{Cl}$: 2266.6788, found: 2266.6823.

F8/16: Synthesized from **F8/16A** (220 mg, 0.09 mmol), PPTS (47 mg, 0.19 mmol) in MeOH/THF (1:1, 30/30 mL), purification by column chromatography (eluent CHCl₃/THF 3:1). Yellow solid $C_{104}H_{112}F_{42}O_8$, $M = 2287.96$ g/mol, yield: 134 mg (0.06 mmol, 63 %), for phase transitions, see Table 2; **1H NMR** (500 MHz, THF-*d*8) δ / ppm = 7.61 – 7.51 (m, 8H, *Aryl-H*), 7.11 (2s, 2H, *Aryl-H*), 4.42 – 4.36 (m, 2H, $-CH_AH_B-OAr_F$), 4.29 (d, 2H, CH-OH), 4.28 – 4.24 (m, 2H, $-CH_AH_B-OAr_F$), 4.00 (d, $^3J_{H,H} = 5.4$ Hz, 2H, CH-CH₂-OAr), 3.96 (d, $^3J_{H,H} = 5.5$ Hz, 2H, CH-CH₂-OAr), 3.90 – 3.84 (m, 4H, $-CH_2-OH$, CH-OH), 3.5-3.7 (m, overlapping with THF, $-CH_2OH$), 2.22 – 2.09 (m, 4H, $-CH_2-CF_2-$), 1.96 – 1.82 (m, 2H, $-CH-$), 1.70 – 1.22 (m, 72H, $-CH_2-$), 0.88 (t, $^3J_{H,H} = 6.9$ Hz, 6H, $-CH_3$). **^{13}C NMR** (126 MHz, THF-*d*8) δ / ppm = 155.32, 154.96 (*Caryl-O*), 132.80, 132.49, 132.41 (*Caryl-H*), 125.86, 125.71, 122.87, 122.75 (*Caryl*), 117.41 (*Caryl-H*), 115.00, 114.94 (*Caryl*), 100.69, 100.55 (m, $-C\equiv C-C_{ArylF}$), 98.22 (m, *CarylF-quart*, 95.16, 95.10, 89.82, 89.76 ($-C\equiv C-$), 77.91 (m, $-CH_2-O-C_{ArylF}$), 76.62 (m, $-C\equiv C-C_{ArylF}$), 73.03, 72.77 ($-OCH_2-CH$), 72.25 (CH-OH), 63.98 ($-CH_2-OH$), 39.47, 39.14 ($-CH-$), 33.03, 32.65, 32.26 ($-CH_2-$), 31.51 (t, $^3J_{C,F} = 21.6$ Hz, $-CH_2-CF_2-$), 31.25, 31.23, 30.85, 30.83 [2xC], 30.82 [3xC], 30.80, 30.77, 30.47, 28.05, 27.42, 23.71, 21.64, ($-CH_2-$), 14.57 ($-CH_3$). **^{19}F NMR** (470 MHz, THF-*d*8) δ / ppm = -79.93 (m, 6F, $-CF_3$), -112.96 (m, 4F, $-CF_2-$), -120.18 – -120.76 (m, 12F, $-CF_2-$), -121.42 (m, 4F, $-CF_2-$), -122.11 (m, 4F, $-CF_2-$), -124.94 (m, 4F, $-CF_2-$), -138.37 (m, 4F, *Caryl-F*), -156.49 (m, 4F, *Caryl-F*). **HRMS** (m/z): [M] $+\text{Cl}^-$ calcd. for $C_{104}H_{112}F_{42}O_8\text{Cl}$: 2322.7403, found: 2322.7390.

F8₂: Synthesized from **F8₂A** (110 mg, 0.04 mmol), PPTS (19 mg, 0.08 mmol) in MeOH/THF (1:1, 30/30 mL), purification by column chromatography (eluent CHCl₃/THF 3:1). Yellow solid $C_{96}H_{62}F_{76}O_8$, $M = 2787.42$ g/mol, yield: 88.5 mg (0.03 mmol, 83 %), for phase transitions, see Fig. 10a; **1H NMR** (400 MHz, THF-*d*8) δ / ppm = 7.58 (d, $^3J_{H,H} = 8.4$ Hz, 4H, *Aryl-H*), 7.53 (d, $^3J_{H,H} = 8.4$ Hz, 4H, *Aryl-H*), 7.14 (s, 2H, *Aryl-H*), 4.40 (dd, $^2J_{H,H} = 10.1$, $^3J_{H,H} = 4.3$ Hz, 2H, $-CH_AH_B-OAr_F$), 4.34 – 4.25 (m, 4H, CH-OH, $-CH_AH_B-OAr_F$), 4.02 (d, $^3J_{H,H} = 5.4$ Hz, 4H, CH-CH₂-OAr), 3.93 – 3.84 (m, 4H, $-CH_2-OH$, CH-OH), 3.5-3.7 (m, overlapping with THF, $-CH_2OH$), 2.26 – 2.07 (m, 8H, $-CH_2-CF_2-$), 2.00 – 1.87 (m, 2H, $-CH-$), 1.71 – 1.20 (m, 24H, $-CH_2-$). **^{13}C NMR** (101 MHz, THF-*d*8) δ / ppm = 155.10 (*Caryl-O*), 150-147, m, *Caryl-F* 144-141 (m, *Caryl-F*), 140.65 (m, *CarylF-O*), 132.83, 132.39 (*Caryl-H*), 125.62, 122.95 (*Caryl-quart*), 119.66 (m, $-CF_2-$), 117.44 (*Caryl-H*), 114.98 (*Caryl-quart*), 112.1 (m, $-CF_2-$), 109.5 (m, $-CF_2-$), 106.9 (m, $-CF_3$), 100.47 (m, $-C\equiv C-C_{ArylF}$), 98.36 (m, *CarylF-quart*), 95.18, 89.63 ($-C\equiv C-$), 77.89 (t, $^4J_{C,F} = 3.3$ Hz, $-CH_2-O-C_{ArylF}$), 76.64 (t, $^3J_{C,F} = 4.2$ Hz, $-C\equiv C-C_{ArylF}$), 72.73, (-OCH₂-CH), 72.25 (CH-OH), 63.99 ($-CH_2-OH$), 39.13 ($-CH-$), 32.26 ($-CH_2-$), 31.52 (t, $^3J_{C,F} = 22.0$ Hz, $-CH_2-CF_2-$), 27.42, 21.64 ($-CH_2-$). **^{19}F NMR** (376 MHz, THF-*d*8) δ / ppm = -81.81 (m, 12F, $-CF_3$), -114.83 (m, 8F, $-CF_2-$), -122.12 – -122.67 (m, 24F, $-CF_2-$), -123.31 (m, 8F, $-CF_2-$), -124.01 (m, 8F, $-CF_2-$), -126.82 (m, 8F, $-CF_2-$), -140.36 (m, 4F, *Caryl-F*), -158.45 (m, 4F, *Caryl-F*). **HRMS** (m/z): [M] $+\text{Cl}^-$ calcd. for $C_{96}H_{62}F_{76}O_8\text{Cl}$: 2822.2948, found: 2822.2864.

3.4 Representative NMR spectra

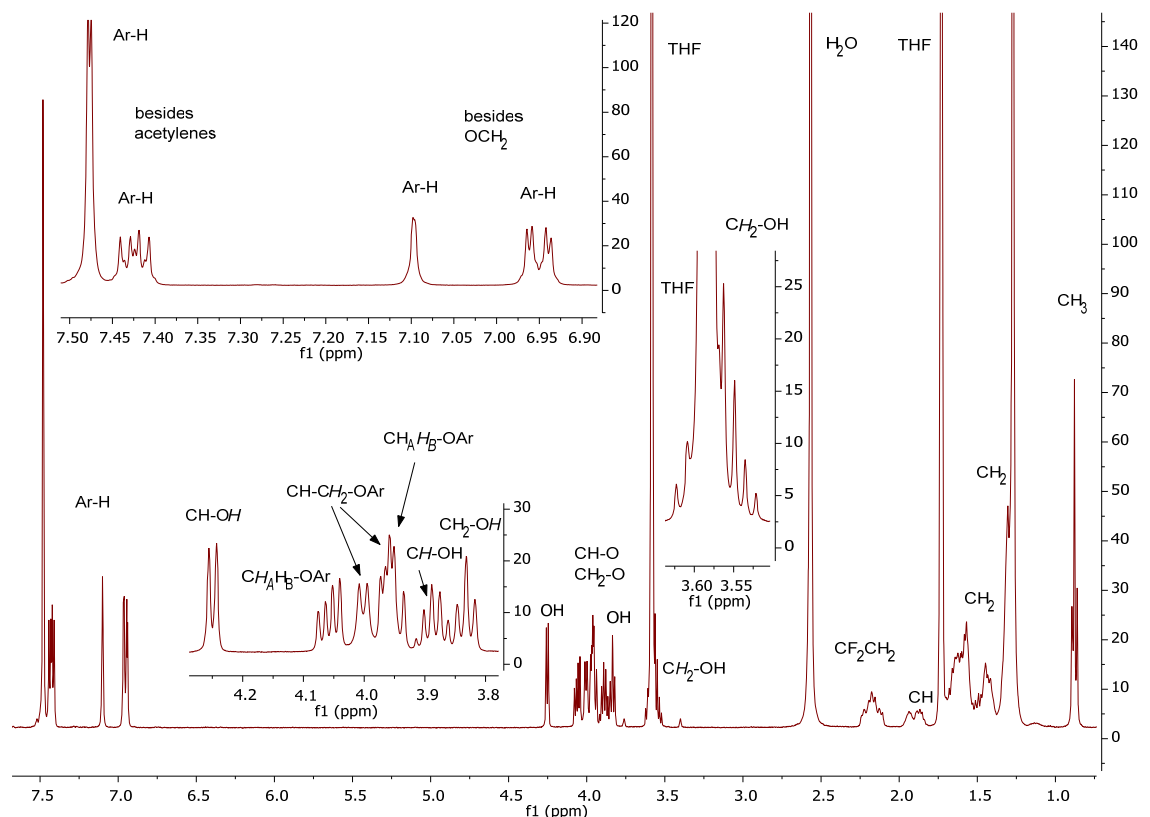


Figure S20: ^1H -NMR of compound H7/14 (400 MHz, THF-d₈, 27 °C); CH_AH_B-OAr = end groups (glycerols), CH-CH₂-OAr = side chains.

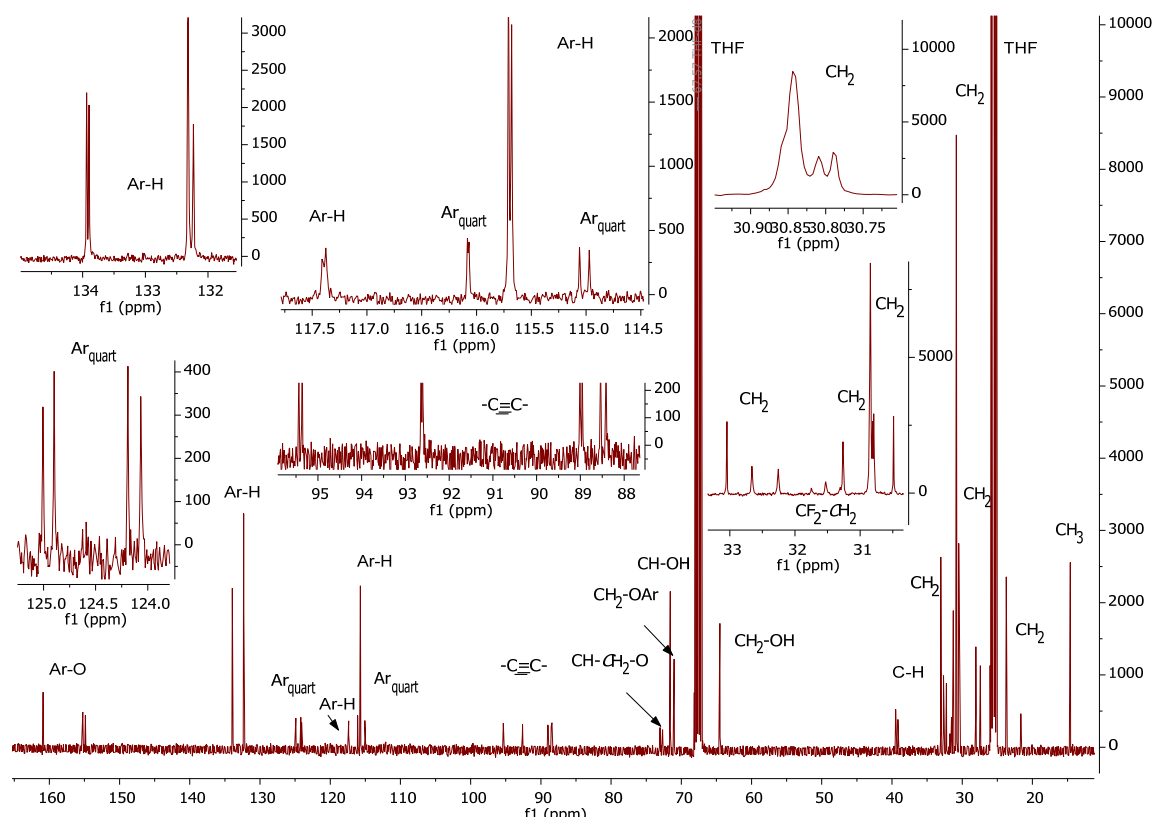


Figure S21: ^{13}C -NMR of compound H7/14 (101 MHz; THF-d₈, 27 °C);

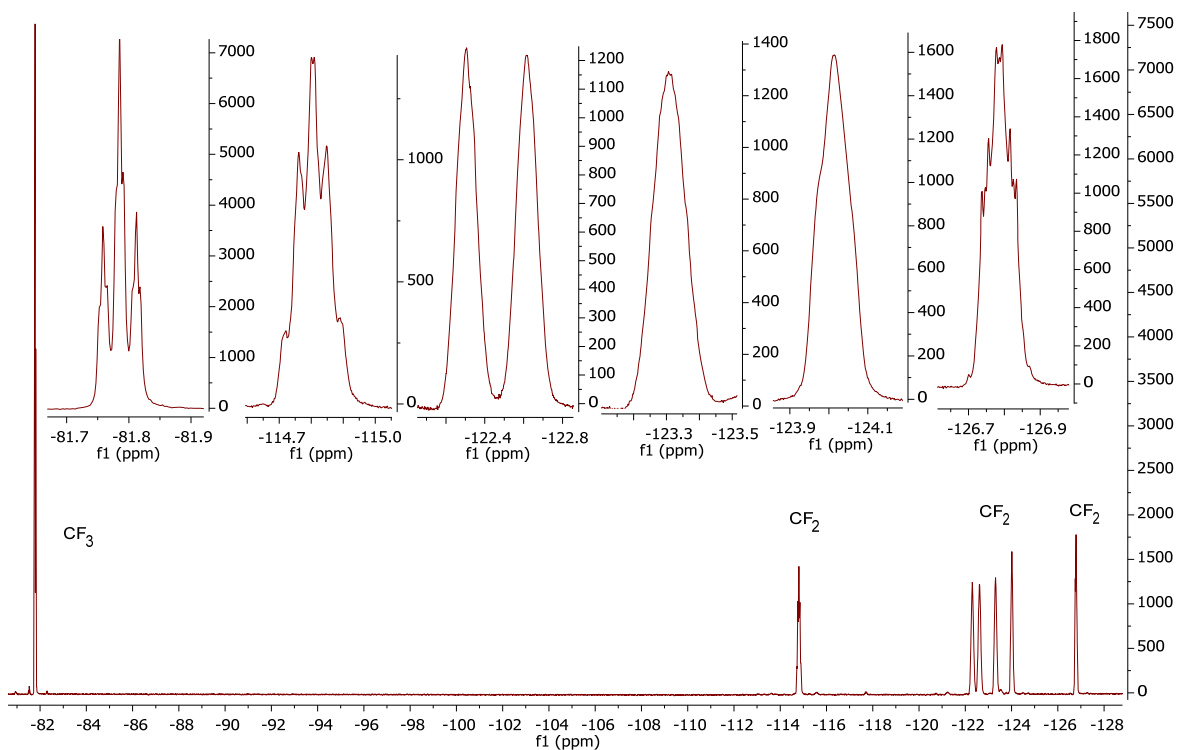


Figure S22: ^{19}F -NMR of compound **H7/14** (376 MHz, THF- d_8 , 27 °C).

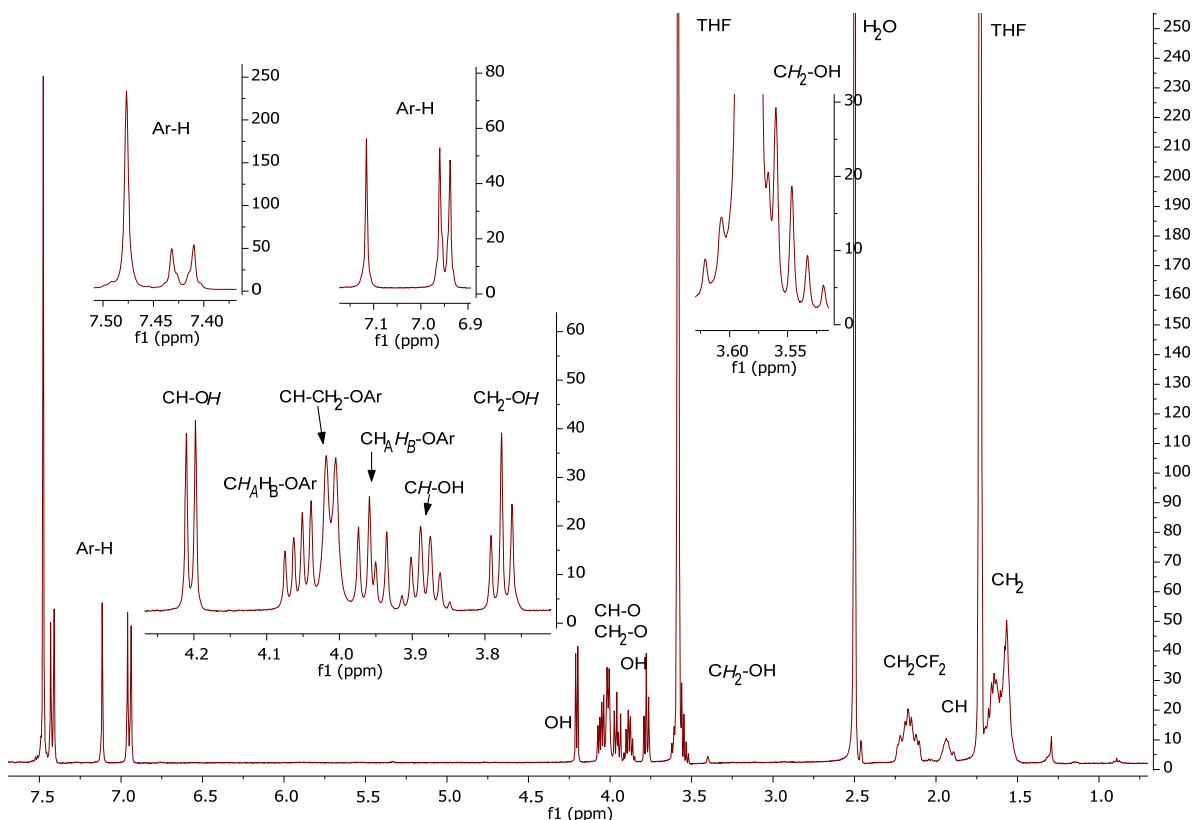


Figure S23: ^1H -NMR of compound **H8²** (400 MHz, THF- d_8 , 27 °C).

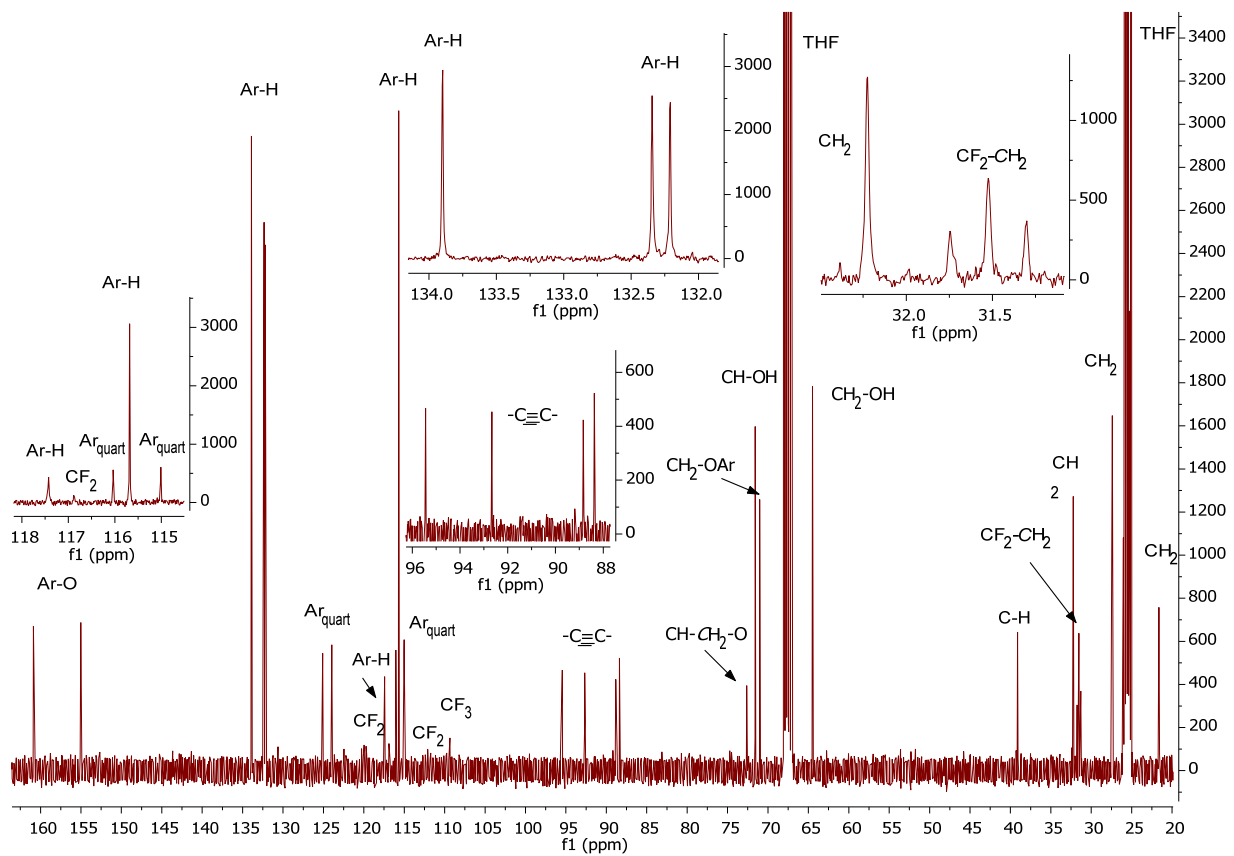


Figure S24: ^{13}C -NMR of compound $\mathbf{H}8^2$ (101 MHz, THF- d_8 , 27 °C).

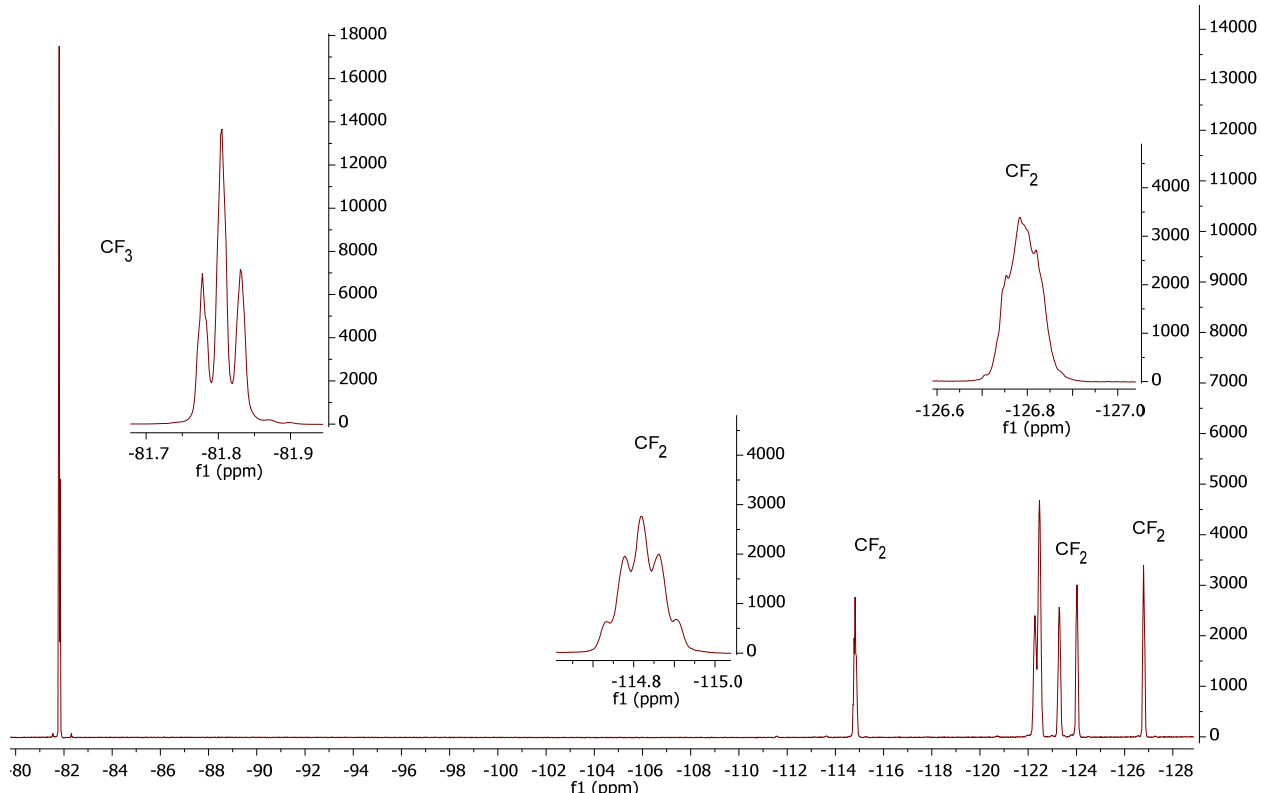


Figure S25: ^{13}F -NMR of compound $\mathbf{H}8^2$ (376 MHz, THF- d_8 , 27 °C).

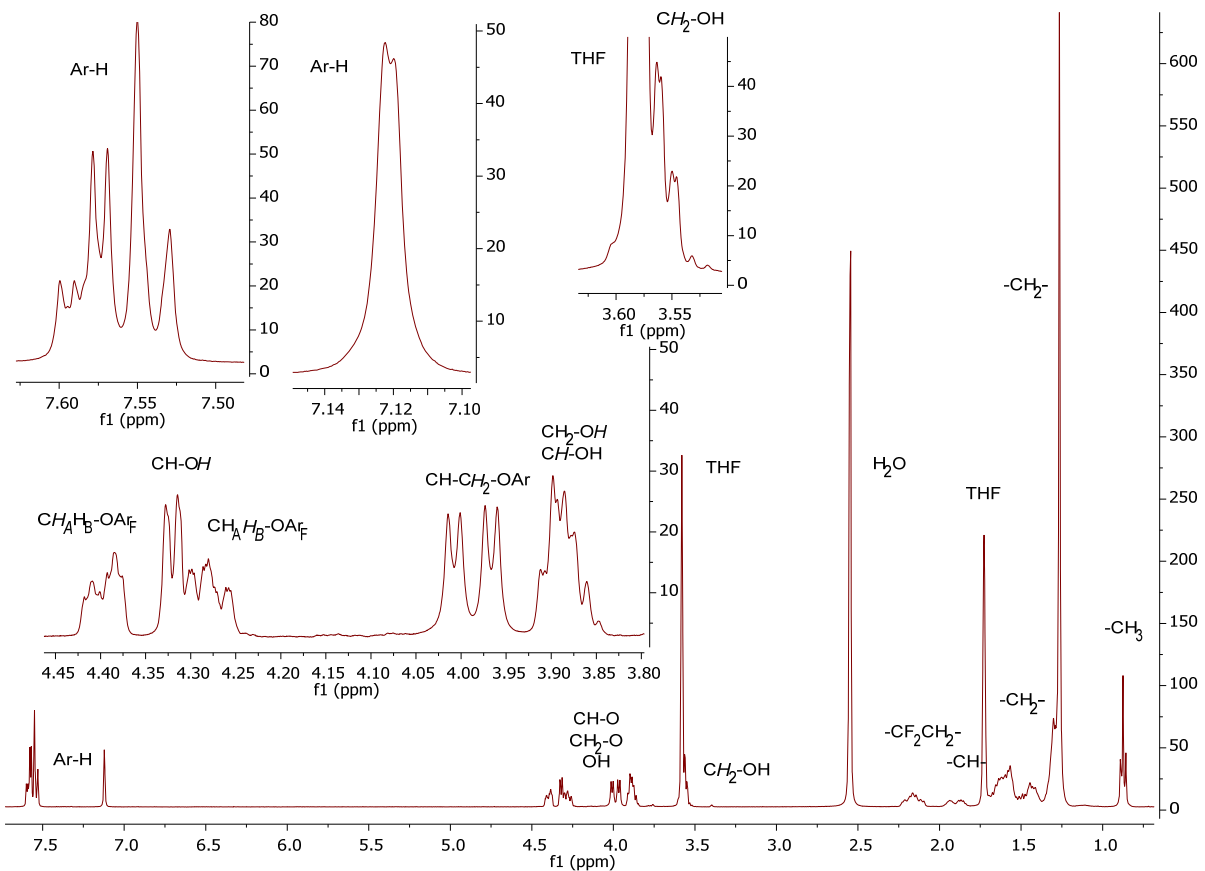


Figure S26: ^1H -NMR of compound F8/14 (400 MHz, THF-d₈, 27 °C).

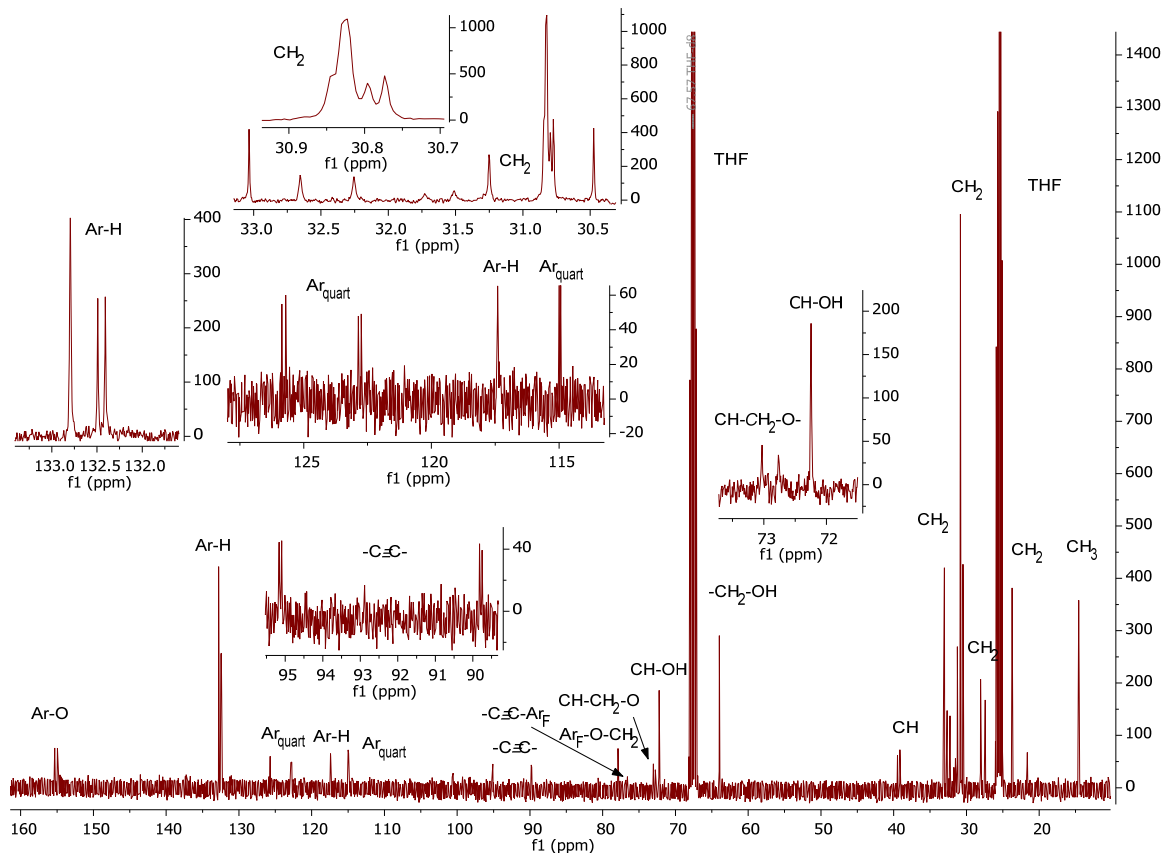


Figure S27: ^{13}C -NMR of compound F8/14 (101 MHz, THF-d₈, 27 °C).

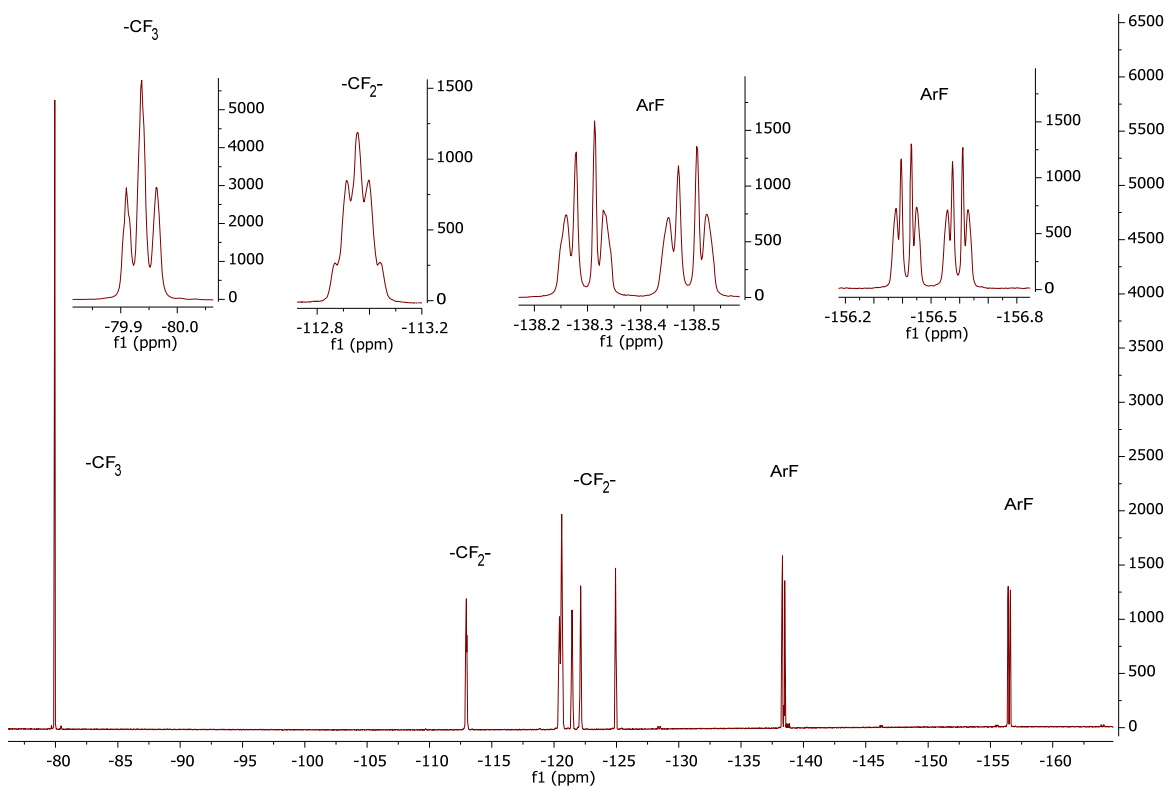


Figure S28: ¹⁹F-NMR of compound F8/14 (376 MHz, THF-d₈, 27 °C).

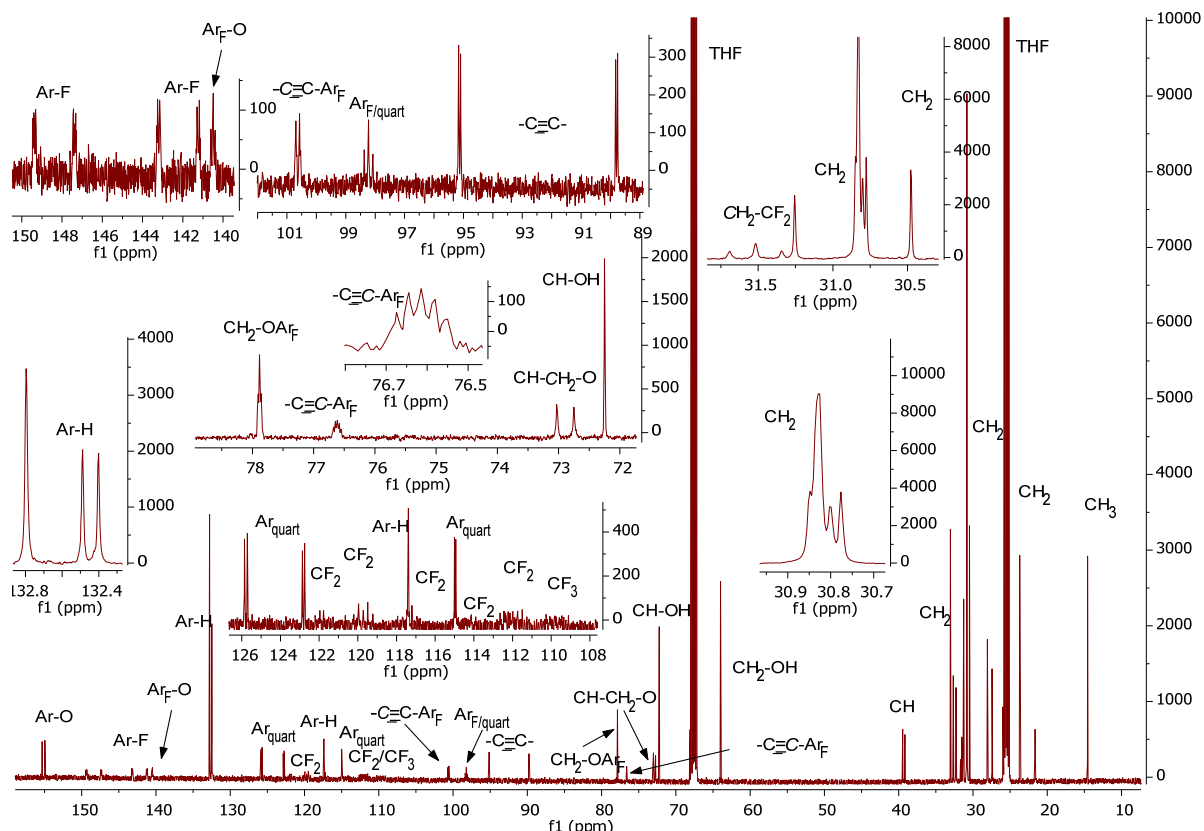
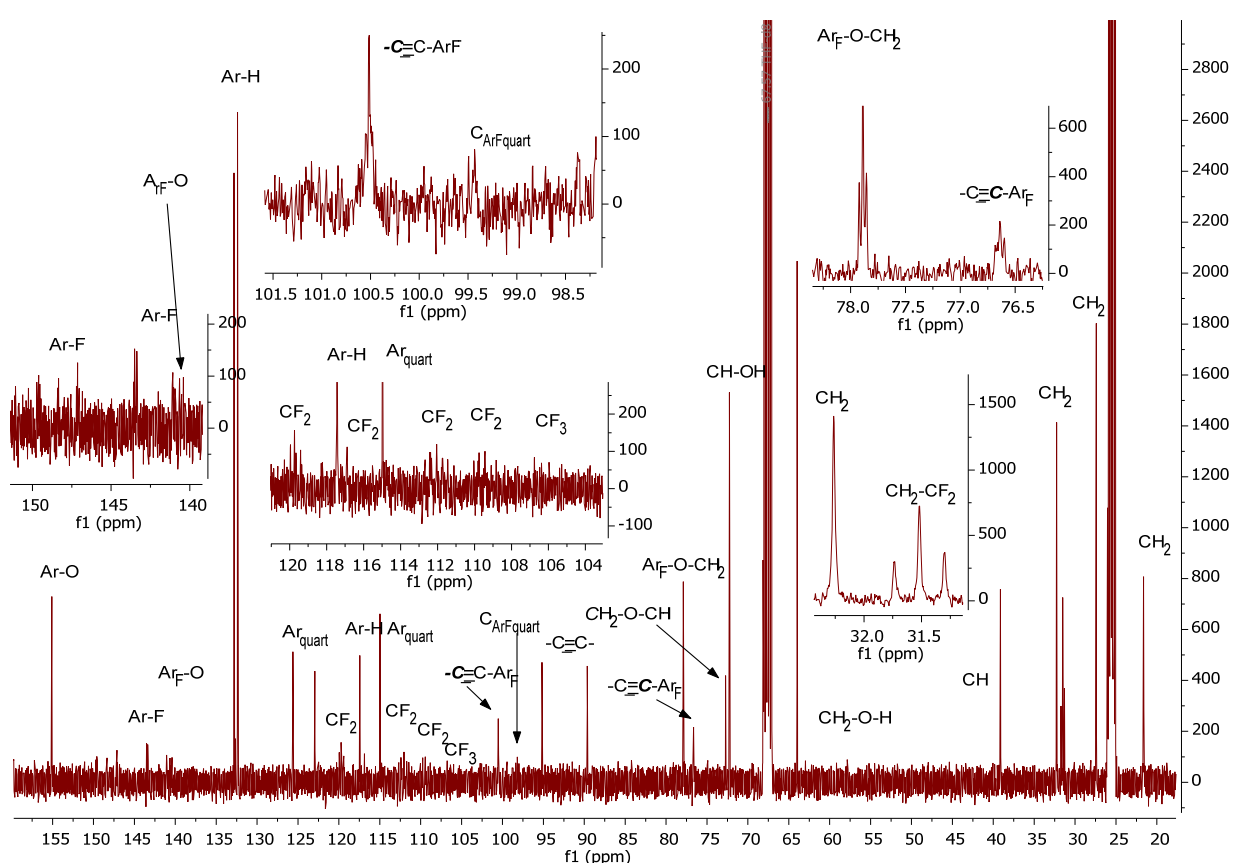
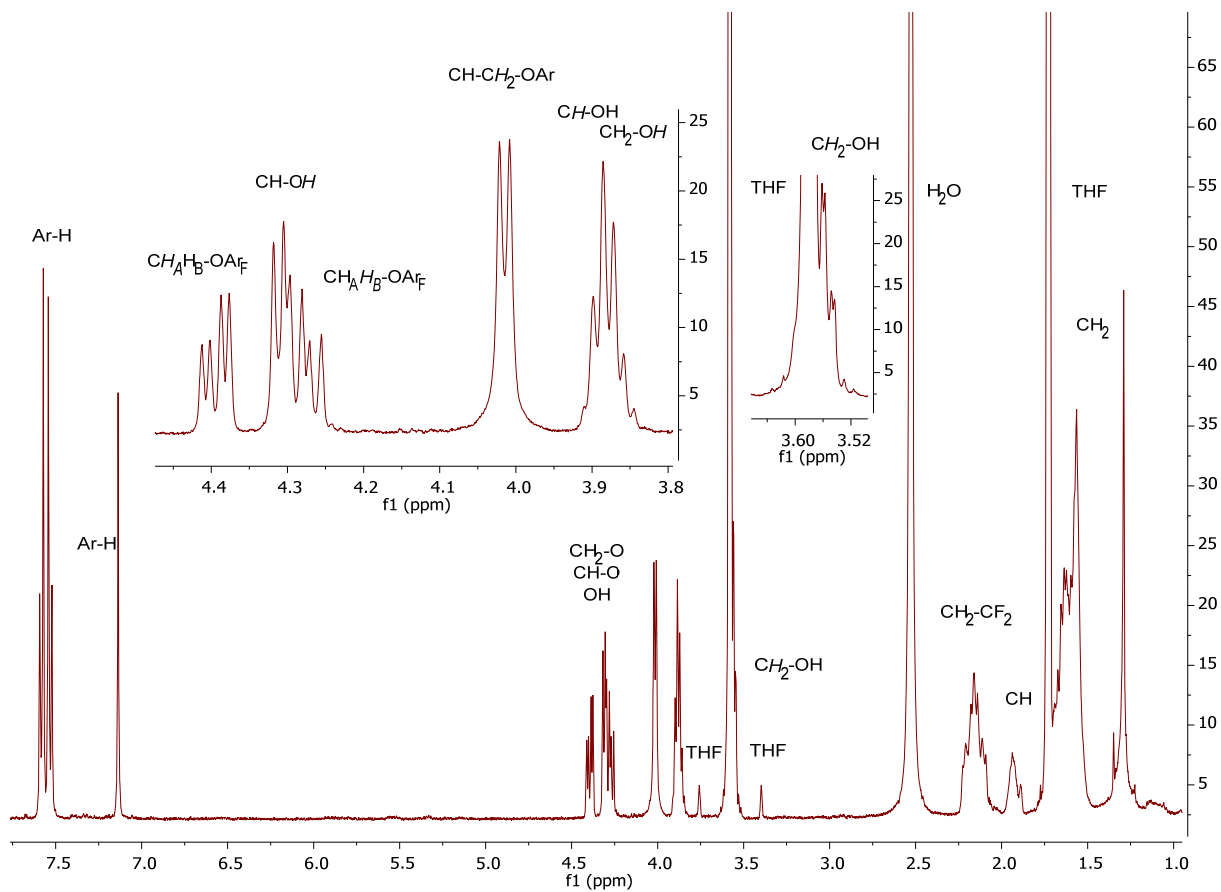


Figure S29: ¹³C-NMR of compound F7/14 (101 MHz, THF-d₈, 27 °C) showing most of the carbons with fluorine coupling.



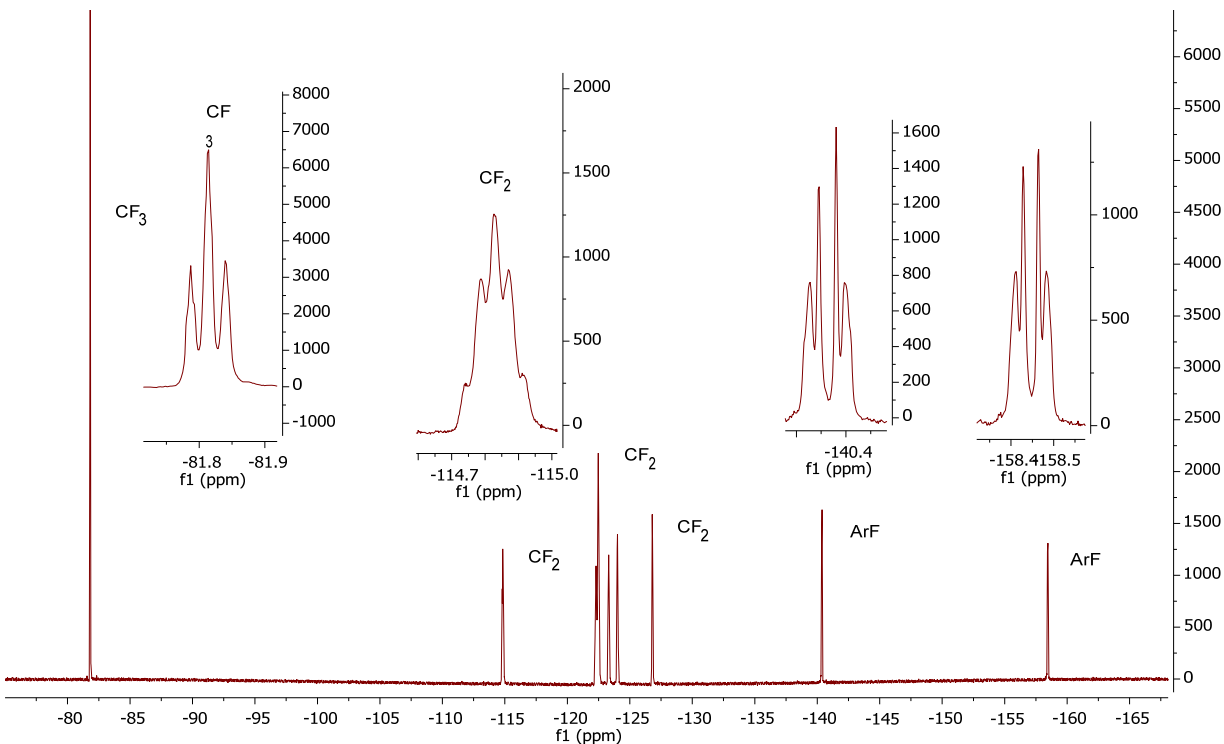


Figure S32: ^{19}F -NMR of compound **F8²** (376 MHz, THF-d₈, 27 °C).

4 References

- S1 A. Immirzi and B. Perini, *Acta Cryst. A*, **1977**, *33*, 216–218.
- S2 W. S. Sheldrick, *Acta Cryst. B*, **1980**, *36*, 2194–2194.
- S3 M. Prehm, F. Liu, X. Zeng, G. Ungar, C. Tschierske, *J. Am. Chem. Soc.* **2011**, *133*, 4906–4916.
- S4 K. Sonogashira, Y. Tohda and N. Hagiwara, *Tetrahedron Lett* **1975**, *50*, 4467-4470.
- S5 a) S. Poppe, M. Poppe, H. Ebert, M. Prehm, C. Chen, F. Liu, S. Werner, K. Bacia, C. Tschierske, *Polymers* **2019**, *7*, 471; b) M. Poppe, C. Chen, F. Liu, S. Poppe and C. Tschierske, *Chem. Eur. J.*, **2017**, *23*, 7196-7200; c) S. Werner, H. Ebert, B.-D. Lechner, F. Lange, A. Achilles, R. Bärenwald, S. Poppe, A. Blume, K. Saalwächter, C. Tschierske and K. Bacia, *Chem. Eur. J.*, **2015**, *21*, 8840-8850.
- S6 N. Iranpoor, H. Firouzabadi, Gh. Aghapour, A. R. Vaezzadeh, *Tetrahedron*, **2002**, *58*, 8669.
- S7 Jr. Lever, O. W. Bell, L. N. Hymna, C. McGuire, R. & M. Ferone, *J. Med. Chem.* **1986**, *29*, 665-670.
- S8 G. Nagarjuna, A. Kokil, J. Kumar, D. Venkataraman, *J. Mater. Chem.* **2012**, *22*, 16091–16094.
- S9 R. van Rijsbergen, M. J. O. Anteunis and A. De Bruyn, *J. Carbohydr. Chem.*, **1983**, *2*, 395-404.
- S10 W.-Y. Chang, D. Shi, X.-Q. Jiang, J.-D. Jiang, Y. Zhao, X.-K. Ren, S. Yang, E.-Q. Chen, *Polym. Chem.*, **2020**, *11*, 1454–1461.